NOAA Technical Memorandum NWS WR-230

SANTA ANA WINDS AND THE FIRE OUTBREAK OF FALL 1993

Ivory J. Small
National Weather Service Forecast Office
Oxnard, California

June 1995

U.S. DEPARTMENT OF COMMERCE / National Oceanic and Atmospheric Administration / National Weather Service

NOAA TECHNICAL MEMORANDA
National Weather Service, Western Region Subseries

The National Weather Service (NWS) Western Region (WR) Subseries provides an informal medium for the documentation and quick dissemination of results not appropriate, or not yet ready, for formal publication. The series is used to report on work in progress, to describe technical procedures and practices, or to relate progress to a limited audience. These Technical Memoranda will report on investigations devoted primarily to regional and local problems of interest mainly to personnel, and hence will not be widely distributed.

Papers 1 to 25 are in the former series, ESSA Technical Memoranda, Western Region Technical Memoranda (WRTM); papers 24 to 59 are in the former series, ESSA Technical Memoranda, Weather Bureau Technical Memoranda (WBTM). Beginning with 60, the papers are part of the series, NOAA Technical Memoranda NWS. Out-of-print memoranda are not listed.

Papers 2 to 22, except for 5 (revised edition), are available from the National Weather Service Western Region, Scientific Services Division, P.O. Box 11188, Federal Building, 125 South State Street, Salt Lake City, Utah 84147. Paper 5 (revised edition), and all others beginning with 25 are available from the National Technical Information Service, U.S. Department of Commerce, Sills Building, 5285 Port Royal Road, Springfield, Virginia 22161. Prices vary for all paper copies; microfiche are $3.50. Order by accession number shown in parentheses at end of each entry.

ESSA Technical Memoranda (WRTM)

2 Climatological Precipitation Probabilities. Compiled by Lucianne Miller, December 1965.
3 Western Region Pre- and Post-FP-3 Program, December 1, 1965, to February 20, 1966. Edward D. Diemer, March 1966.
5 Station Descriptions of Local Effects on Synoptic Weather Patterns. Philip Williams, Jr., April 1966 (Revised November 1967, October 1969). (PB-17800)
8 Interpreting the RAREP. Herbert P. Benner, May 1966 (Revised January 1967).
11 Some Electrical Processes in the Atmosphere. J. Latham, June 1966.
17 A Digitalized Summary of Radar Echoes within 100 Miles of Sacramento, California. J. A. Youngberg and L. B. Overaas, December 1966.
21 An Objective Aid for Forecasting the End of East Winds in the Columbia Gorge, July through October. D. John Coparanis, April 1967.
22 Derivation of Radar Horizons in Mountainous Terrain. Roger G. Pappas, April 1967.

ESSA Technical Memoranda, Weather Bureau Technical Memoranda (WBTM)

25 Verification of Operation Probability of Precipitation Forecasts, April 1966-March 1967. W. W. Dickey, October 1967. (PB-176240)
26 A Study of Winds in the Lake Mead Recreation Area. R. P. Augulis, January 1968. (PB-177830)
28 Weather Extremes. R. J. Schmidli, April 1968 (Revised March 1986). (PB86 177672/AS). (Revised October 1991 - PB92-115062/AS)
29 Small-Scale Analysis and Prediction. Philip Williams, Jr., May 1968. (PB178425)
30 Numerical Weather Prediction and Synoptic Meteorology. CPT Thomas D. Murphy, USAF, May 1968. (AD 673365)
31 Precipitation Detection Probabilities by Salt Lake ARTC Radars. Robert K. Belesky, July 1968. (PB 179084)
32 Probability Forecasting--A Problem Analysis with Reference to the Portland Fire Weather District. Harold S. Ayer, July 1968. (PB 179289)
36 Temperature Trends in Sacramento--Another Heat Island. Anthony D. Lentini, February 1969. (PB 183055)
37 Disposal of Logging Residues Without Damage to Air Quality. Owen P. Cramer, March 1969. (PB 183057)
39 Upper-Air Lows Over Northwestern United States. A.L. Jacobson, April 1969. PB 184296)
40 The Man-Machine Mix in Applied Weather Forecasting in the 1970s. L.W. Snellman, August 1969. (PB 185068)
43 Forecasting Maximum Temperatures at Helena, Montana. David E. Olsen, October 1969. (PB 185762)
44 Estimated Return Periods for Short-Duration Precipitation in Arizona. Paul C. Kangieser, October 1969. (PB 187763)
46 Applications of the Net Radiometer to Short-Range Fog and Stratus Forecasting at Eugene, Oregon. L. Yee and E. Bates, December 1969. (PB 190476)
47 Statistical Analysis as a Flood Routing Tool. Robert J.C. Burnash, December 1969. (PB 188744)
48 Tsunami. Richard P. Augulis, February 1970. (PB 190157)
49 Predicting Precipitation Type. Robert J.C. Burnash and Floyd E. Hug, March 1970. (PB 190962)
50 Statistical Report on Aeroallergens (Pollens and Molds) Fort Huachuca, Arizona, 1969. Wayne S. Johnson, April 1970. (PB 191743)
51 Western Region Sea State and Surf Forecaster's Manual. Gordon C. Shields and Gerald B. Burdwell, July 1970. (PB 193102)
52 Sacramento Weather Radar Climatology. R.G. Pappas and C. M. Veliquette, July 1970. (PB 193347)
54 A Refinement of the Vorticity Field to Delineate Areas of Significant Precipitation. Barry B. Aronovitch, August 1970.
55 Application of the SSARR Model to a Basin without Discharge Record. Vail Schermerhorn and Donal W. Kuehl, August 1970. (PB 194394)
56 Areal Coverage of Precipitation in Northwestern Utah. Philip Williams, Jr., and Werner J. Heck, September 1970. (PB 194389)
57 Preliminary Report on Agricultural Field Burning vs. Atmospheric Visibility in the Willamette Valley of Oregon. Earl M. Bates and David O. Chilcote, September 1970. (PB 194710)
58 Air Pollution by Jet Aircraft at Seattle-Tacoma Airport. Wallace R. Donaldson, October 1970. (COM 71 00017)
59 Application of PE Model Forecast Parameters to Local-Area Forecasting. Leonard W. Snellman, October 1970. (COM 71 00016)
60 An Aid for Forecasting the Minimum Temperature at Medford, Oregon, Arthur W. Fritz, October 1970. (COM 71 00120)
63 700-mb Warm Air Advection as a Forecasting Tool for Montana and Northern Idaho. Norris E. Woerner, February 1971. (COM 71 00349)
64 Wind and Weather Regimes at Great Falls, Montana. Warren B. Price, March 1971.
65 Climate of Sacramento, California. Tony Martini, April 1990. (Fifth Revision) (PB89 207781/AS)
66 A Preliminary Report on Correlation of ARTCC Radar Echoes and Precipitation. Wilbur K. Hall, June 1971. (COM 71 00829)
69 National Weather Service Support to Soaring Activities. Ellis Burton, August 1971. (COM 71 00956)
71 Western Region Synoptic Analysis-Problems and Methods. Philip Williams, Jr., February 1972. (COM 72 10433)
74 Thunderstorms and Hail Days Probabilities in Nevada. Clarence M. Sakamoto, April 1972. (COM 72 10554)
75 A Study of the Low Level Jet Stream of the San Joaquin Valley. Ronald A. Willis and Philip Williams, Jr., May 1972. (COM 72 10707)
76 Monthly Climatological Charts of the Behavior of Fog and Low Stratus at Los Angeles International Airport. Donald M. Gales, July 1972. (COM 72 11140)
77 A Study of Radar Echo Distribution in Arizona During July and August. John E. Hales, Jr., July 1972. (COM 72 11136)
78 Forecasting Precipitation at Bakersfield, California, Using Pressure Gradient Vectors. Earl T. Riddiough, July 1972. (COM 72 11146)
79 Climate of Stockton, California. Robert C. Nelson, July 1972. (COM 72 10920)
80 Estimation of Number of Days Above or Below Selected Temperatures. Clarence M. Sakamoto, October 1972. (COM 72 10021)
81 An Aid for Forecasting Summer Maximum Temperatures at Seattle, Washington. Edgar G. Johnson, November 1972. (COM 73 10150)
82 Flash Flood Forecasting and Warning Program in the Western Region. Philip Williams, Jr., Chester L. Glenn, and Roland L. Raetz, December 1972, (Revised March 1978). (COM 73 10251)
83 A comparison of Manual and Semiautomatic Methods of Digitizing Analog Wind Records. Glenn E. Rasch, March 1973. (COM 73 10669)
86 Conditional Probabilities for Sequences of Wet Days at Phoenix, Arizona. Paul C. Kangieser, June 1973. (COM 73 11264)
87 A Refinement of the Use of K-Values in Forecasting Thunderstorms in Washington and Oregon. Robert Y.G. Lee, June 1973. (COM 73 11276)
89 Objective Forecast Precipitation Over the Western Region of the United States. Julia N. Paegle and Larry P. Kierulff, September 1973. (COM 73 11946/3AS)
91 Arizona "Eddy" Tornadoes. Robert S. Ingram, October 1973. (COM 73 10465)
92 Smoke Management in the Willamette Valley. Earl M. Bates, May 1974. (COM 74 11277/AS)
93 An Operational Evaluation of 500-mb Type Regression Equations. Alexander E. MacDonald, June 1974. (COM 74 11407/AS)
94 Conditional Probability of Visibility Less than One-Half Mile in Radiation Fog at Fresno, California. John D. Thomas, August 1974. (COM 74 11555/AS)
95 Climate of Flagstaff, Arizona. Paul W. Sorenson, and updated by Reginald W. Preston, January 1987. (PB87 143160/AS)
96 Map type Precipitation Probabilities for the Western Region. Glenn E. Rasch and Alexander E. MacDonald, February 1975. (COM 75 10428/AS)
97 Eastern Pacific Cut-Off Low of April 21-28, 1974. William J. Alder and George R. Miller, January 1976. (PB 250 711/AS)
98 Study on a Significant Precipitation Episode in Western United States. Ira S. Brenner, April 1976. (COM 75 10719/AS)
99 A Study of Flash Flood Susceptibility-A Basin in Southern Arizona. Gerald Williams, August 1975. (COM 75 11360/AS)
102 A Set of Rules for Forecasting Temperatures in Napa and Sonoma Counties. Wesley L. Tuft, October 1975. (PB 246 902/AS)
103 Application of the National Weather Service Flash-Flood Program in the Western Region. Gerald Williams, January 1976. (PB 253 053/AS)
104 Objective Aids for Forecasting Minimum Temperatures at Reno, Nevada, During the Summer Months. Christopher D. Hill, January 1976. (PB 252 866/AS)
105 Forecasting the Mono Wind. Charles P. Ruscha, Jr., February 1976. (PB 254 650)
106 Use of MOS Forecast Parameters in Temperature Forecasting. John C. Plankinton, Jr., March 1976. (PB 254 649)
107 Map Types as Aids in Using MOS PoPs in Western United States. Ira S. Brenner, August 1976. (PB 259 594)
108 Other Kinds of Wind Shear. Christopher D. Hill, August 1976. (PB 260 437/AS)
109 Forecasting North Winds in the Upper Sacramento Valley and Adjoining Forests. Christopher E. Fontana, September 1976. (PB 273 677/AS)
110 Cool Inflow as a Weakening Influence on Eastern Pacific Tropical Cyclones. William J. Denney, November 1976. (PB 264 655/AS)
112 The MAN/MOS Program. Alexander E. MacDonald, February 1977. (PB 265 941/AS)
113 Winter Season Minimum Temperature Formula for Bakersfield, California, Using Multiple Regression. Michael J. Oard, February 1977. (PB 273 694/AS)
114 Tropical Cyclone Kathleen. James R. Fors, February 1977. (PB 273 676/AS)
116 A Study of Wind Gusts on Lake Mead. Bradley Colman, April 1977. (PB 268 847)
117 The Relative Frequency of Cumulonimbus Clouds at the Nevada Test Site as a Function of K-Value. R.F. Quiring, April 1977. (PB 272 831)
118 Moisture Distribution Modification by Upward Vertical Motion. Ira S. Brenner, April 1977. (PB 268 740)
119 Relative Frequency of Occurrence of Warm Season Echo Activity as a Function of Stability Indices Computed from the Yucca Flat, Nevada, Rawinsonde. Darryl Randerson, June 1977. (PB 271 290/AS)
121 Climatological Prediction of Cumulonimbus Clouds in the Vicinity of the Yucca Flat Weather Station. R.F. Quiring, June 1977. (PB 271 704/AS)
122 A Method for Transforming Temperature Distribution to Normality. Morris S. Webb, Jr., June 1977. (PB 271 742/AS)
124 Statistical Guidance for Prediction of Eastern North Pacific Tropical Cyclone Motion - Part I. Charles J. Neumann and Preston W. Leftwich, August 1977. (PB 272 661)
125 Statistical Guidance on the Prediction of Eastern North Pacific Tropical Cyclone Motion - Part II. Preston W. Leftwich and Charles J. Neumann, August 1977. (PB 273 155/AS)
126 Climate of San Francisco. E. Jan Null, February 1978. Revised by George T. Pericht, April 1988. (PB88 208624/AS)
127 Development of a Probability Equation for Winter-Type Precipitation Patterns in Great Falls, Montana. Kenneth B. Mielke, February 1978. (PB 281 387/AS)
128 Hand Calculator Program to Compute Parcel Thermal Dynamics. Dan Gudgel, April 1978. (PB 283 080/AS)
129 Fire whirls. David W. Goens, May 1978. (PB 283 866/AS)
130 Flash-Flood Procedure. Ralph C. Hatch and Gerald Williams, May 1978. (PB 286 014/AS)
131 Automated Fire-Weather Forecasts. Mark A. Mollner and David E. Olsen, September 1978. (PB 289 916/AS)
132 Estimates of the Effects of Terrain Blocking on the Los Angeles WSR-74C Weather Radar. R.G. Pappas, R.Y. Lee, B.W. Finke, October 1978. (PB 289767/AS)
133 Spectral Techniques in Ocean Wave Forecasting. John A. Jannuzzi, October 1978. (PB291317/AS)
134 Solar Radiation. John A. Jannuzzi, November 1978. (PB291195/AS)
135 Application of a Spectrum Analyzer in Forecasting Ocean Swell in Southern California Coastal Waters. Lawrence P. Kierulff, January 1979. (PB292716/AS)
136 Basic Hydrologic Principles. Thomas L. Dietrich, January 1979. (PB292247/AS)
137 LFM 24-Hour Prediction of Eastern Pacific Cyclones Refined by Satellite Images. John R. Zimmerman and Charles P. Ruscha, Jr., January 1979. (PB294324/AS)
138 A Simple Analysis/Diagnosis System for Real Time Evaluation of Vertical Motion. Scott Heflick and James R. Fors, February 1979. (PB294216/AS)
139 Aids for Forecasting Minimum Temperature in the Wenatchee Frost District. Robert S. Robinson, April 1979. (PB298339/AS)
140 Influence of Cloudiness on Summertime Temperatures in the Eastern Washington Fire Weather district. James Holcomb, April 1979. (PB298674/AS)
141 Comparison of LFM and MFM Precipitation Guidance for Nevada During Doreen. Christopher Hill, April 1979. (PB298613/AS)

NOAA Technical Memorandum NWS WR-230

SANTA ANA WINDS AND THE FIRE OUTBREAK OF FALL 1993

Ivory J. Small
National Weather Service Forecast Office
Oxnard, California

June 1995

UNITED STATES DEPARTMENT OF COMMERCE
Ronald H. Brown, Secretary

National Oceanic and Atmospheric Administration
D. James Baker, Under Secretary and Administrator

National Weather Service
Elbert W. Friday, Jr., Assistant Administrator for Weather Services

This publication has been reviewed
and is approved for publication by
Scientific Services Division,
Western Region

Delain A. Edman, Chief
Scientific Services Division
Salt Lake City, Utah

TABLE OF CONTENTS

TABLES AND FIGURES

SANTA ANA WINDS AND THE FIRE OUTBREAK OF FALL 1993

Ivory J. Small - NWSFO Los Angeles/Oxnard

I. INTRODUCTION

From late October 1993 through early November of 1993, one of the worst fire outbreaks in recent history occurred in southern California. The fires were the result of a near-perfect combination of several factors; strong Santa Ana winds, high temperatures, low relative humidities, the abundance of vegetation due to well-above normal rainfall during the last two winters, and the lack of significant precipitation over the previous six months. A brief description of Santa Ana winds and how the current conceptual models relate to the winds will be given in section II. In section III, the typical synoptic and mesoscale patterns as well as the current methodology used by the Los Angeles/ Oxnard National Weather Service Forecast Office (NWSFO LOX) to forecast Santa Ana winds will be given. In section IV, the synoptic and mesoscale conditions associated with five Santa Ana wind cases, including a comparison to the PCGRIDS forecasts, will be presented to further illustrate this methodology. In section V, an overview of conditions common to fire outbreaks will be presented by comparing the fall 1993 scenario to the Panorama Fire scenario of fall 1980. Finally, additional problems and a summary of the possible improvements to the forecasting of Santa Ana winds will be presented.

II. OVERVIEW OF SANTA ANA WIND

a. Definition of Santa Ana Winds

In the Glossary of Meteorology, (Huschke 1959) the Santa Ana wind is defined as a "...hot, dry foehn-like desert wind, generally from the northeast or east, especially in the passes and river valley of Santa Ana, California, where it is further modified as a mountain gap wind...". Generally these winds occur on the southwestern slopes below the passes and canyons of the coastal ranges and in the Los Angeles Basin. The Los Angeles Basin is bounded to the north through east by the coastal ranges, with peaks to above 11,000 feet, and on the west by the Pacific Ocean. Figures 1, 2, and 3 show the location of the Los Angeles Basin as well as the locations of the cross sections that will be used.

The above definition of the Santa Ana wind has been modified somewhat by forecasters at NWSFO LOX, who have placed speed minimums on the winds, reserving the use of "Santa Ana" for more significant events (with speeds in excess of about 25 knots in heavily populated areas). Also, since "hot" is not defined, forecasters do not put a temperature restriction on the winds. Occasionally, spotty precipitation occurs during the early or later stages of these events. During the times when spotty precipitation is in the forecast, the event is known locally as a "wet" Santa Ana.

Santa Ana winds can blow violently over the southwestern slopes of the coastal ranges in heavily populated areas of the basin. These events most commonly occur between October and February, but can occur anytime after August and before June. Mid-summer Santa Ana events are extremely rare, while December has the highest frequency of events.

Wind speeds are typically north to east at about 35 knots in and below passes and canyons in the mountains and favored basin locations, with gusts to 50 knots. Stronger Santa Ana winds can have gusts to 60 knots or higher over widespread areas, and over 100 knots in favored areas. During the widespread Santa Ana episode of 14-15 November 1993, a peak wind of over 65 knots was recorded on the western slopes of the Santa Ana Mountains on both days.

According to Fosberg et al. (1966), the Santa Ana wind is primarily a lee wave phenomenon, and the air flow is along an isentropic surface. The altocumulus standing lenticular reported at the Ontario Airport during the morning of the 27 October 1993 gives strong support to this statement (Table 1).

Santa Ana winds are an important forecast problem because of the hazards associated with them; high fire danger, wind damage to property, and severe turbulence and low-level wind shear for aircraft. Also, as the winds blow offshore, they can be dangerous for boaters.

Although the most favored locations for Santa Ana winds are the western slopes of the mountains, and the portion of the basin near the mountains, the winds can extend over the coastal waters and reach the islands some 50 miles offshore. During widespread, strong Santa Ana episodes, the winds can blow over all of southern California. Usually, the strongest winds occur near the Cajon Pass, Santa Ana Canyon, the Santa Clara River Valley, and Banning Pass. These areas, henceforth called the "favored areas", can be seen in Fig. 1.

b. Conceptual Models and the Santa Ana Wind

The Santa Ana wind is a type of windstorm that can occur without strong gradients aloft, and produce strong winds at the surface through the downward transfer of momentum (however, many Santa Ana events occur with strong gradients aloft). Therefore, the Santa Ana can be categorized as a type of vertically propagating wave. In order to properly address the "amplified mountain wave" characteristics of the Santa Ana, some discussion of the conceptual models must be included.

Durran (1990) discusses downslope winds by comparing three theoretical models. The first compares downslope windstorms to hydraulic jumps of shallow water theory. The assumption is that a homogeneous fluid bounded by a free surface is in hydrostatic balance and flows over a ridge-like obstacle. Using the shallow-water momentum and continuity equations, the Froud number (Fr), is defined as the ratio of the fluid velocity to the speed of linear shallow water gravity waves, $Fr^2 = u^2/gD$. Figure 4a is the supercritical flow case where $Fr > 1$. The fluid actually thickens, slows to a minimum speed at ridgetop, then returns to the ambient speed after traversing the obstacle. Figure 4b is the case of $Fr < 1$ (subcritical flow), where the fluid thins, reaches a maximum speed at the crest, then decelerates on the other side to the ambient flow speed. The subcritical flow speed at the crest is greater than the mean flow speed. Figure 4c is the flow regime that was proposed to be

analogous to downslope windstorms. In this case, the supercritical fluid flow on the windward side of the obstacle thins and accelerates, eventually becoming subcritical at the crest. The fluid continues to accelerate on the leeward side. Finally, the flow undergoes a hydraulic jump to conform to the ambient downstream conditions.

A second possible explanation discussed by Durran utilizes theory presented by Eliassen and Palm (1960) for gravity waves, with an extension by Klemp and Lilly (1975) for a multilayered atmosphere. It was suggested that downslope windstorms occur when upward propagating gravity waves are partially reflected by layers in the atmosphere where the Scorer parameter changes rapidly. (The Scorer parameter is dependent on vertical shear and stability, so regions of rapidly changing vertical shear and stability can cause rapid changes of the Scorer parameter. From this point on, layers of rapidly changing Scorer parameter will be referred to as "critical levels"). If the atmosphere is "tuned" such that the reflected energy due to the critical levels results in an optimal superpositions of upward and downward propagating waves (which determines wave amplitude), downslope windstorms may result. The optimal static stability structure for high amplitude waves consists of a relatively deep conditionally unstable layer in the middle troposphere, bounded above by the stratosphere, and below by a shallow layer of high static stability air in the lower troposphere.

The third explanation mentioned in Durran was proposed based on numerical models. In the models, breaking waves resulted in a critical layer, which as seen in the second explanation, can reflect upward propagating waves downward.

In the case of the Santa Ana wind, it is possible that the critical layer is not produced by a breaking wave, but rather by an evolving synoptic pattern. While high pressure at the surface moves into the Great Basin, and pushes into the desert areas of southern California from the north and east, a ridge of high pressure aloft pushes inland from the northwest, creating a critical layer. This is similar to the critical layer creation process noted for "Sundowner Winds", another type of southern California windstorm, discussed in Western Region Technical Attachment 90-31.

III. CHARACTERISTIC PATTERNS AND FORECASTING TECHNIQUES

a. Synoptic and Mesoscale Patterns

The synoptic scale situation that characterizes many offshore flow patterns, including the subset known as the "Santa Ana", begins with a developing short-wave trough, moving in a northwest to southeast direction through Nevada, Arizona, or southern California. The trough is usually followed by rapidly building surface high pressure over northern and central California, eventually spilling over into Nevada and Utah. (Nevada and Utah are frequently referred to as the "Great Basin"). When the surface pressure over central California or the Great Basin exceeds that found along the southern California coast, offshore flow develops.

A chief upper-air pattern for the strongest winds is when an upper-level low develops over southern Nevada, western Arizona, extreme northwest Mexico, or southern California. This results in a moderate to strong southeast to northwest height gradient and moderate to strong north to northeast flow at 500 mb and 700 mb over

southern California. (Moderate would be considered to be a 30 to 50 meter height change over a distance of 200 miles, and strong is greater than about 50 meters.) Also, the temperature difference at 700 mb between the southern California coast and southern Nevada (called "thermal support") forms almost simultaneously (Harvey, 1959). A three to six degree temperature difference between the warmer Vandenberg, California (VBG) and Desert Rock, Nevada (DRA) would be considered moderate.

The complex topography of the mountains in southern California significantly influences the location, strength, and direction of the Santa Ana winds, making the forecasting of these parameters very difficult.

During a typical Santa Ana wind episode, when the surface pressure gradient to the Great Basin is strong (surface pressure at Tonapah, Nevada (TPH) exceeds that at Los Angeles (LAX) by 10 mb or more), but the surface pressure gradient to central California is weak (surface pressure at San Francisco (SFO) is no more than about 4 mb higher than the value at LAX), wind gusts in excess of 60 knots can occur in the mountains and in the favored coastal areas shown in Fig. 1. At the same time, only weak sustained northeast winds of less than 10 knots, or even southwest winds can blow over the western Los Angeles Basin, where the Los Angeles International Airport (LAX) is located. During one such episode in January 1989, northeast winds at the Ontario International Airport (ONT) gusted to 60 knots for several hours, while only weak northeast winds occurred at LAX. During another episode in December 1993, northeast winds at ONT gusted to 65 knots, closing the airport, while the strongest wind from any direction at LAX was 7 knots during the course of the event.

Events with widespread Santa Ana winds occur when, (in addition to strong upper-level height gradients, a strong 700 mb thermal gradient, and a strong offshore surface pressure gradient to the Great Basin), a cold front sweeps over southern California from the north or northeast, and the surface pressure difference at SFO exceeds that at LAX by more than about 8 mb. Fronts of this type are usually indicators of rapidly building high pressure over northern and central California and cold air advection. It is during these episodes that the winds finally surface at LAX and the nearby beaches and coastal waters of Santa Monica, Marina Del Rey, and Venice. This type of pattern occurred during the November 14-15 1993 Santa Ana episode, which will be presented later. Wind gusts to 33 knots were reported at LAX on the 14th, still less than half the speeds reported in the mountains, but a matter of much concern to the residents of Los Angeles.

b. Forecasting Techniques

NWSFO LOX uses two systems to predict the occurrence and strength of a Santa Ana wind. The first method, called the Santa Ana Objective System (Sergius and Huntoon, 1949), determines the probability of a Santa Ana occurring 18-42 hours in the future. The second system, called the Fontana System (Harvey, 1959) gives an expected wind speed for the Fontana-Chino area (below the Cajon Pass), where some of the strongest winds are usually found. The Fontana System was developed using a wind speed indicator mounted on a building at the Kaiser Steel Plant in Fontana, just below the pass. Unfortunately, the sensor is no longer in that location so this system is used with extreme caution.

To determine the probability of Santa Ana winds, the first system uses the following

data. (Keep in mind that stronger gradients usually result in higher probabilities of Santa Ana winds):

a. The surface pressure gradient between the Oregon coast and Los Angeles, with higher pressure over Oregon. (Surface high pressure building behind a trough.)

b. The west to east height gradient at 500 mb between northern California and eastern Nevada, with lower heights over the Great Basin. (Ridge of high pressure building over the Pacific Northwest with a trough of low pressure moving southeast through the Great Basin.)

c. The 500 mb temperature gradient between eastern Washington and eastern Nevada with colder air over eastern Washington. (Cold air aloft moving into the Great Basin behind the trough.)

To decide on the wind speed just below the Cajon Pass, the Fontana System looks for offshore surface pressure gradients and 700 mb thermal support. Wind speeds are determined using the following data. (Bear in mind that larger differences usually indicate stronger winds):

a. The difference (in degrees Celsius) between the 700 mb temperatures at Desert Rock (DRA), Nevada and Vandenberg Air Force Base (VBG), California. (Stronger winds if the colder air is over Nevada.)

b. The difference (in millibars) between the surface pressure at the Los Angeles International Airport (LAX) and Tonopah (TPH) Nevada, (Stronger winds if the higher pressure is over Nevada).

c. The difference (in geopotential meters) between the 850-700 mb thickness at VBG and the 850-700 mb thickness at DRA.

Unfortunately, forecasted values of surface pressure gradient and 700 mb temperatures must be used in order to predict wind speeds 18-42 hours in advance.

In addition, forecasters make use of the 700 mb vertical velocity forecasts to determine what type of synoptic-scale subsidence can be expected.

Based on the conceptual models discussed in section II, the forecaster should also look for wind directions roughly within 30 degrees of perpendicular to the ridgeline with wind speed at mountaintop level exceeding a terrain dependent 15 to 30 knots. Also an upstream temperature profile with an inversion or layer of strong stability near the mountaintop is desirable.

In the next section, a remarkable resemblance between the conceptual models and the conditions during recent Santa Ana wind episodes emerges.

IV. OVERVIEWS OF RECENT "DRY" AND "WET" SANTA ANA WINDS

There were two distinct Santa Ana wind maxima during the period between 26 October 1993 and 2 November 1993, coinciding with the most damaging fires in late October and early November. On 27 October, with winds gusting to over 50 knots at ONT, and 60 knots near Santa Ana Canyon, a vicious fire raced through the community of Laguna Hills. During the early morning hours of 2 November 1993, with 10 consecutive hours of sustained 30 knot winds and gusts to as high as 45 knots at ONT, another fire

ravaged the seaside community of Malibu. Ontario International Airport was closed due to strong winds on 23 December 1993 when winds gusting to 65 knots raked across the airport. Another event occurred on 8 December 1994 when winds gusted to 40 knots at ONT, and gusts above 55 knots occurred in the Malibu area, again. The synoptic and mesoscale features of these "dry" Santa Ana wind cases will be presented. Following immediately, the synoptic and mesoscale features surrounding the 14-15 November 1993 "wet" Santa Ana will be presented. Tables 1 through 5 show the winds at Ontario International Airport associated with each event.

a. The "dry" Santa Ana Event of 26-27 October 1993 (The Laguna Hills Fire)

Figures 5a and 5b show the synoptic condition at 1200 UTC 26 October 1993 that led to the Santa Ana event during the morning of 27 October 1993. The Santa Ana system gave a 61 percent chance of a Santa Ana wind for the period between 0600 UTC 27 October 1993 and 0600 UTC 28 October 1993.

Figures 6a through 7b show the synoptic conditions during the Laguna Hills Fire. The 1200 UTC 27 October 1993 NGM 500 mb analysis showed a 500 mb low center moving through southern Arizona (Fig. 6a). There was a rather tight height gradient over southern California. The 1200 UTC 27 October 1993 NGM 700 mb analysis indicated a 6 degree temperature gradient between VBG and DRA (Fig. 6b). The 1200 UTC 27 October 1993 NGM 700 mb analysis and 1200 UTC 27 October 1993 NGM 850 mb analysis showed a 61 meter difference in 850-700 mb thickness between VBG and DRA (Figs. 6b and 7a). The 1200 UTC 27 October 1993 surface analysis showed a low over southern Arizona with a strong offshore (-12.2 mb) LAX to TPH pressure gradient (Fig. 7b). As previously mentioned, maximum winds at ONT were 42 knots with gusts to 54 knots (Table 1). Without a strong frontal passage or strong pressure gradient to SFO to bring the winds to LAX, winds at LAX remained light.

Fortunately, the availability of PCGRIDS has allowed us to observe downslope windstorms such as the Santa Ana in much greater detail. The following is an analysis of the 27 October 1993 event as seen through PCGRIDS. The forecasts and analysis will be presented for this case.

Figure 8a shows the 24-hour forecasted 700 mb heights, vertical velocities, and winds valid at 1200 UTC 27 October 1993. Figure 8b shows the 700 mb heights, vertical velocities, and winds at 1200 UTC 27 October 1993. There is good agreement in the wind speed over the Los Angeles Basin. The actual vertical velocities were weaker over the Los Angeles Basin than forecast. Nevertheless, winds at mountaintop levels are perpendicular to the barrier and exceed 30 knots.

Figure 9a shows the 24-hour forecasted 850 mb heights, vertical velocities, and winds valid at 1200 UTC 27 October 1993. Figure 9b shows the 850 mb heights, vertical velocities, and winds at 1200 UTC 27 October 1993. The winds were weaker than the forecast, and vertical velocities were weaker as well. Figure 10a shows the 24-hour forecasted surface pressure map valid for 1200 UTC 27 October 1993, and Fig. 10b shows the surface pressure map valid 1200 UTC 27 October 1993. There is good agreement on the pressure difference along the cross section. Note the surface pressure gradient between the plateau and southern California. Time-height cross sections of winds, vertical velocities, and relative humidity at 34°N/117°W are shown for 1200 UTC 26 October 1993 and

1200 UTC 27 October 1993 in Figs. 11a and 11b, respectively. Notice the downward vertical velocity maximum forecast for 1200 UTC October 27 1993. The 24-hour forecasted winds and vertical velocities cross section valid 1200 UTC 27 October 1993 are shown in Fig. 12, and the 1200 UTC 27 October 1993 cross section is shown in Fig. 13. Both figures show a maximum in vertical velocities west of the coastal mountains from about 800 to 850 mb, with the maximum sloping upward to the east. The 24-hour forecasted winds and potential temperature cross section valid 1200 UTC 27 October 1993 is shown in Fig. 14. The 1200 UTC 27 October 1993 cross section is shown in Fig. 15. To assist in the evaluation of stability, the 24-hour forecasted winds and potential temperature cross section valid 1200 UTC 27 October 1993 is shown in Fig. 16, and the 1200 UTC 27 October 1993 cross section is shown in Fig. 17 at a higher temperature resolution. Both show a critical layer near mountaintop level. This critical layer is also noted on the 1200 UTC 27 October 1993 raob from Desert Rock, Nevada, upstream from the mountains (Fig. 18). Also, notice the sloping of the isentropes in Fig. 17, implying downward motion from the plateau to the coastal areas. The Q-vector divergence for 0000 UTC 27 October 1993 is shown in Fig. 19a. The Q-vector divergence at 1200 UTC 27 October 1993 is shown in Fig. 19b. Examination of other layers revealed a similar pattern. Notice the quasi-geostrophic downward motion over southern California.

b. The Santa Ana event of 24 December 1993

Figure 20a shows the 700 mb heights, vertical velocities, and winds at 0000 UTC 24 December 1993. Winds at mountaintop levels are perpendicular to the barrier and exceed 30 knots. Figure 20b shows the 850 mb heights, vertical velocities, and winds at 0000 UTC 24 December 1993. Figure 21a shows the surface pressure map valid for 0000 UTC 24 December 1993. The surface pressure gradient is sufficient for a windstorm in southern California. Time-height cross sections of winds, vertical velocities, and relative humidity at 34°N/117°W are shown for 0000 UTC 24 December 1993 in Fig. 21b. Notice the downward vertical velocity maximum near 850 mb, similar to the 1200 UTC 27 October 1993 case. The 0000 UTC 24 December 1993 cross section is shown in Fig. 22. Notice the maximum in vertical velocities west of the coastal mountains near 850 mb, with the maximum sloping upward to the east, also similar to the 1200 UTC 27 October 1993 case. A critical layer is noted on the 0000 UTC 24 December 1993 raob from Desert Rock, Nevada, upstream from the mountains (Fig. 23). The winds and potential temperature cross section valid 0000 UTC 24 December 1993 is shown in Fig. 24. To further assist in the evaluation of stability, the winds and potential temperature cross section valid 0000 UTC 24 December 1993 is again shown in Fig. 25, but this time, at a higher temperature resolution. Both show a critical layer near mountaintop level. Also, notice the sloping of the isentropes, implying downward motion from the plateau to the coastal areas. Another important feature is the appearance of three critical levels on the cross section. This may be a strong reason behind the strength of this particular windstorm.

The Q-vector divergence valid 1200 UTC 23 December 1993 and 0000 UTC 24 December 1993 shows downward quasi-geostrophic forcing moving over southern California in Figs. 26 and 27. The winds associated with this case at ONT are shown in Table 2.

c. *The Santa Ana Event of 9 December 1994*

Figure 28a shows the 700 mb heights, vertical velocities, and winds at 0000 UTC 9 December 1994. Winds at mountaintop levels are perpendicular to the barrier, but do not exceed 30 knots. Figure 28b shows the 850 mb heights, vertical velocities, and winds at 0000 UTC 9 December 1994. Figure 29a shows the surface pressure map valid for 0000 UTC 9 December 1994. Note the surface pressure gradient between the plateau and southern California. Time-height cross sections of winds, vertical velocities, and relative humidity at 34°N/117°W is shown for 0000 UTC 9 December 1994 in Fig. 29b. Notice the downward vertical velocity maximum is near 850 mb, similar to the 1200 UTC 27 October 1993 case and 0000 UTC 24 December 1993 case. The 0000 UTC 9 December 1994 cross section is shown in Fig. 30. Notice the maximum in vertical velocities west of the coastal mountains near 850 mb, with the maximum sloping upward to the east, also similar to the 1200 UTC 27 October 1993 and 0000 UTC 24 December 1993 cases. In Fig. 31, a critical layer is noted on the 0000 UTC 9 December 1993 raob from Desert Rock (DRA), Nevada. The winds and potential temperature cross section valid 0000 UTC 9 December 1994 is shown in Fig. 32. To further assist in the evaluation of stability, the winds and potential temperature cross section valid 0000 UTC 9 December 1994 is again shown in Fig. 33, but this time at a higher temperature resolution. Both show a critical layer near mountaintop level. Also, notice the sloping of the isentropes, implying downward motion from the plateau to the coastal areas. In Figs. 34 and 35, the Q-vector divergence valid 1200 UTC 8 December 1994 and 0000 UTC 9 December 1994 shows downward quasi-geostrophic forcing moving over southern California. The winds at ONT associated with this case are shown in Table 3.

d. *The Santa Ana Event of 2 November 1993 (The Malibu Fire)*

Figure 36a shows the 700 mb heights, vertical velocities, and winds at 1200 UTC 2 November 1993. Winds at mountaintop levels are perpendicular to the barrier at approximately 20 to 25 knots. Figure 36b shows the 850 mb heights, vertical velocities, and winds at 1200 UTC 2 November 1993. Figure 37a shows the surface pressure map valid for 1200 UTC 2 November 1993. Note the surface pressure gradient between the plateau and southern California. Time-height cross sections of winds, vertical velocities, and relative humidity at 34°N/117°W are shown for 1200 UTC 2 November 1993 in Fig. 37b. The 1200 UTC 2 November 1993 cross section is shown in Fig. 38. Notice the maximum in vertical velocities is near 700 mb, somewhat higher than that seen in previous cases. There is also no slope. The 1200 UTC 2 November 1993 raob from Desert Rock, Nevada, upstream from the mountains, shows the airmass becoming more stable between about 800 mb and 600 mb in Fig. 39. The winds and potential temperature cross section valid 1200 UTC 2 November 1993 is shown in Fig. 40. To assist in the evaluation of stability, the winds and potential temperature cross section valid 1200 UTC 2 November 1993 is again shown in Fig. 41 at a higher temperature resolution. Both show a weak critical layer near mountaintop level. Also, notice the sloping of the isentropes, implying downward motion from the plateau to the coastal areas. The 700 mb Q-vector divergence for 1200 UTC 2 November 1993 shows downward quasi-geostrophic forcing over southern California in Fig. 42. The winds associated with this case at ONT are shown in Table 4.

e. The "wet" Santa Ana of 14-15 November 1993

Figures 43a and 43b show the synoptic condition at 1200 UTC 13 November 1993 that led to the "wet" Santa Ana event during the mornings of 14-15 November 1993. The Santa Ana system gave an 87 percent chance of a Santa Ana wind for the period between 0600 UTC 14 November 1993 and 0600 UTC 15 November 1993.

Figures 44a through 45b show the typical synoptic conditions associated with a wet Santa Ana. The 0000 UTC 15 November 1993 NGM 500 mb analysis showed a 500 mb low moving southwest from a position over southern Nevada to a position near the California/Mexican border (Fig. 44a). The 0000 UTC 15 November 1993 NGM 700 mb analysis showed a strong height gradient over the southern California coast, in addition to a 3 degree temperature gradient between VBG and DRA (Fig. 44b), down from 10 degrees 12 hours earlier. The 0000 UTC 15 November 1993 NGM 700 mb analysis and 0000 UTC 15 November 1993 NGM 850 mb analysis showed a 16 meter difference in 850-700 mb thickness between VBG and DRA (Figs. 44b and 45a). The 0000 UTC 15 November 1993 surface analysis showed an offshore (-8.8) mb surface pressure gradient from LAX to TPH that would increase to -12.1 mb over the next three hours (Fig. 45b). Lastly, thunderstorms associated with the surface cold front swept past the LAX area at about 1400 UTC with falling dewpoints and increasing winds, heralding its passage at LAX and the other nearby airports. Surface pressure at SFO at 0000 UTC 15 November 1993 was over 7 mb higher than at LAX. Maximum winds at ONT were 32 knots at 2000 UTC 14 November and 30 knots with gusts to 40 knots at 0400 UTC 15 November.

To get a more detailed look at this "wet" Santa Ana, PCGRIDS will be employed.

Figure 46a shows the 24-hour forecasted 700 mb heights, vertical velocities, and winds valid at 0000 UTC 15 November 1993. Figure 46b shows the 700 mb heights, vertical velocities, and winds at 0000 UTC 15 November 1993. There is good agreement in the wind speed over the Los Angeles Basin. The position of the low center forecast by the model was almost exact. The winds at mountaintop levels are between 20 and 30 knots and are perpendicular to the barrier. Figure 47a shows the 24-hour forecasted 850 mb heights, vertical velocities, and winds valid at 0000 UTC 15 November 1993. Figure 47b shows the 850 mb heights, vertical velocities, and winds at 0000 UTC 15 November 1993. Although the low was forecast a bit far east, the wind speeds and vertical velocities are forecast well over the Los Angeles Basin. Figure 48a shows the 24-hour forecasted surface pressure map valid for 0000 UTC 15 November 1993, and Fig. 48b shows the surface pressure map valid 0000 UTC 15 November 1993. Both show the surface trough over the California coast, with high pressure over the plateau. Note the surface pressure gradient between southern California and northern California, as well as between southern California and the plateau. Time-height cross sections of winds, vertical velocities, and relative humidity at 34°N/117°W are shown for 0000 UTC 14 November 1993 and 0000 UTC 15 November 1993 in Figs. 49a and 49b, respectively. Notice that the downward vertical velocity maximum is higher (around 500 mb) in comparison to the other cases. The 24-hour forecasted winds and vertical velocities cross section valid 0000 UTC 15 November 1993 are shown in Fig. 50. The 0000 UTC 15 November 1993 cross section is shown in Fig. 51. Similar to the 1200 UTC 27 October 1993 and 0000 UTC 24 December

1993 cases, the maximum vertical velocity is west of the mountains, but centered higher. The maximum slopes upward to the east in both the forecast and the analysis. The 24-hour forecasted winds and potential temperature cross section valid 0000 UTC 15 November 1993 is shown in Fig. 52. The 0000 UTC 15 November 1993 cross section is shown in Fig. 53. To assist in the evaluation of stability, the 24-hour forecasted winds and potential temperature cross section valid 0000 UTC 15 November 1993 is shown in Fig. 54, and the 0000 UTC 15 November 1993 cross section is shown in Fig. 55, but this time, at a higher temperature resolution. Both the analysis and forecasted cross sections show a critical layer near mountaintop levels. This critical layer is also noted on the 0000 UTC 15 November 1993 raob from Desert Rock, Nevada, upstream from the mountains (Fig. 56). Also, notice the sloping of the isentropes on the cross sections, implying downward motion from the plateau to the coastal areas. The winds associated with this case at ONT are shown in Table 5. The Q-vector divergence at 0000 UTC 15 November 1993 is shown in Fig. 57. Notice the quasi-geostrophic downward motion over southern California.

f. Forecasting the Santa Ana Wind

Based on the conceptual models discussed in section II, the forecaster should look for wind directions roughly within 30 degrees of perpendicular to the ridgeline with wind speed at mountaintop levels exceeding a terrain dependent 15 to 30 knots. This condition was satisfied by all cases evaluated.

Also based on the conceptual models, an upstream temperature profile, with an inversion or layer of strong stability near the mountaintop level, is desirable (Durran 1990). The raobs from all cases discussed showed an increase in stability, and sometimes an inversion, near mountaintop level. This is also seen in the cross sections via the packing of the isentropes.

These features are in addition to the surface pressure gradient, height gradient aloft, and thermal gradient aloft discussed in section III-b.

There were other features that were common among the cases. First, cases a and b showed a maximum in downward vertical velocity west of the mountains near 850 mb, with a slope to the northeast. The winds at ONT were strongest in these two cases. It appears that PCGRIDS did pick up on the conditions necessary for vertically propagating waves, as this profile was well forecast by PCGRIDS on 27 October 1993. Case c showed the maximum in the downward vertical velocity sloping as well, but the maximum was further northeast than in cases a and b. Case d showed the maximum in downward vertical velocity further east and higher in the troposphere. Notice also that the increase in stability at mountaintop level was not nearly as prominent as in the cases where the maximum in vertical velocity was sloping. In case e, the "wet" case, there was some detectable slope in the maximum in vertical velocity, but not as prominent as in cases a, b, and c. Similar to case d, the increase in stability at mountaintop level was not as prominent as in cases a, b, and c.

Throughout this discussion, we have seen that there is rather strong subsidence over much of southern California during Santa Ana episodes. This can be partially explained via lee wave theory west of the mountains. To explain the downward vertical velocities over the remainder of southern California, we can use Q-vector divergence. From the figures, it can be seen that there is downward quasi-geostrophic forcing over much of the area

during a Santa Ana. It is possible that the mesoscale lee subsidence associated with the mountain wave can "phase" with the synoptic scale subsidence indicated by Q-vector divergence. Therefore, the quasi-geostrophic forcing phased with the downslope flow of the lee wave may result in the strong winds associated with Santa Ana conditions.

V. COMPARISONS TO THE FALL 1980 PANORAMA FIRE

Outside of the summer thunderstorms in the mountains and deserts, very little rain falls in southern California between mid-May and mid-October. This makes the area very vulnerable to wildfires on a yearly basis. If significant rains are delayed until late in the fall, similar to what has happened in 1993, the fire danger can become extreme.

Over the combined 1991-1992 and 1992-1993 rainy seasons, southern California received rainfall in excess of 150 percent of normal. In addition, there was a long period of very dry weather before the fires. This is very similar to the situation that developed before the devastating Panorama Fire of November 1980. The Panorama Fire, pushed by very strong Santa Ana winds below the Cajon Pass, destroyed hundreds of homes as it burned from the Cajon Pass to Banning Pass in San Bernardino County. Rainfall totals for the combined 1978-1979 and 1979-1980 seasons were also in excess of 150 percent of normal. As a result, there was plenty of growth available to fuel wildfires in both instances.

VI. ADDITIONAL PROBLEMS

Another factor that has come into play is the pressure to build housing in and below canyons as the Los Angeles metropolitan area expands. Areas, where wildfires did nothing more than burn excess growth in the past, have now become the sites of major urban fire disasters.

Other problems associated with the Santa Ana wind is forecasting the location and areal coverage of the strongest winds. Occasionally, ONT reports west winds of less than 10 knots. At the same time, Chino Airport (CNO), approximately 5 miles to the south, reports northeast winds 20 to 30 knots. At other times, the winds will oscillate wildly, from northeast at 40 knots to west at 20 knots. This could be the result of return flow or a mountain wave rotor, and can wreak havoc during both fire-fighting and aviation operations.

VII. SUMMARY

The uses of forecasting methodology described here have resulted in some skill in forecasting Santa Ana wind probability, and wind speeds at Fontana, but there is still much work to be done. The forecasting of wind speed maxima in other areas of southern California must be addressed, since the various areas of southern California respond differently to various synoptic and mesoscale conditions. In order to address this issue, the creation of forecast methodology for other areas of southern California based on gridded data will be the topic of continued research. A network of profilers and strategically-placed ASOS units would be very helpful in this regard. After building a database of information on Santa Ana winds and using the above tools, we can improve on both lead time and forecast accuracy for these events.

VIII. ACKNOWLEDGEMENTS

I would like to thank Glen Sampson, of SSD, Western Region Headquarters for his insightful review of this paper, and NWSFO Los Angeles/Oxnard forecaster Edward Wentworth for his invaluable input concerning Santa Ana wind characteristics. I would also like to thank NWSFO Los Angeles/Oxnard forecasters David Gomberg, Greg Martin, Andrew Rorke, and Michael Wofford for their input as well as graphical assistance.

IX. REFERENCES

Durran, D. R., 1990: Mountain Waves and Downslope Winds. *Atmospheric Processes over Complex Terrain.* William Blumen, *Ed., Meteor. Monogr.*, **23**, No. 45, 59-81.

Eliassen, A. and E. Palm, 1960: On the transfer of energy in stationary mountain waves. *Geofys. Publ., 22, 1-23*

Fosberg, M. A., C. A. O'Dell, and M. J. Schroeder, 1966: Some characteristics of the three-dimensional structure of Santa Ana Winds, *U. S. Forest Service Research Paper PSW-30*, Pacific Southwest Forest and Range Experiment Station, Forest Service, U. S. Department of Agriculture, 35 pp.

Harvey, H. C., 1959: *Fontana System*, Local study, Weather Service Office Riverside, California, 2 pp.

Huschke, R. E., ed., 1959: *Glossary of Meteorology*, American Meteorological Society, Boston, 638 pp.

Klemp, J. B. and D. K. Lilly, 1975: The dynamics of induced Downslope winds. *J. Atmos Sci.*, **32**, 320-339.

Sergius, L. A., J. K. Huntoon, 1949: *An Objective Method For Forecasting The Santa Ana*, Local study, Weather Bureau Airport Station, Los Angeles, California (now Weather Service Forecast Office, Oxnard, California), 7 pp.

Ulrickson, B. L., and C. F. Mass, 1990: Numerical Investigation of Mesoscale Circulations over the Los Angeles Basin. Part II: Synoptic Influences and Pollutant Transport. *Mon. Wea. Rev.*, **118**, 2163

Western Region Technical Attachment, No. 90-31, Downslope Windstorms and Mountain Waves.

TABLE 1. Observations taken at ONT starting at 1100 UTC 27 October 1993 and ending at 2000 UTC 27 October 1993.

```
27 ONT SA 1046 200 -SCT 20 77/8/0835G48/995/OCNL BD ALQDS
27 ONT SA 1146 200 -SCT 20 75/8/0742g54/993/BD ALQDS PK WND 0754/42
27 ONT SA 1250 200 -SCT 15 75/7/0420g30/002/BD ALQDS PRESRR
27 ONT SA 1348 200 -SCT 20 72/7/0720g30/003/BD ALQDS
27 ONT SA 1446 200 SCT 20 72/7/0725g30/004/BD ALQDS/K SE
27 ONT SA 1553 200 -SCT 20 73/8/0925g35/005/BD ALQDS
27 ONT SA 1651 200 SCT 20 77/11/0725g35/005/BD ALQDS ACSL W
27 ONT SA 1746 200 SCT 20 77/12/0730g43/005/BD K ALQDS ACSL W
27 ONT SA 1846 200 -SCT 20 79/13/0630g42/001/BD K ALQDS
27 ONT SA 1946 CLR 30 80/14/0535g50/000/BD K ALQDS
```

TABLE 2. Observations taken at ONT starting at 1800 UTC 23 December 1993 and ending at 0700 UTC 24 December 1993.

```
23 ONT SA 1750 200 -BKN 40 63/38/3115/019/ BD BN SE-SW
23 ONT SA 1846 E200 BKN 30 63/38/0735G50/020/ BD E-SE VSBY LWR S
23 ONT SA 1946 E150 BKN 63/38/0635G55/015/ BD S-W VSBY LWR SW
23 ONT SA 2046 150 SCT 20 64/37/0755G65/011/ BD SE-W VSBY LWR W
23 ONT SA 2149 150 SCT 20 64/38/0650G60/012/ BD SE-SW VSBY LWR S
23 ONT SA 2246 150 -SCT 20 64/36/0650G65/012/ BD SE-SW
23 ONT SA 23Z  MISSING
24 ONT SA 0048 CLR 50 62/36/0530G50/018
24 ONT SA 0149 CLR 35 61/33/0535G55/020/ BD S-SW
24 ONT SA 0250 CLR 35 59/33/0640G55/026/PRESRR
24 ONT SA 0346 CLR 50 59/32/0630G45/027
24 ONT SA 0450 CLR 50 60/33/0630G50/027
24 ONT SA 0548 CLR 50 59/32/0740G55/028
24 ONT SA 0646 CLR 35 55/32/1805/037
24 ONT SA 0746 CLR 35 56/33/1506/037
```

TABLE 3. Observations taken at ONT starting at 1000 UTC 8 December 1994 and ending at 0200 UTC 9 December 1993.

---

08 ONT SA 1046 CLR 15 40/36/3605/013
08 ONT SA 1158 CLR 20 40/35/3406/013
08 ONT SA 1255 CLR 40 50/29/0623/016/ WSHFT 44 BD
08 ONT SA 1346 CLR 20 54/17/0426/015
08 ONT SA 1446 CLR 30 51/18/0625G32/019
08 ONT SA 1546 CLR 55 53/16/*0630G40*/020/ BD ALQDS
08 ONT SA 1646 CLR 15 53/14/0725G40/020 BD ALQDS
08 ONT SA 1746 150 SCT 15 55/17/*0330G40*/019/ BD ALQDS
08 ONT SA 1846 250 SCT 10 58/19/*0830G40*/020/ BD ALQDS
08 ONT SA 1946 CLR 40 59/20/0525G35/017/ BD SW
08 ONT SA 2055 CLR 40 60/21/0625G35/017/ BD E-S
08 ONT SA 2146 CLR 30 61/22/0520G35/016/ BD E-SW
08 ONT SA 2246 CLR 20 62/32/0615G25/016/BD S
08 ONT SA 2346 CLR 40 60/21/0610/016
09 ONT SA 0046 CLR 40 57/16/0620/017
09 ONT SA 0148 CLR 40 54/13/0715/017
09 ONT SA 0250 CLR 40 50/8/0608/017

TABLE 4. Observations taken at ONT starting at 0700 UTC 2 November 1993 and ending at 0100 UTC 3 November 1993.

---

02 ONT SA 0647 CLR 30 75/25/0615/001
02 ONT SA 0747 CLR 40 74/28/0520G30/002
02 ONT SA 0848 CLR 40 73/20/0520G30/004
02 ONT SA 1047 CLR 40 73/17/0330G40/002
02 ONT SA 1146 CLR 40 72/17/0730G40/001
02 ONT SA 1246 CLR 40 73/14/*0730G45*/006
02 ONT SA 1346 CLR 50 72/11/0730G40/007/ OCNL BD
02 ONT SA 1446 CLR 50 72/12/0930G40/012/ BD NE-SW
02 ONT SA 1551 CLR 50 74/14/0730/015
02 ONT SA 1659 CLR 55 76/15/0830/013/ BD E-S
02 ONT SA 1749 CLR 55 78/17/0630G40/014/ BD E-S
02 ONT SA 1852 CLR 55 79/17/0630G40/012/ BD E-S
02 ONT SA 1946 CLR 55 81/19/0630G40/012/ BD K E-S
02 ONT SA 2049 CLR 55 81/19/0725G35/011
02 ONT SA 2146 CLR 40 83/21/0425G35/011/ BD K E-SE
02 ONT SA 2246 CLR 30 82/21/0520G30/011/ BD K E-S
02 ONT SA 2346 CLR 30 82/19/0615G25/012/ K E-S
03 ONT SA 0046 CLR 30 79/17/0315/014/ BD K E-SE

TABLE 5. Observations taken at ONT starting at 1200 UTC 14 November 1993 and ending at 0700 UTC 15 November 1993.

14 ONT SA 1146 20 SCT E60 BKN 15 51/49/0000/980
14 ONT SA 1246 20 SCT E60 BKN 15 50/48/0000/977
14 ONT SA 1346 28 SCT E60 BKN 15 50/48/0706/975/***OCNL LTGICCC S***
14 ONT SA 1446 15 SCT E30 BKN 65 BKN 15 53/37/3612/976/ ***CIG RGD RWU SE***
14 ONT SP 1521 15 SCT E30 BKN 65 BKN 15 53/34/0602/976
14 ONT SA 1546 15 SCT E50 BKN 15 54/31/0618/975
14 ONT SP 1559 50 SCT 15 55/36/2608/976
14 ONT SA 1650 50 SCT 80 SCT 25 56/34/2715/975
14 ONT SP 1720 50 SCT 80 SCT 25 59/27/0620/976
14 ONT SA 1750 45 SCT 100 SCT 40 58/27/0630/978
14 ONT SA 1850 45 SCT 90 SCT 40 59/26/0630/978
14 ONT SA 1946 45 SCT 80 SCT 40 62/26/0632/978
14 ONT SA 2056 45 SCT 80 SCT 40 62/25/0425/977
14 ONT SA 2146 50 SCT 150 SCT 50 61/28/0525G35/978
14 ONT SA 2254 50 SCT 100 SCT 30 60/25/0420G30/979
14 ONT SA 2350 70 SCT E150 BKN 30 60/25/0420G30/981
15 ONT SA 0046 70 SCT E110 BKN 30 59/22/0515G25/982
15 ONT SA 0150 70 SCT 100 SCT 30 58/23/3208/983
15 ONT SA 03Z MISSING
15 ONT SA 0347 70 SCT 110 SCT 30 60/27/*0330G40*/985
15 ONT SA 0450 70 SCT 110 SCT 30 56/26/0215/985
15 ONT SA 0546 70 SCT 110 SCT 30 57/25/3510/989
15 ONT SA 0646 110 SCT 25 62/25/0420G28/989

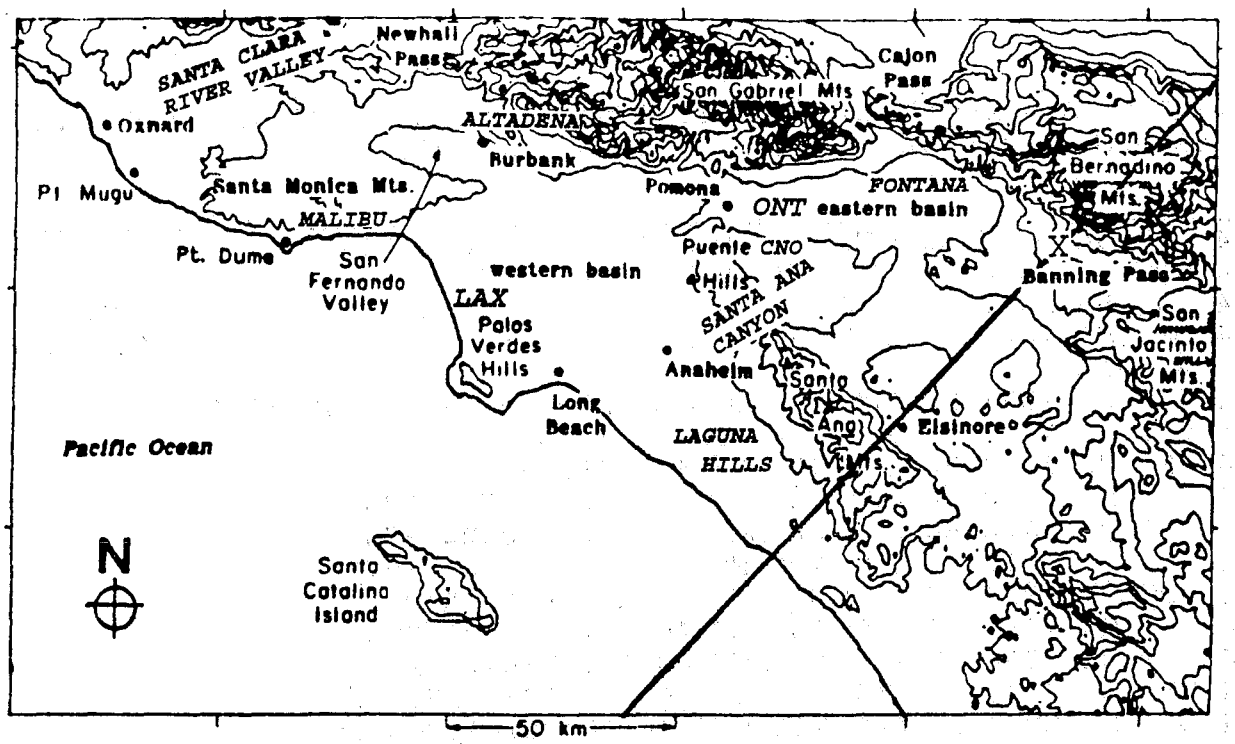

Figure 1. Map of the Los Angeles Basin and surrounding region, redrafted from Ulrickson and Mass, 1990. Terrain contours every 250 meters. Diagonal line indicates approximate position of crossection. The "X" on the crossection indicates the approximate position of the time/height crossection.

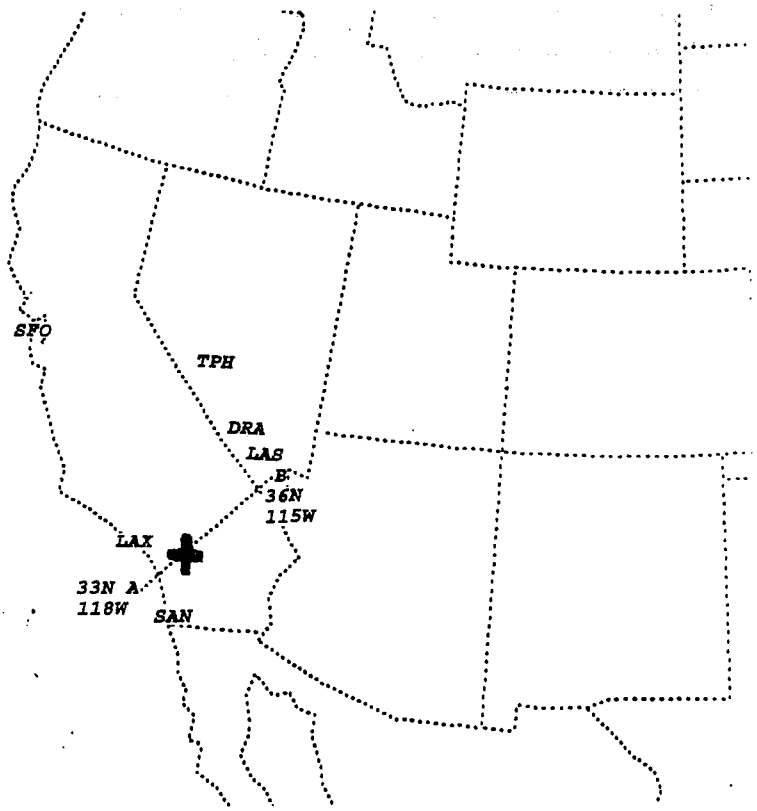

Figure 2. Locations of crossections and station identifiers.

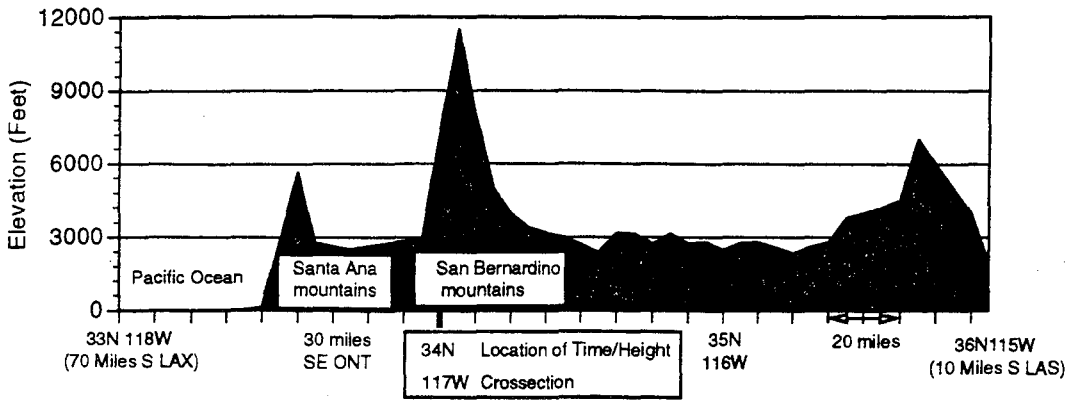

Figure 3. Topography along the crossection from 33N/118W to 36N/115WN.

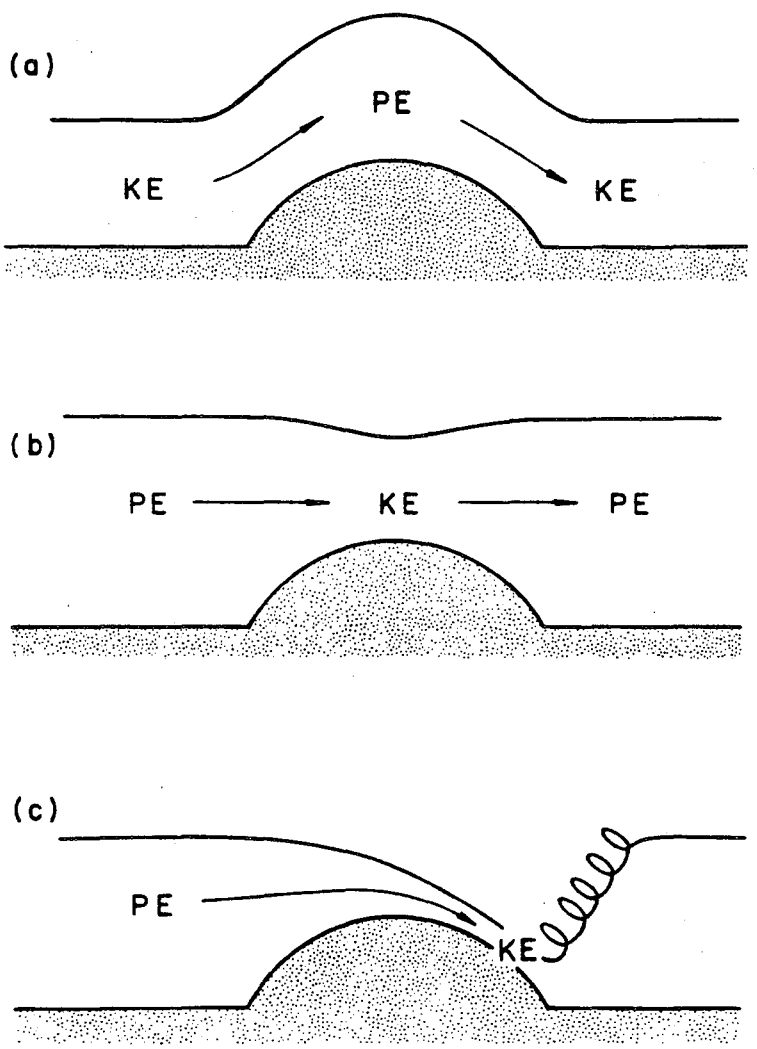

Figure 4. Behavior of shallow water flowing over an obstacle: (a) everywhere supercritical flow, (b) everywhere subcritical flow, (c) hydraulic jump.

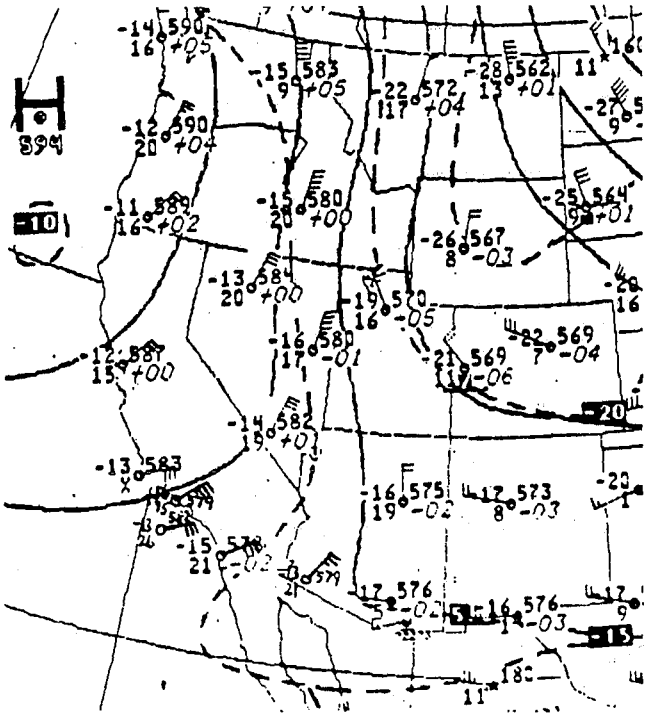

Figure 5a.
1200 UTC 26 October 1993
500mb analysis
heights/temperature

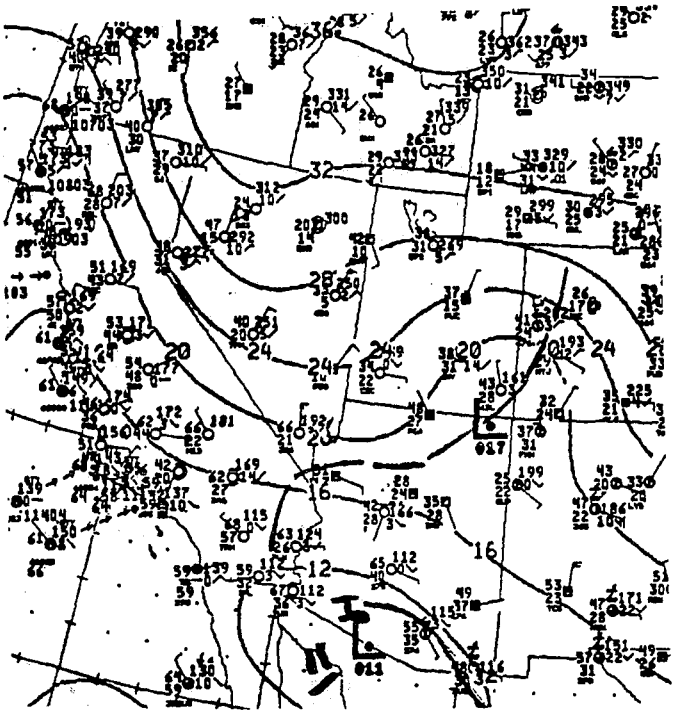

Figure 5b.
1200 UTC 26 October 1993
NMC surface analysis

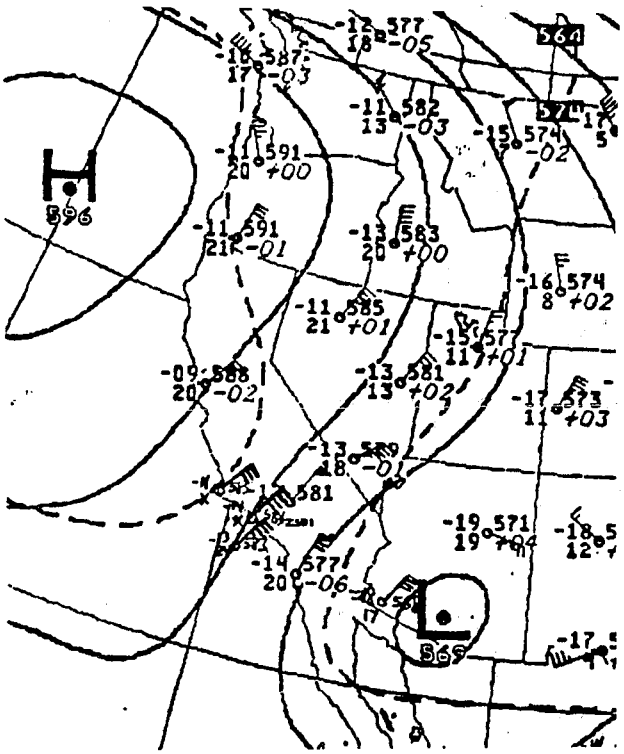

FIGURE 6a.
1200 UTC 27 October 1993
500mb analysis
heights/temperature

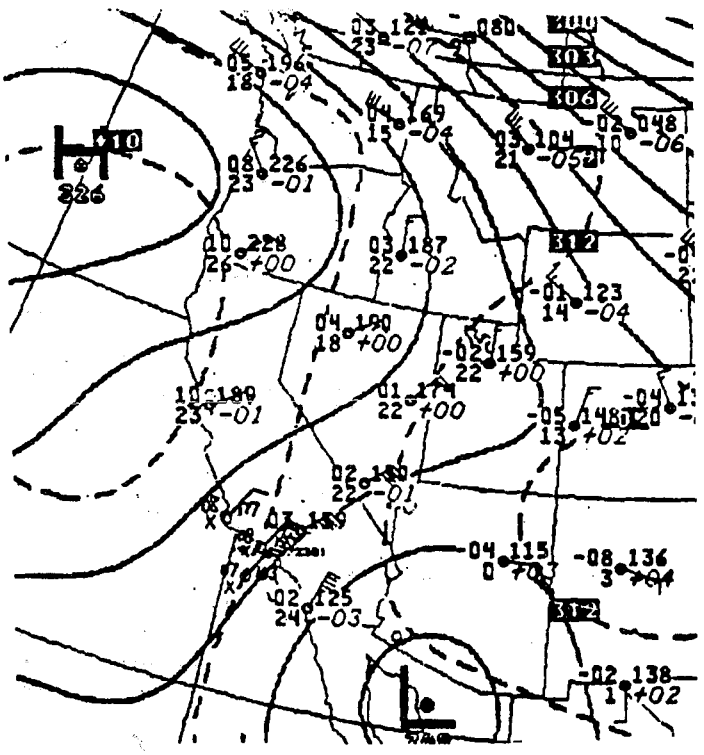

Figure 6b.
1200 UTC 27 October 1993
700mb analysis
heights/temperature

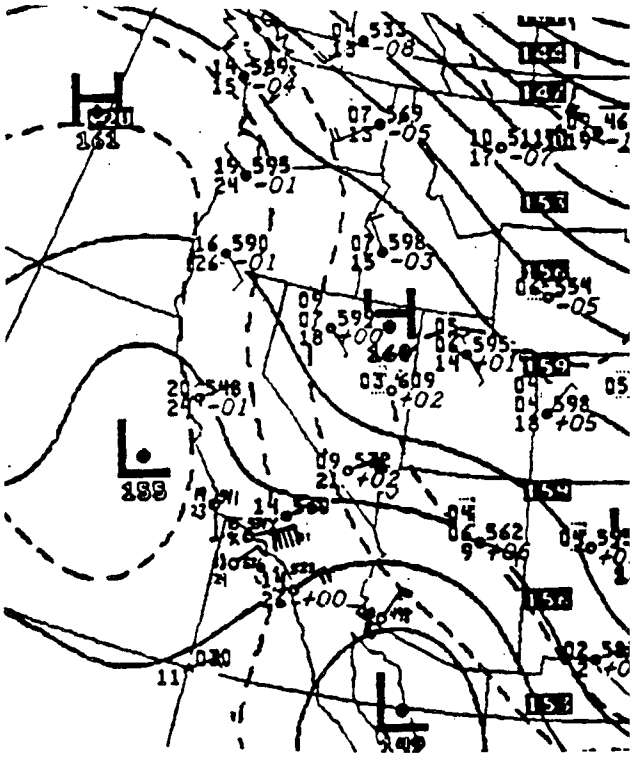

Figure 7a.
1200 UTC 27 October 1993
850mb analysis
heights/temperature

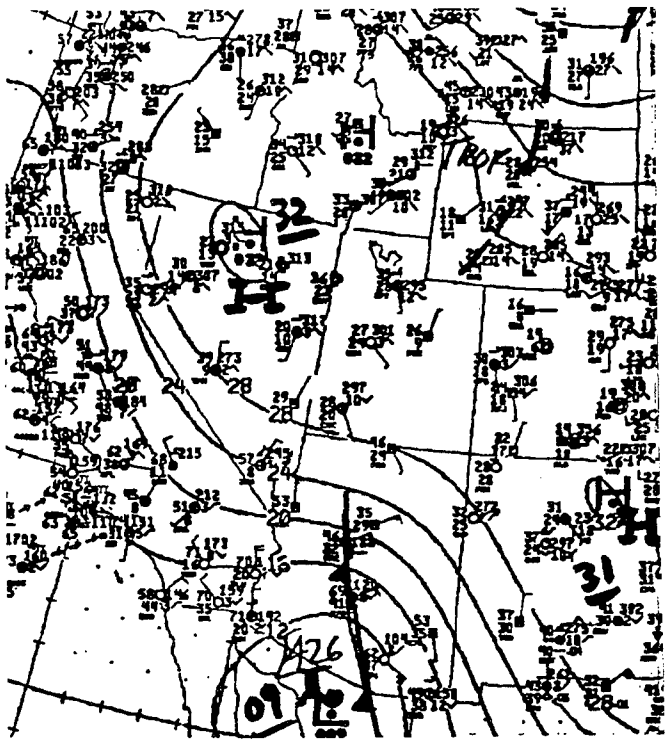

Figure 7b.
1200 UTC 27 October 1993
NMC surface analysis

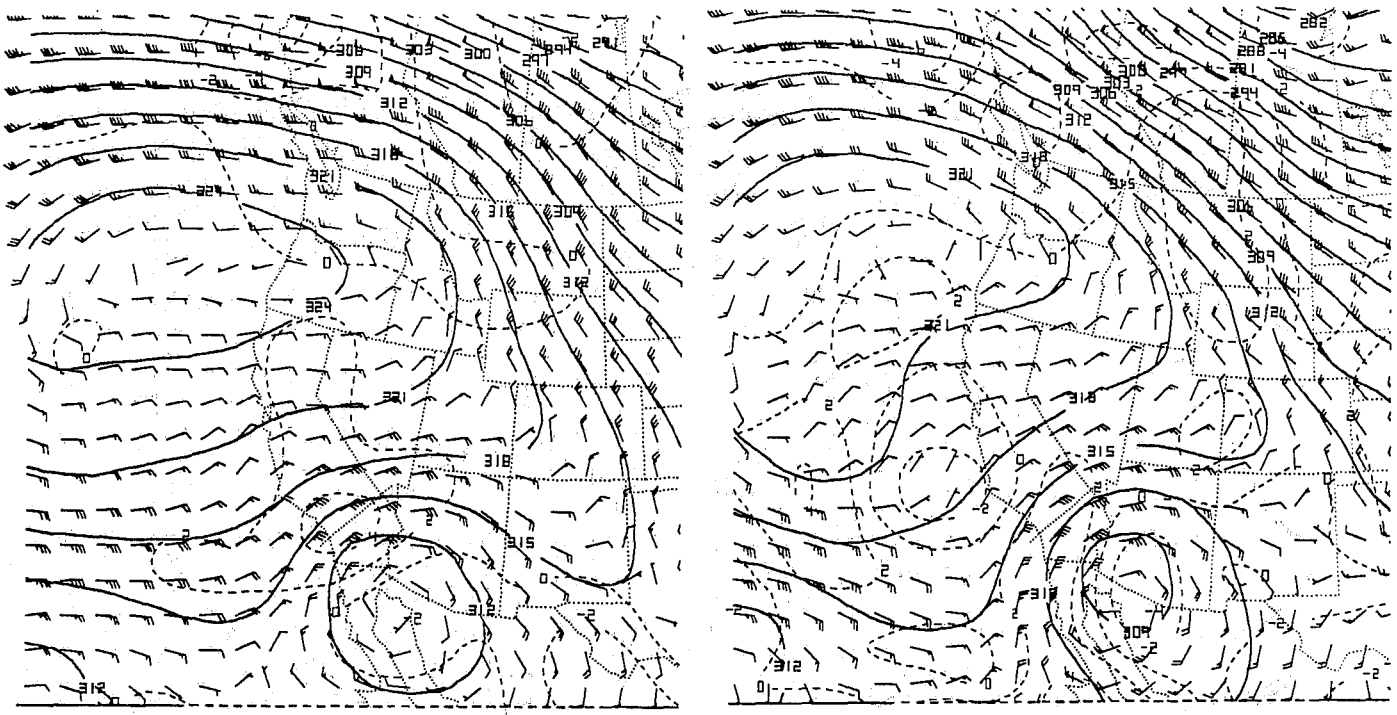

a. b.

Figure 8. (a) ETA 24 hour forecast 700 mb heights (dekameters), vertical velocities (microbars per second), and winds (knots) valid 1200 UTC 27 October 1993. Height contours (solid) every 30 meters and vertical velocity contours (dashed) every 2 microbars per second.
(b) ETA 700 mb heights, vertical velocities,and winds at 1200 UTC 27 October 1993. Same units and contour intervals.

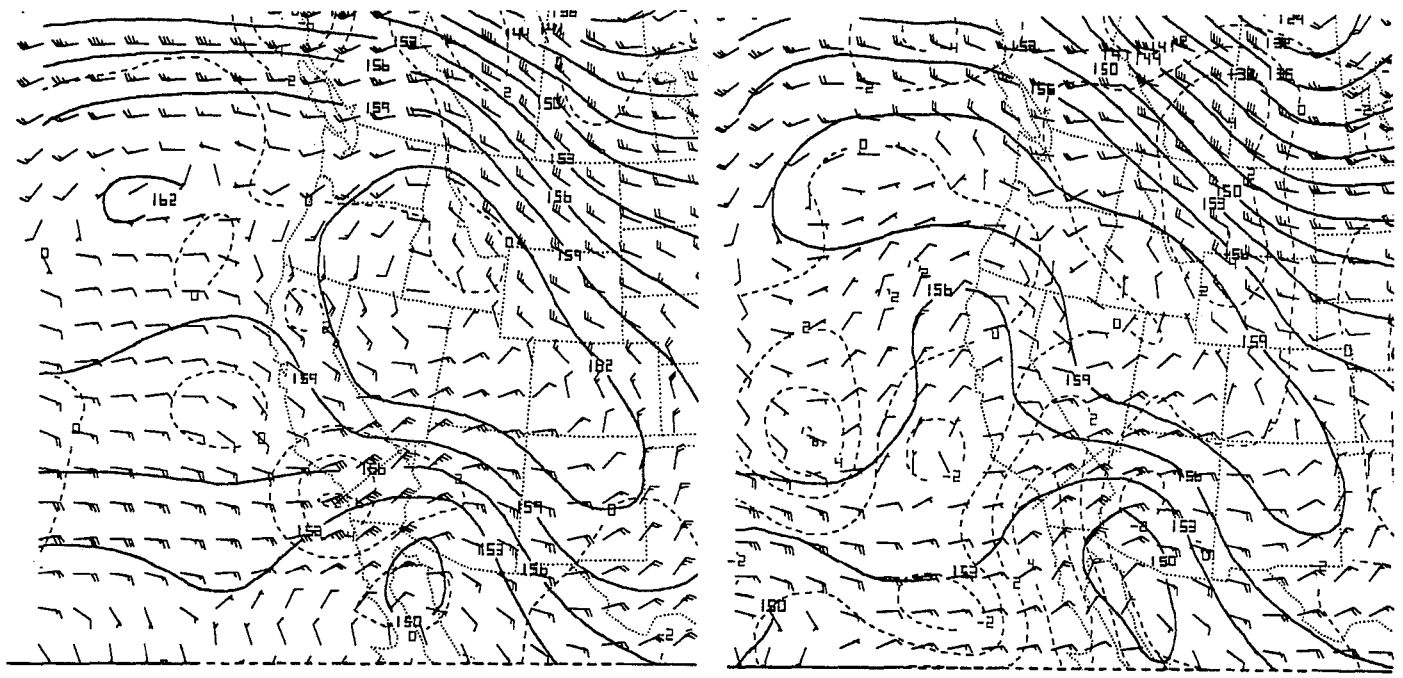

a. b.

Figure 9. (a) ETA 24 hour forecast 850 mb heights (dekameters), vertical velocities (microbars per second), and winds (knots) valid 1200 UTC 27 October 1993. Height contours are every 30 meters and vertical velocity contours are every 2 microbars per second.
(b) ETA 850 mb heights (dekameters), vertical velocities (microbars per second), and winds (knots) at 1200 UTC 27 October 1993. Same units and contour intervals.

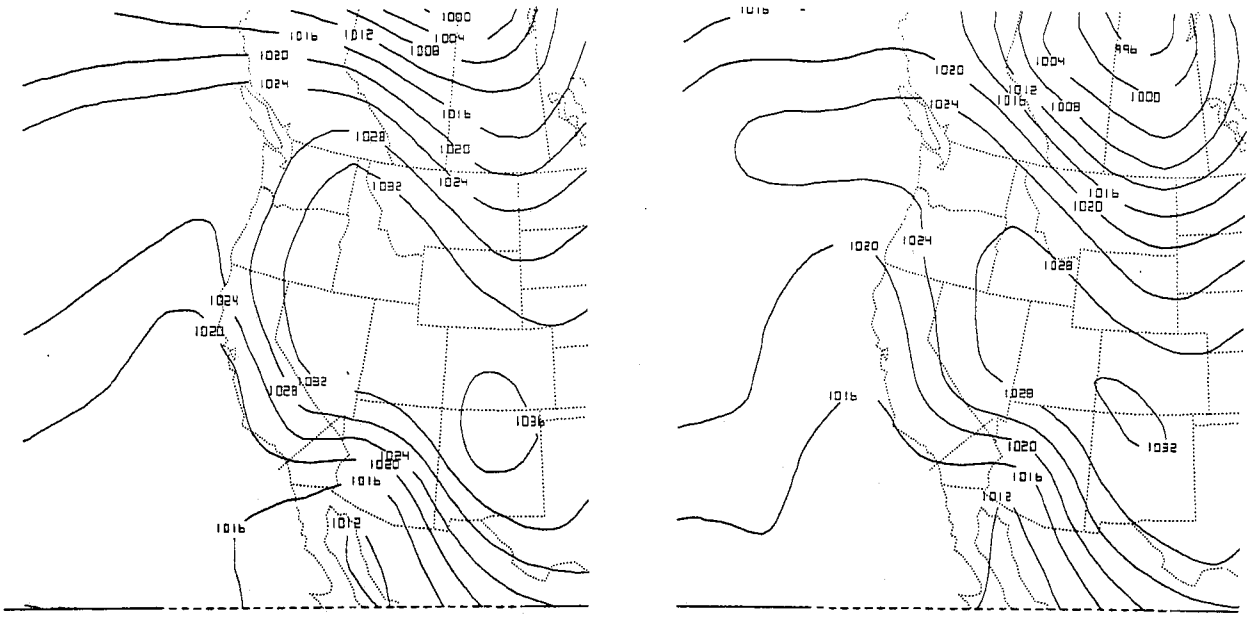

a. b.

Figure 10. (a) ETA 24 hour forecast Mean Sea Level Pressure (millibars) valid 1200 UTC 27 October 1993. Pressure contours every 4 millibars.
(b) ETA Mean Sea Level Pressure (millibars) at 1200 UTC 27 October 1993. Pressure contours every 4 millibars.

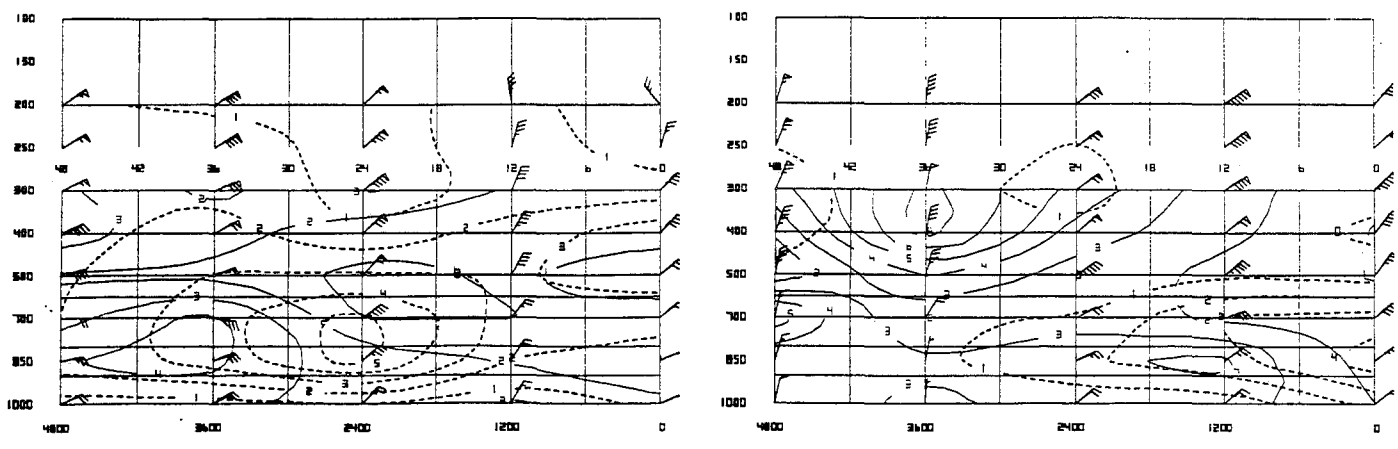

a. b.

Figure 11. (a) ETA Time/Height Crossection of winds (knots), vertical velocity (microbars per second) and relative humidity (percent) at 1200 UTC October 26 1993. Vertical velocity (dashed) every 1 microbar per second, and relative humidity (solid) every 10 percent.
(b) Same, except at 1200 UTC 27 October 1993.

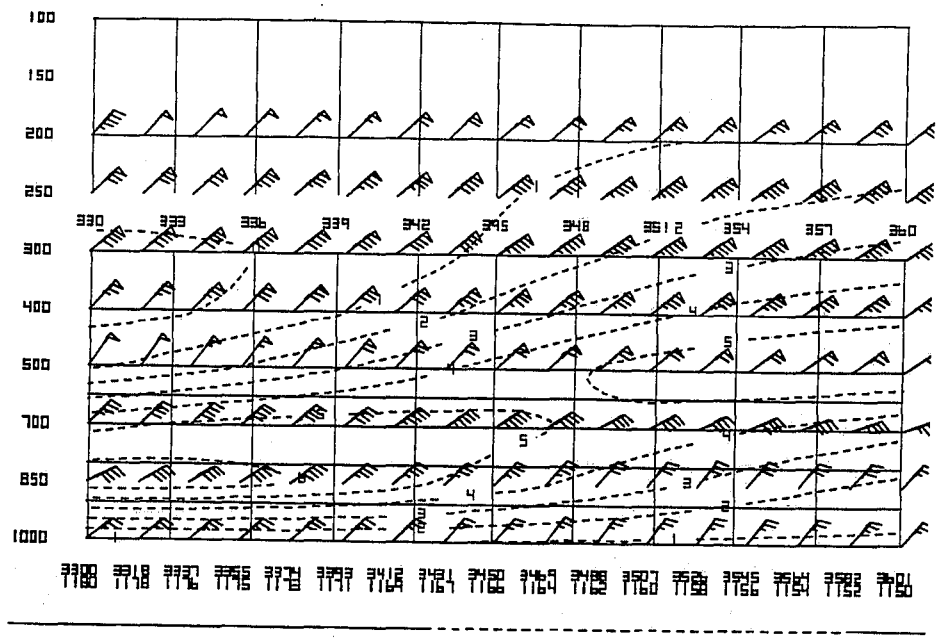

Figure 12. ETA 24 hour forecast crossection of winds (knots) and vertical velocity (microbars per second) valid 1200 UTC 27 October 1993. Vertical velocity (dashed) every 1 microbar per second.

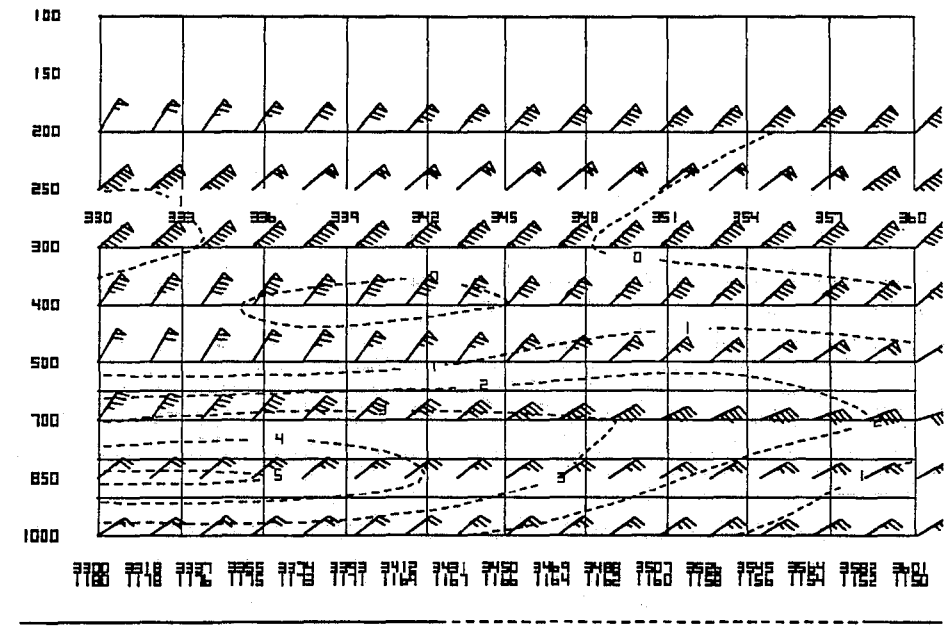

Figure 13. ETA crossection of winds (knots) and vertical velocity (microbars per second) at 1200 UTC 27 October 1993. Vertical velocity (dashed) every 1 microbar per second.

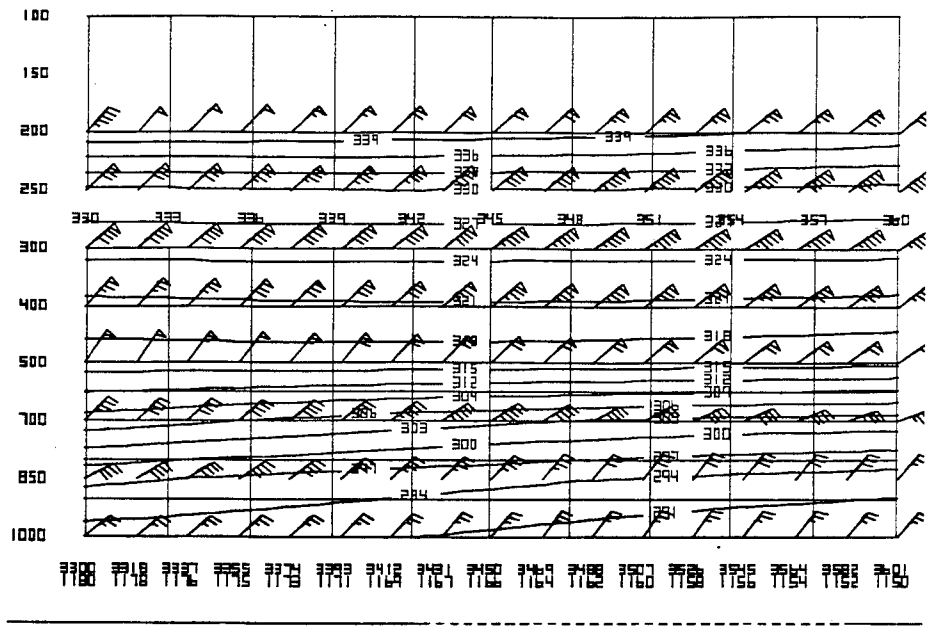

Figure 14. ETA 24 hour forecast crossection of winds (knots) and potential temperature (degrees kelvin) valid 1200 UTC 27 October 1993. Potential temperature contours every 3 degrees kelvin.

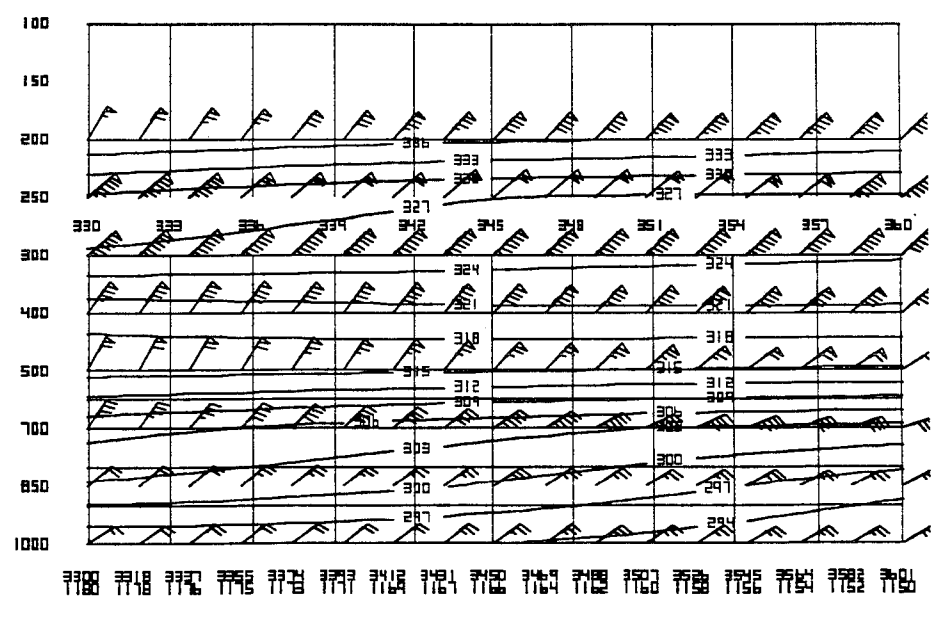

Figure 15. ETA crossection of winds (knots) and potential temperature (degrees kelvin) at 1200 UTC 27 October 1993. Potential temperature contours every 3 degrees kelvin.

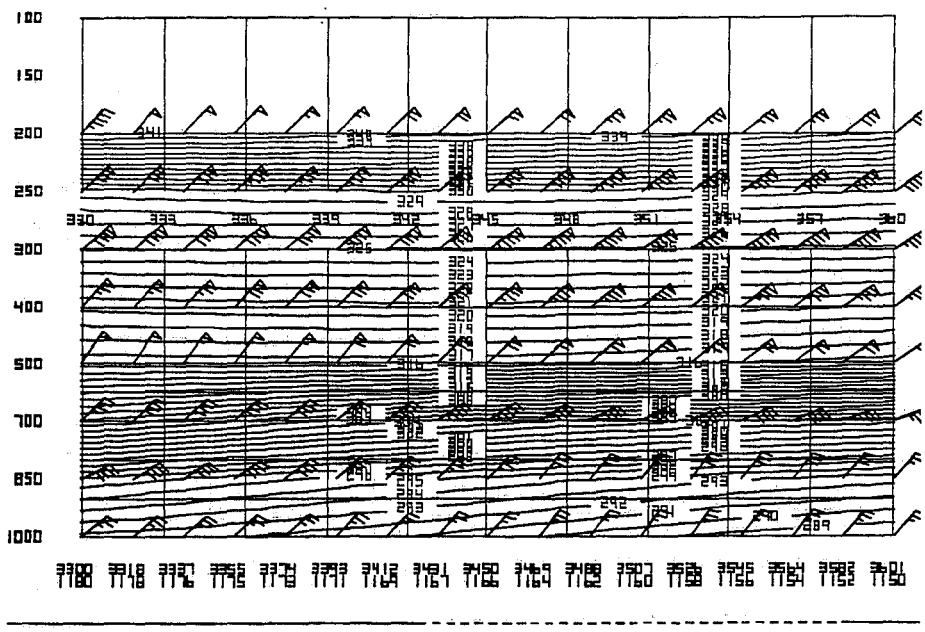

Figure 16. ETA 24 hour forecast crossection of winds (knots) and potential temperature (degrees kelvin) valid 1200 UTC 27 October 1993. Potential temperature contours every 1 degree kelvin.

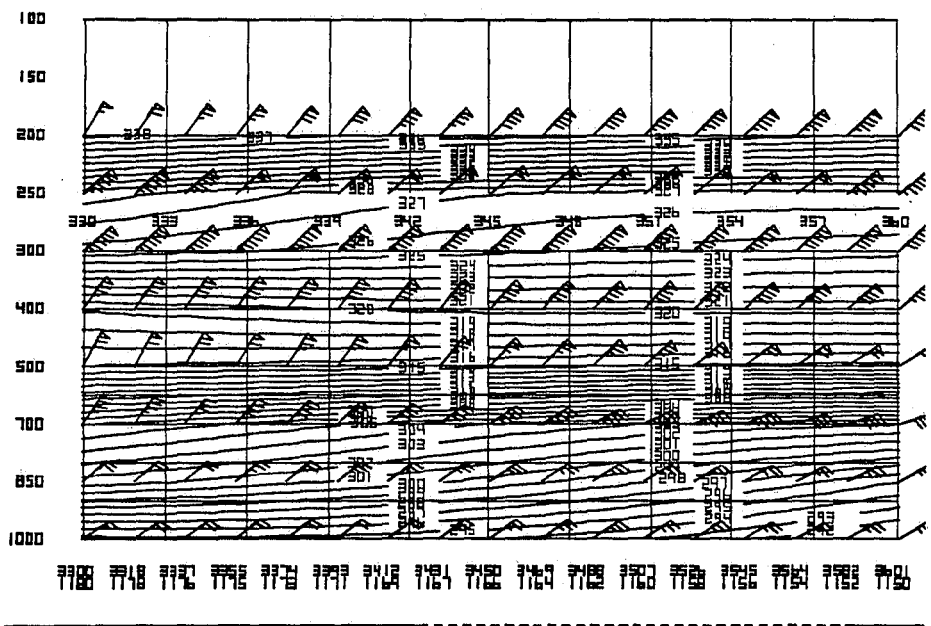

Figure 17. ETA crossection of winds (knots) and potential temperature (degrees kelvin) at 1200 UTC 27 October 1993. Potential temperature contours every 1 degree kelvin.

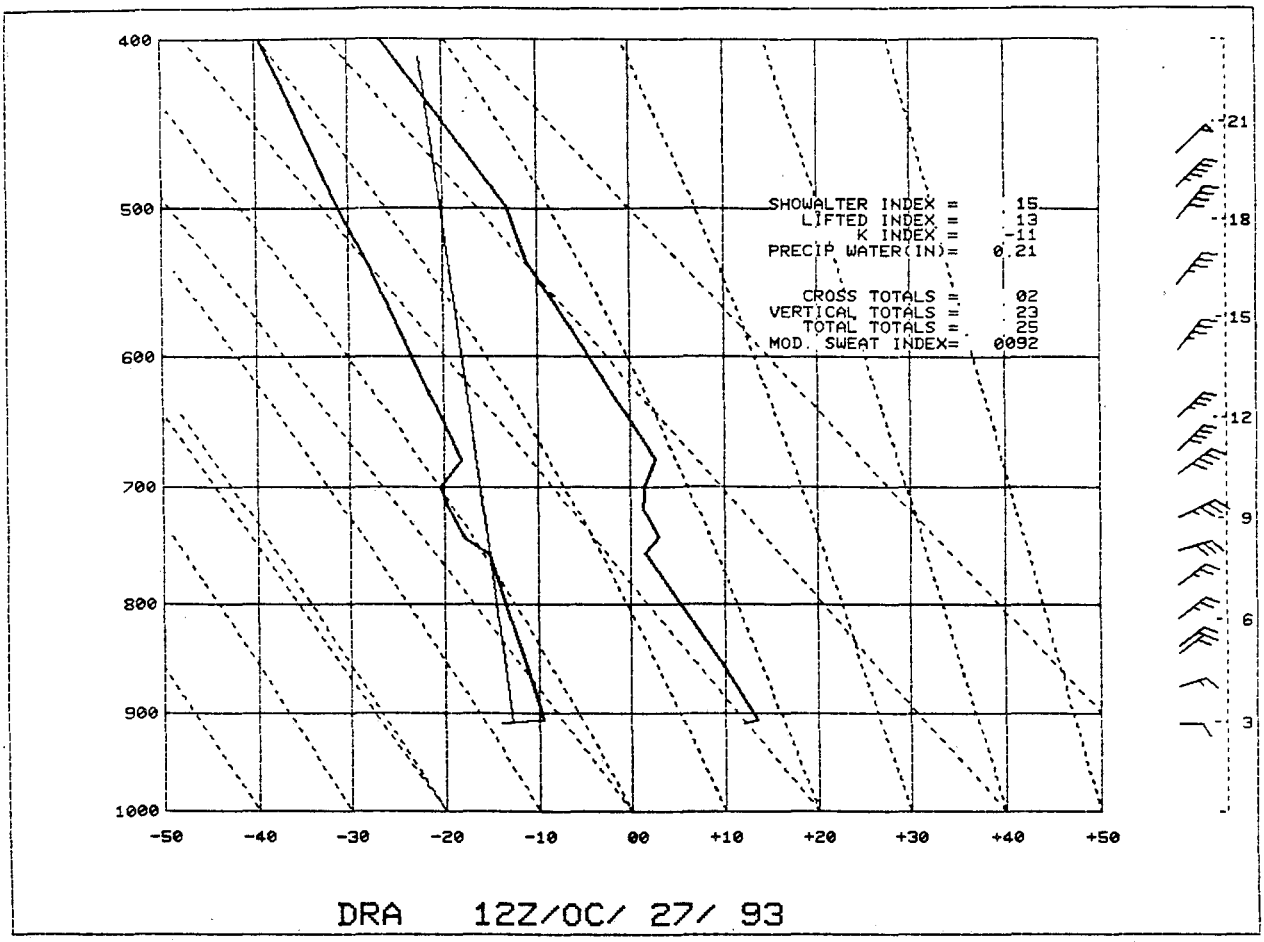

Figure 18. 1200 UTC 27 October 1993 Raob from Desert Rock (DRA) Nevada.

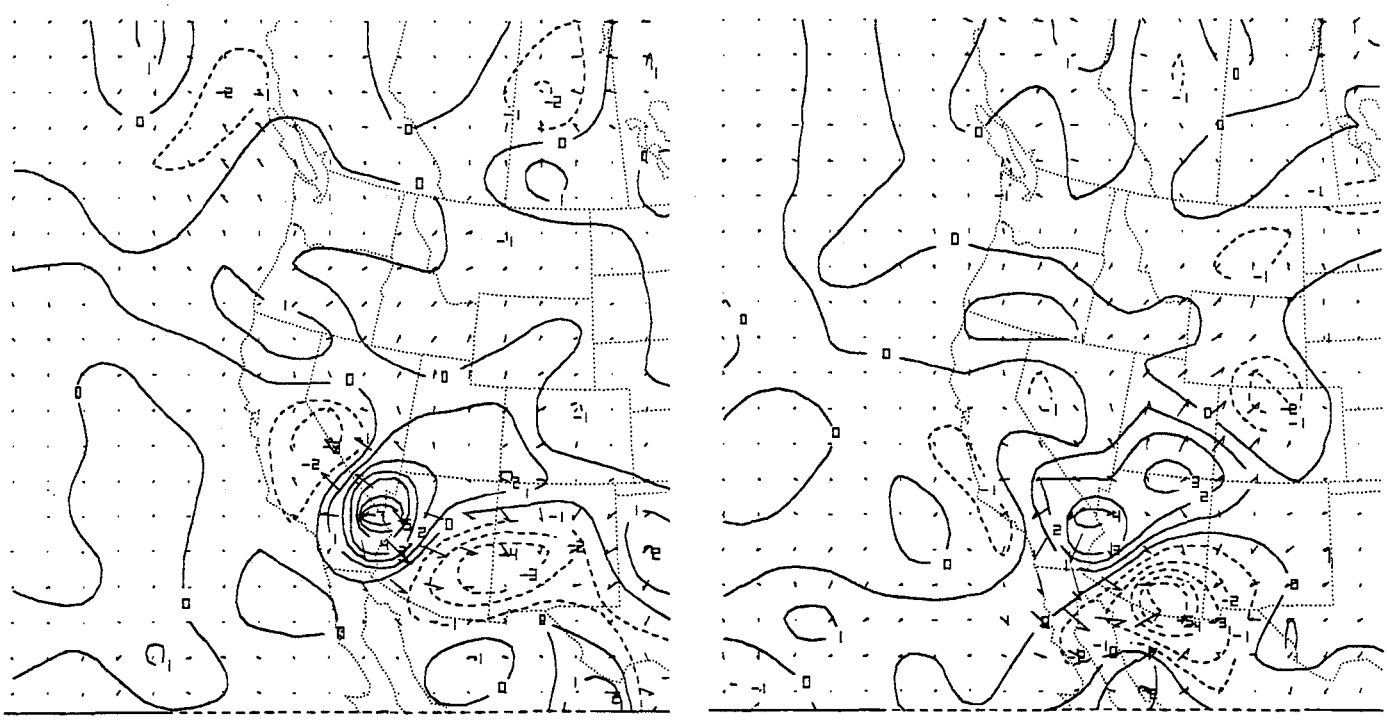

a. b.

Figure 19. (a) 0000 UTC 27 October 1993 700 millibar Q-vector divergence. Contours every $1x10^{-10}$ C m^{-2} s^{-1}.
(b) 1200 UTC 27 October 1993 700 millibar Q-vector divergence. Contours every $1x10^{-10}$ C m^{-2} s^{-1}.

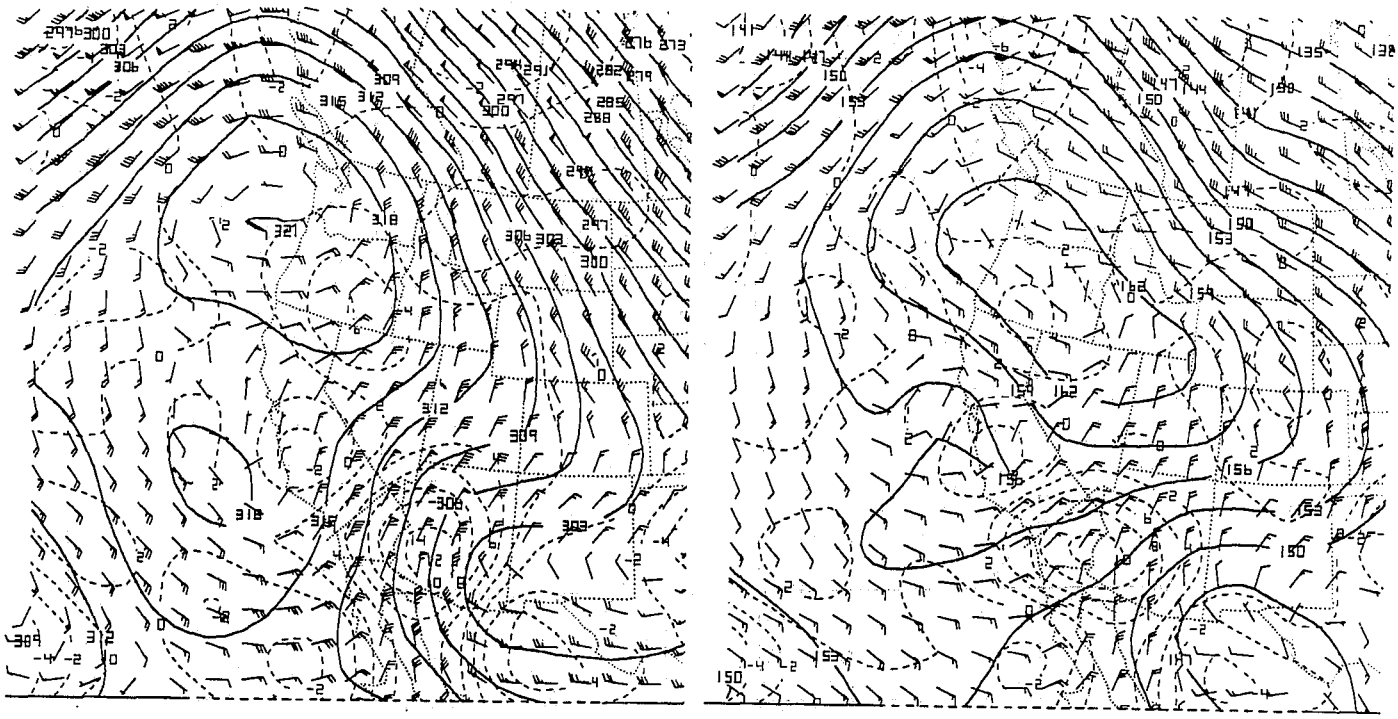

a. b.

Figure 20. (a) ETA 700 mb heights (dekameters), vertical velocities (microbars per second), and winds (knots) valid 0000 UTC 24 December 1993. Height contours (solid) every 30 meters and vertical velocity contours (dashed) every 2 microbars per second. (b) ETA 850 mb heights (dekameters), vertical velocities (microbars per second), and winds (knots) valid 0000 UTC 24 December 1993. Height contours are every 30 meters and vertical velocity contours are every 2 microbars per second.

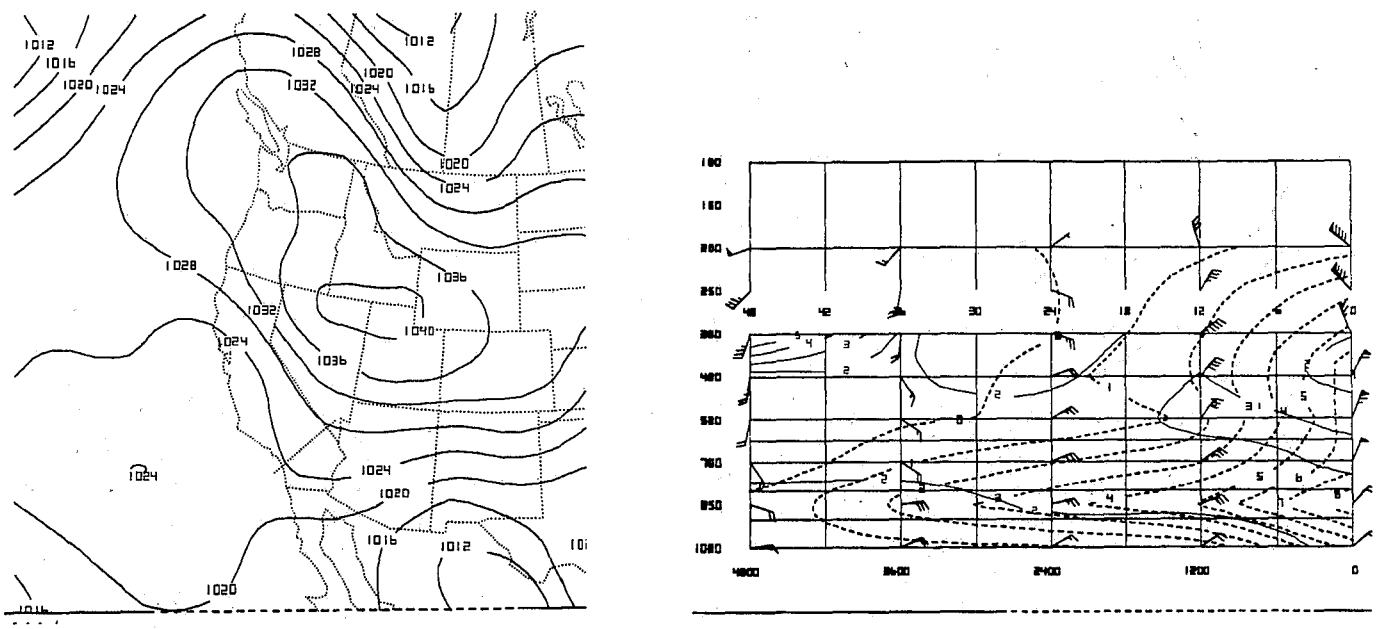

a. b.

Figure 21. (a) ETA Mean Sea Level Pressure (millibars) valid 0000 UTC 24 December 1993. Pressure contours every 4 millibars. (b) ETA Time/Height Crossection of winds (knots), vertical velocity (microbars per second) and relative humidity (percent) at 0000 UTC 24 December 1993. Vertical velocity (dashed) every 1 microbar per second, and relative humidity (solid) every 10 percent.

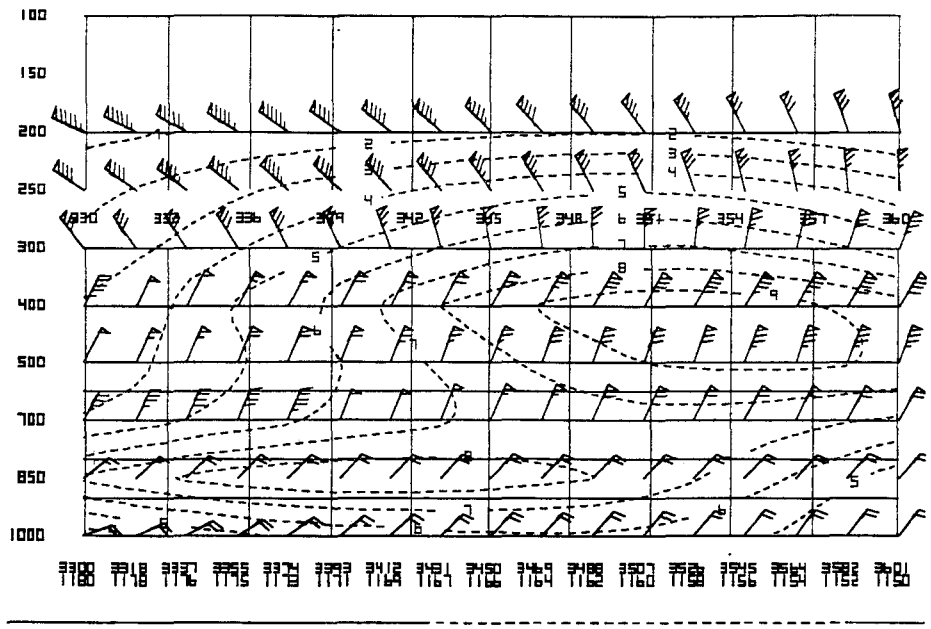

Figure 22. ETA crossection of winds (knots) and vertical velocity (microbars per second) valid 0000 UTC 24 December 1993. Vertical velocity (dashed) every 1 microbar per second.

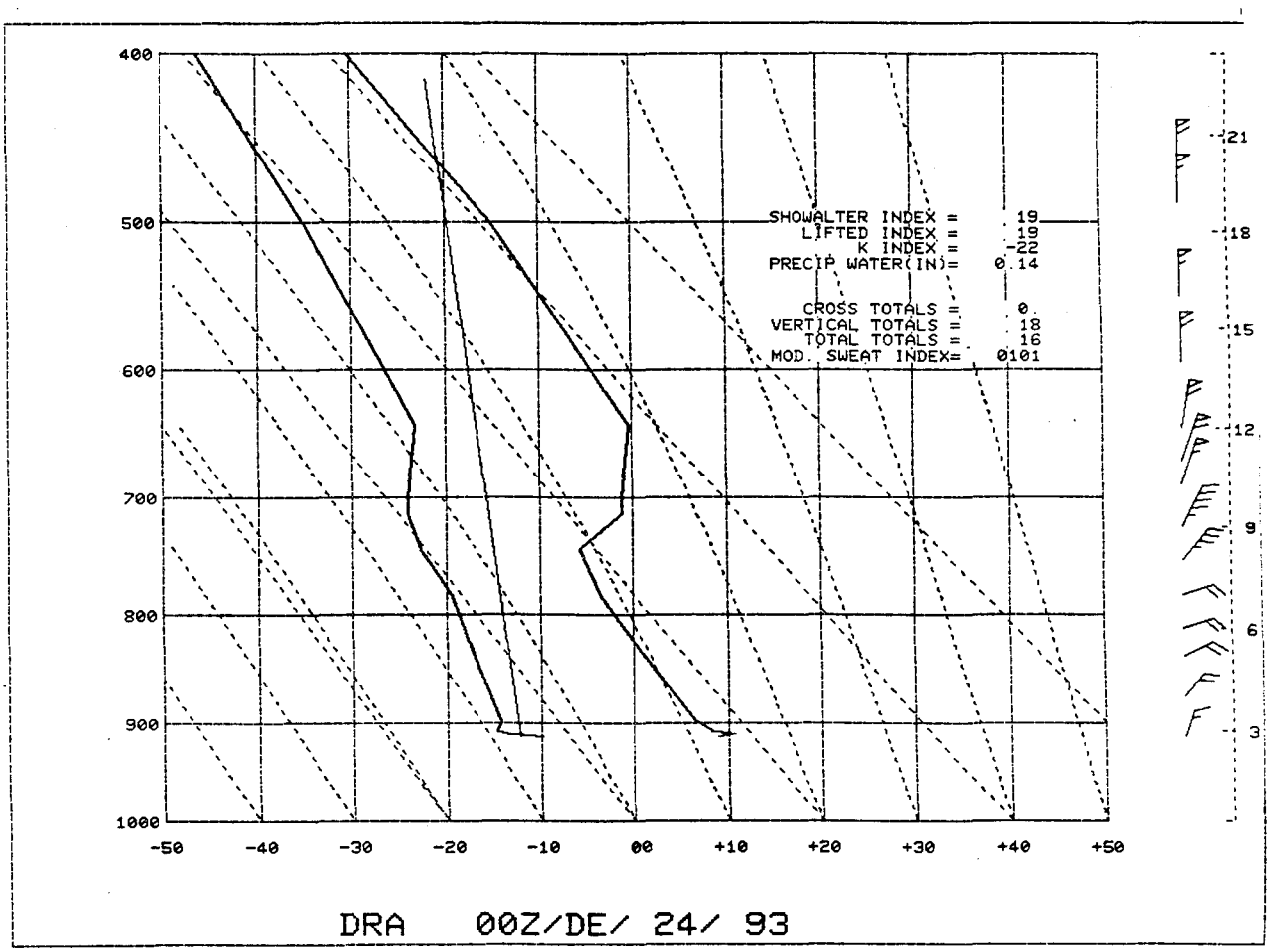

Figure 23. 0000 UTC 24 December 1993 Raob from Desert Rock (DRA) Nevada.

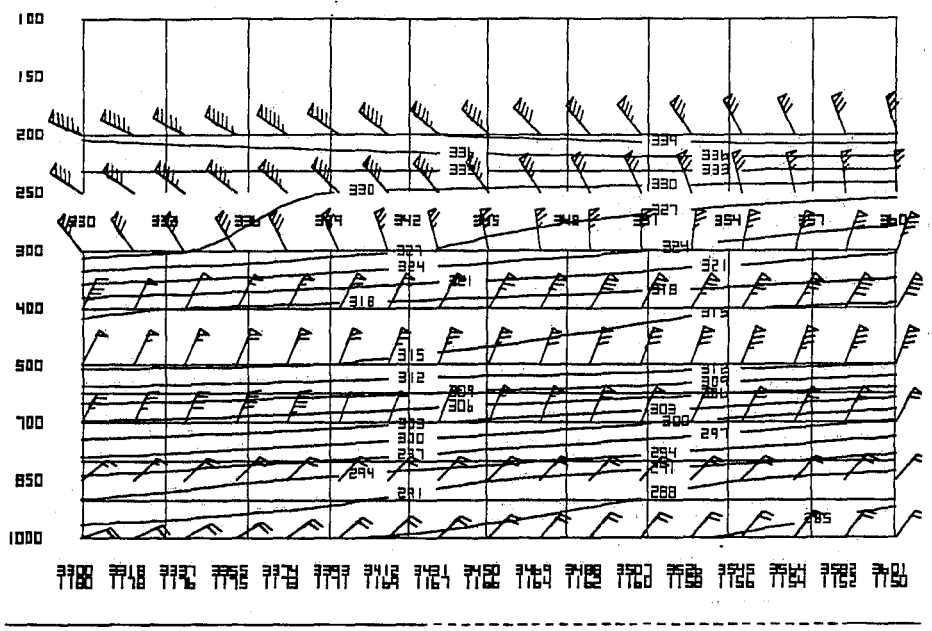

Figure 24. ETA crossection of winds (knots) and potential temperature (degrees kelvin) at 0000 UTC 24 December 1993. Potential temperature contours every 3 degrees kelvin.

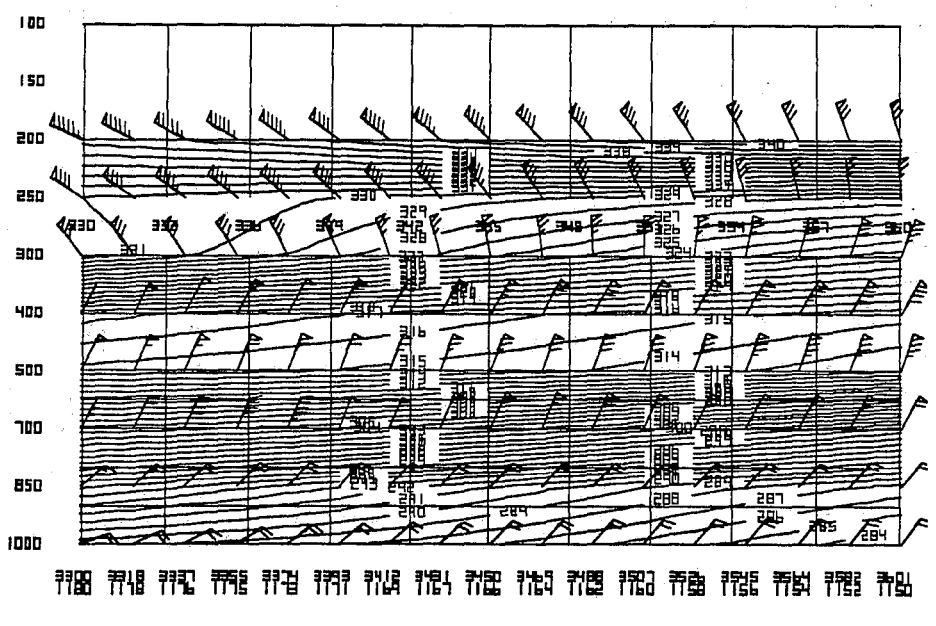

Figure 25. ETA crossection of winds (knots) and potential temperature (degrees kelvin) at 0000 UTC 24 December 1993. Potential temperature contours every 1 degree kelvin.

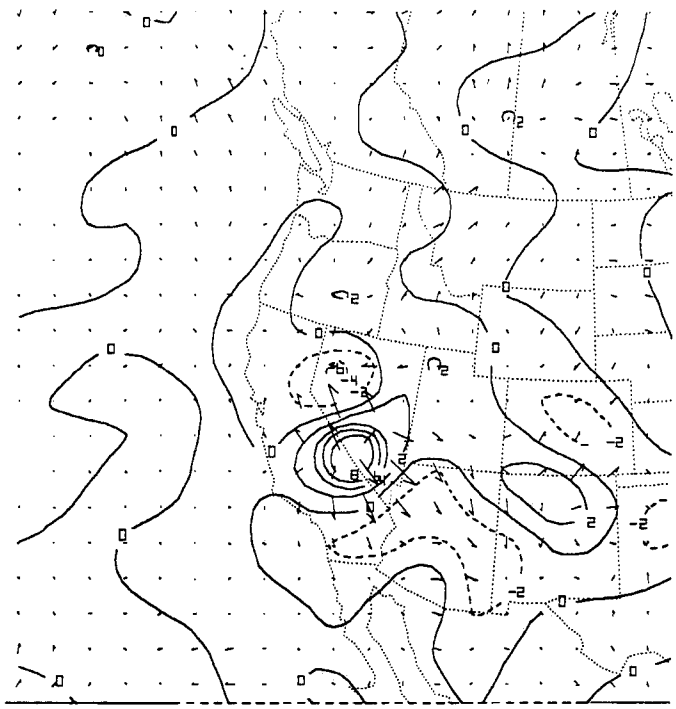

Figure 26. 1200 UTC 23 December 1993 700 millibar Q-vector divergence. Contours every 2×10^{-10} C m^{-2} s^{-1}.

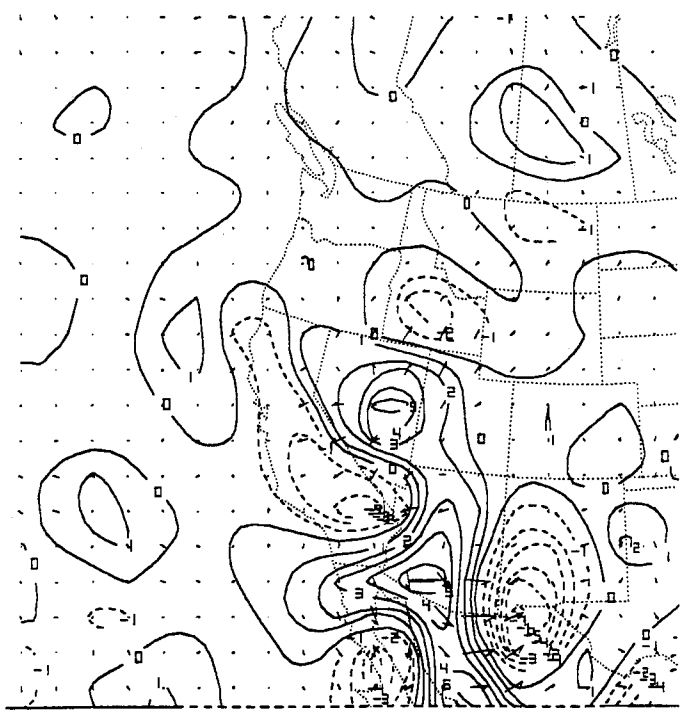

Figure 27. 0000 UTC 24 December 1993 700 millibar Q-vector divergence. Contours every 1×10^{-10} C m^{-2} s^{-1}.

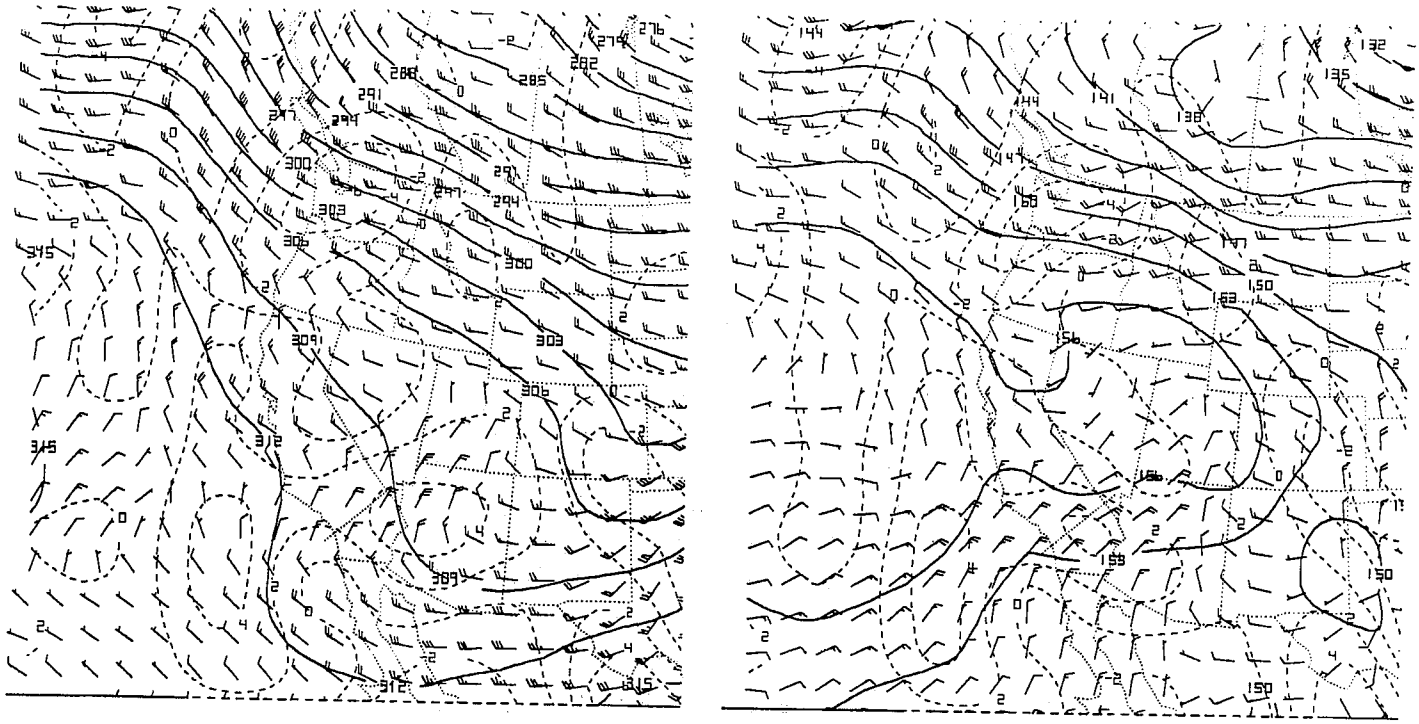

a. b.

Figure 28. (a) ETA 700 mb heights (dekameters), vertical velocities (microbars per second), and winds (knots) valid 0000 UTC 9 December 1994. Height contours (solid) every 30 meters and vertical velocity contours (dashed) every 2 microbars per second. (b) ETA 850 mb heights (dekameters), vertical velocities (microbars per second), and winds (knots) valid 0000 UTC 9 December 1994. Height contours are every 30 meters and vertical velocity contours are every 2 microbars per second.

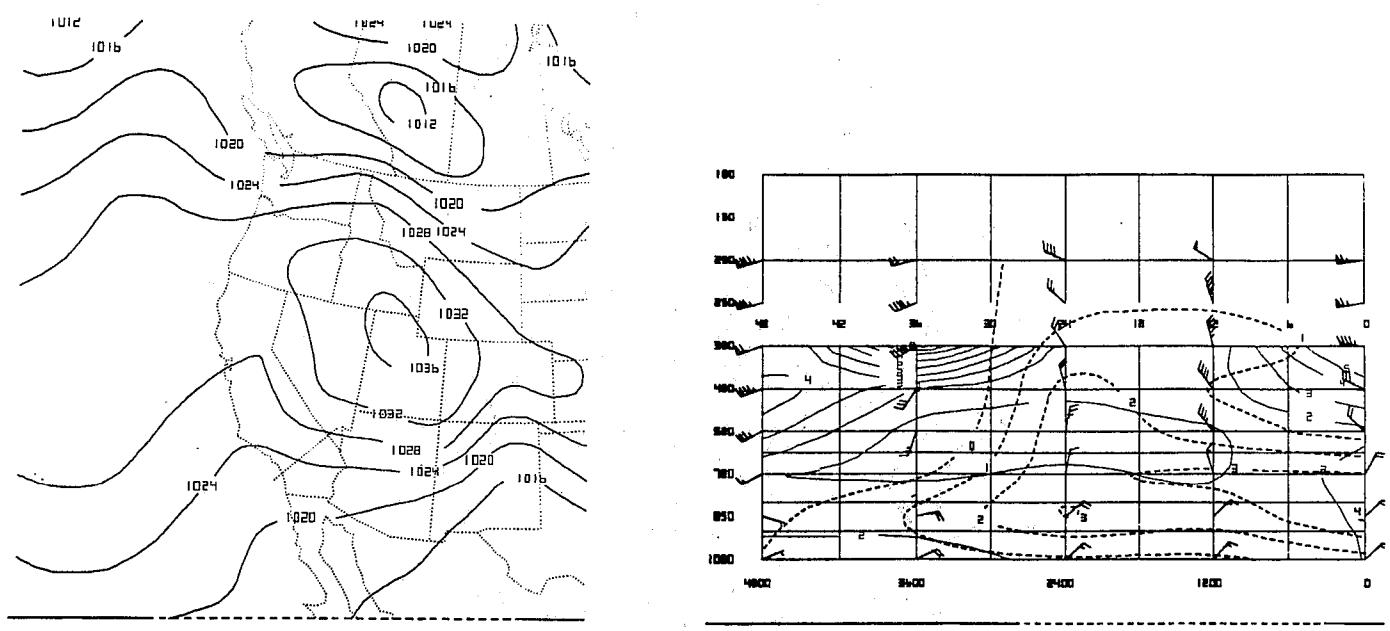

a. b.

Figure 29. (a) ETA Mean Sea Level Pressure (millibars) valid 0000 UTC 9 December 1994. Pressure contours every 4 millibars. (b) ETA Time/Height Crossection of winds (knots), vertical velocity (microbars per second) and relative humidity (percent) at 0000 UTC 9 December 1994. Vertical velocity (dashed) every 1 microbar per second, and relative humidity (solid) every 10 percent.

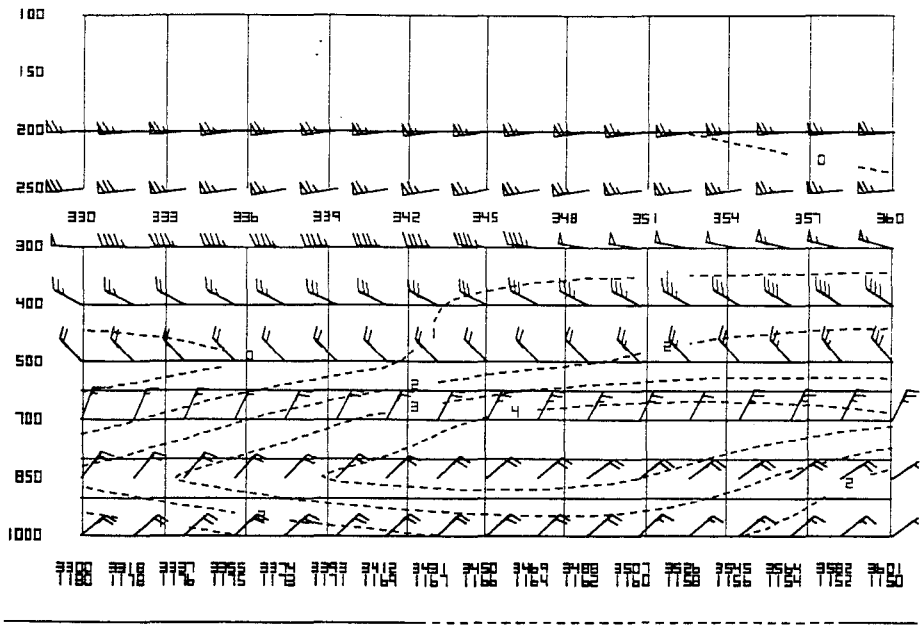

Figure 30. ETA crossection of winds (knots) and vertical velocity (microbars per second) valid 0000 UTC 9 December 1994. Vertical velocity (dashed) every 1 microbar per second.

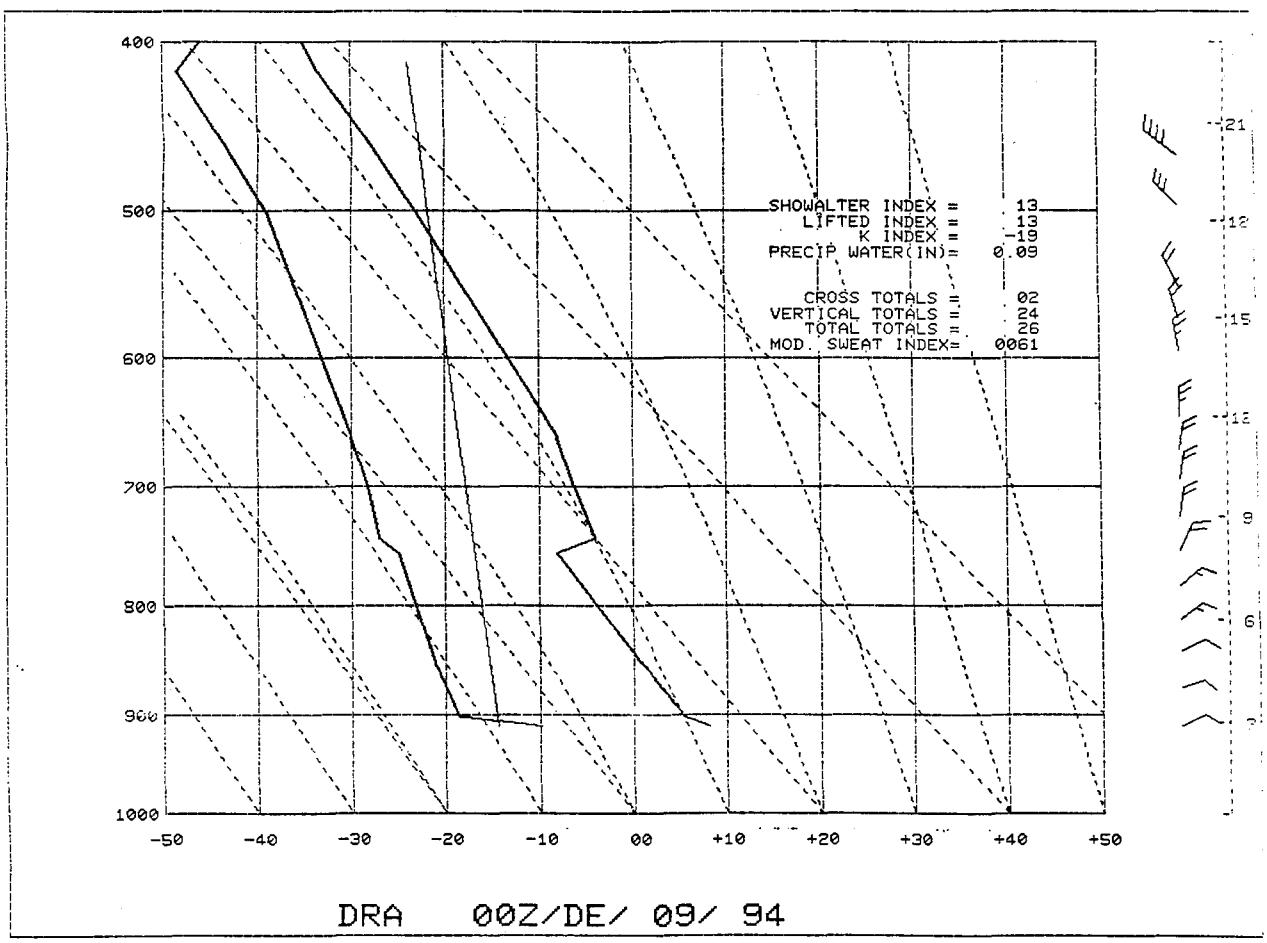

Figure 31. 0000 UTC 9 December 1994 Raob from Desert Rock (DRA) Nevada.

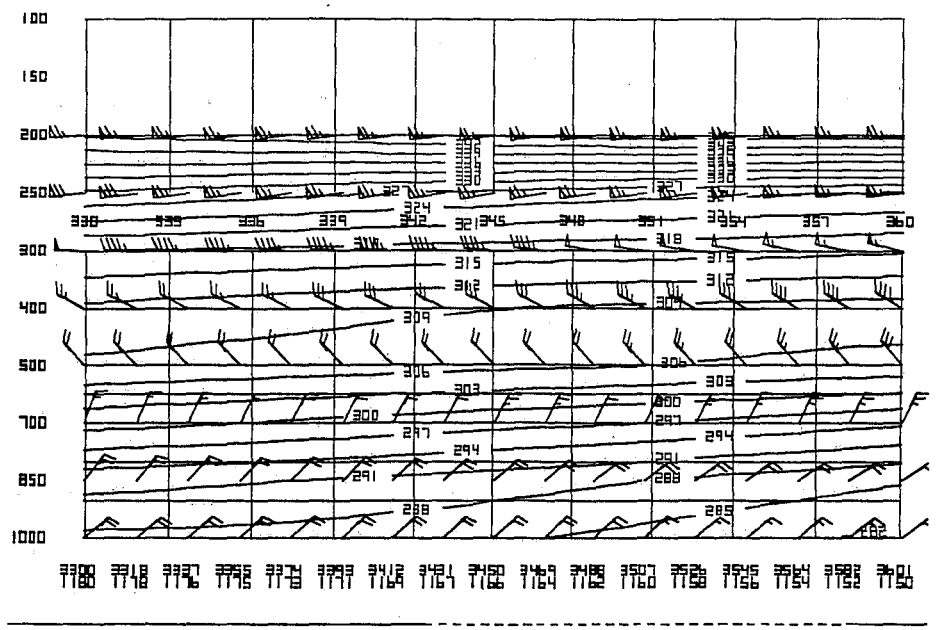

Figure 32. ETA crossection of winds (knots) and potential temperature (degrees kelvin) at 0000 UTC 9 December 1994. Potential temperature contours every 3 degrees kelvin.

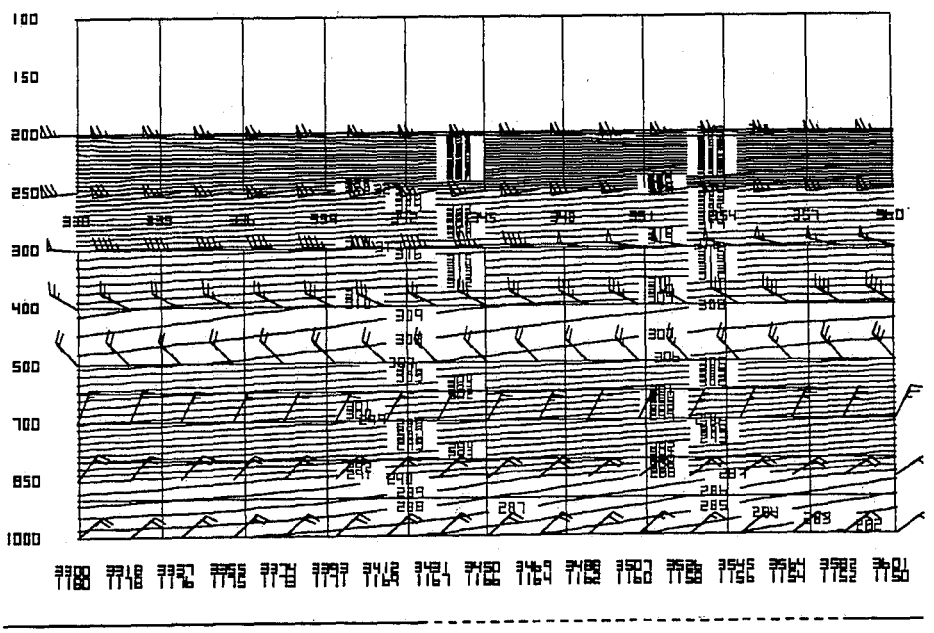

Figure 33. ETA crossection of winds (knots) and potential temperature (degrees kelvin) at 0000 UTC 9 December 1994. Potential temperature contours every 1 degree kelvin.

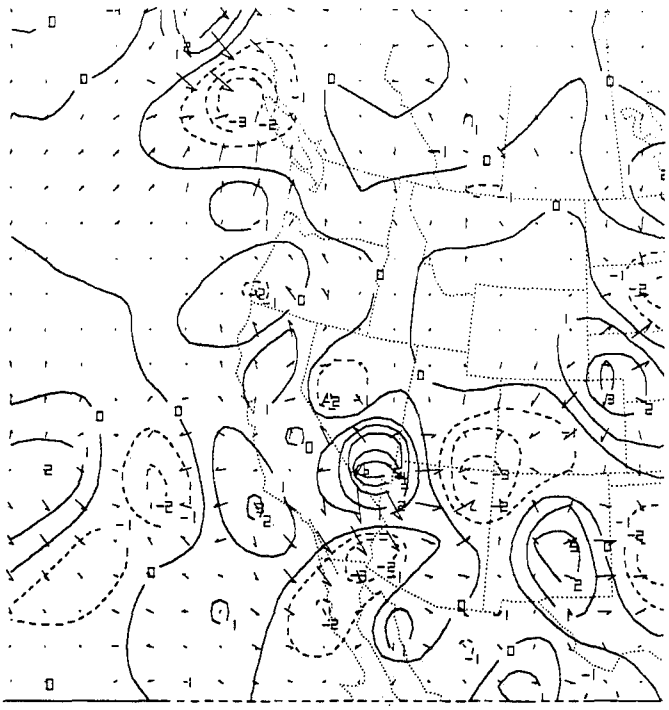

Figure 34. 1200 UTC 8 December 1994 700 millibar Q-vector divergence. Contours every $1x10^{-10}$ C m^{-2} s^{-1}.

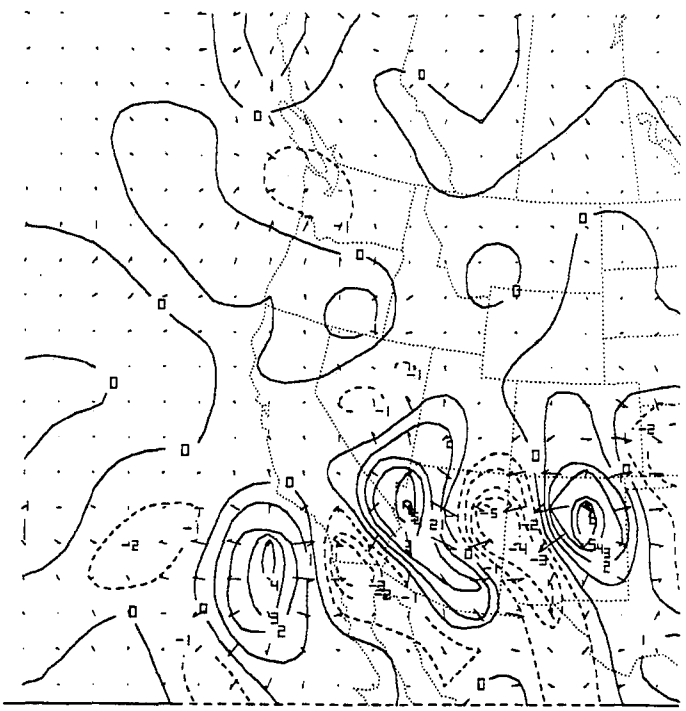

Figure 35. 0000 UTC 9 December 1994 700 millibar Q-vector divergence. Contours every $1x10^{-10}$ C m^{-2} s^{-1}.

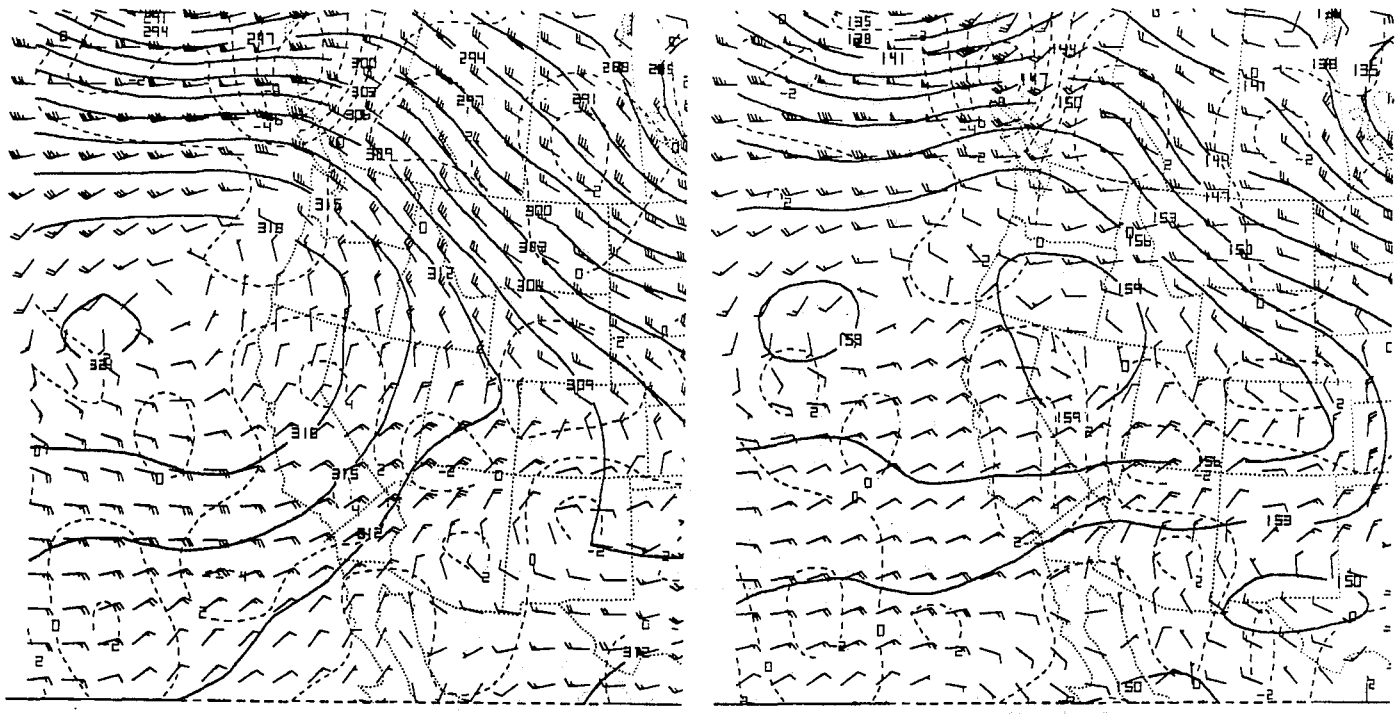

a. b.

Figure 36. (a) ETA 700 mb heights (dekameters), vertical velocities (microbars per second), and winds (knots) at 1200 UTC 2 November 1993. Height contours (solid) every 30 meters and vertical velocity contours (dashed) every 2 microbars per second. (b) ETA 850 mb heights (dekameters), vertical velocities (microbars per second), and winds (knots) at 1200 UTC 2 November 1993. Height contours are every 30 meters and vertical velocity contours are every 2 microbars per second.

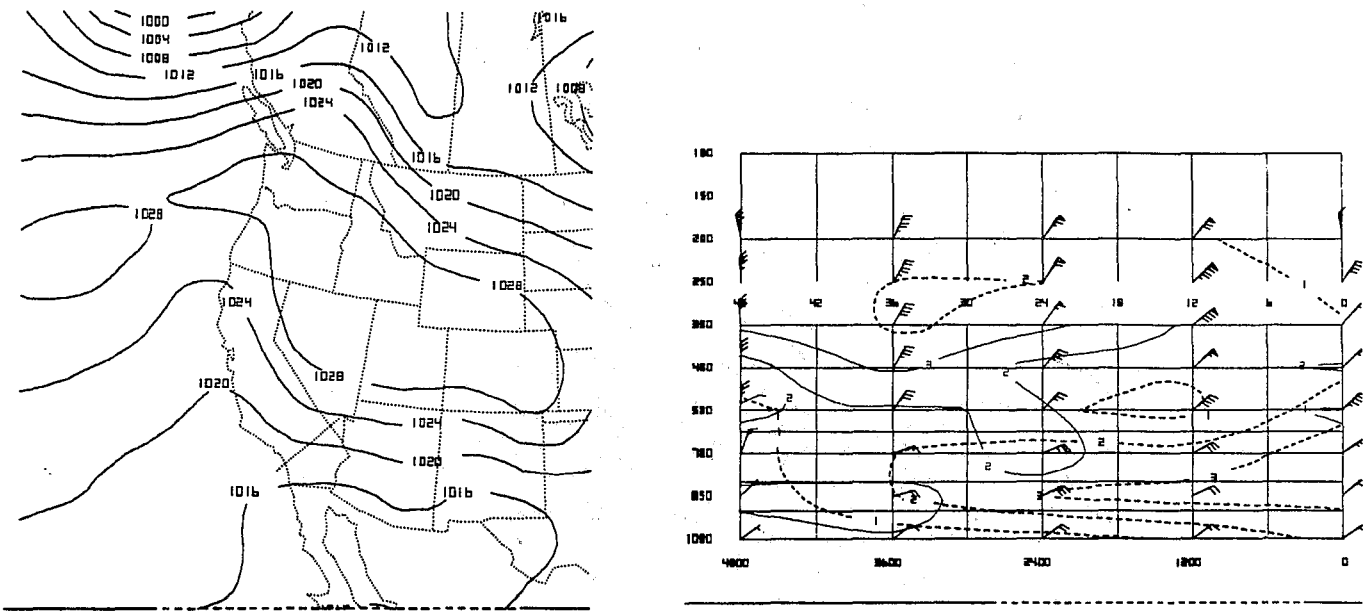

a. b.

Figure 37. (a) ETA Mean Sea Level Pressure (millibars) at 1200 UTC 2 November 1993. Pressure contours every 4 millibars. (b) ETA Time/Height Crossection of winds (knots), vertical velocity (microbars per second) and relative humidity (percent) at 1200 UTC 2 November 1993. Vertical velocity (dashed) every 1 microbar per second, and relative humidity (solid) every 10 percent.

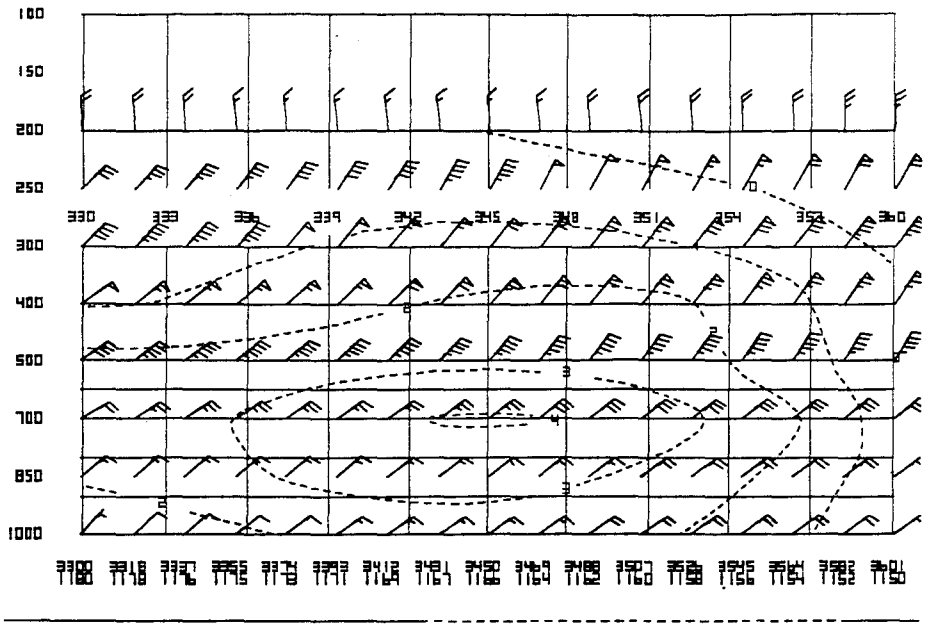

Figure 38. ETA crossection of winds (knots) and vertical velocity (microbars per second) at 1200 UTC 2 November 1993. Vertical velocity (dashed) every 1 microbar per second.

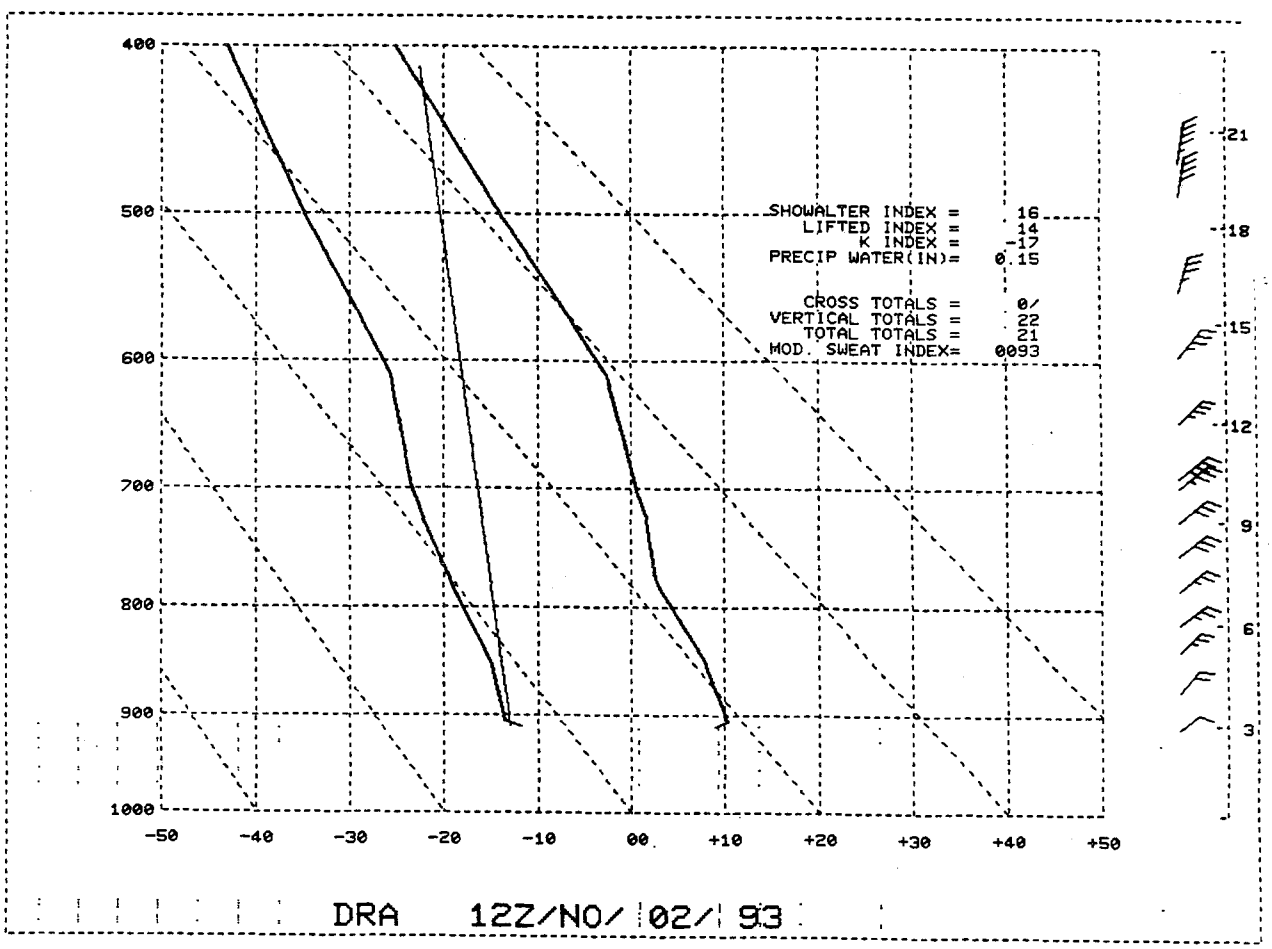

Figure 39. 1200 UTC 2 November 1993 Raob from Desert Rock (DRA) Nevada.

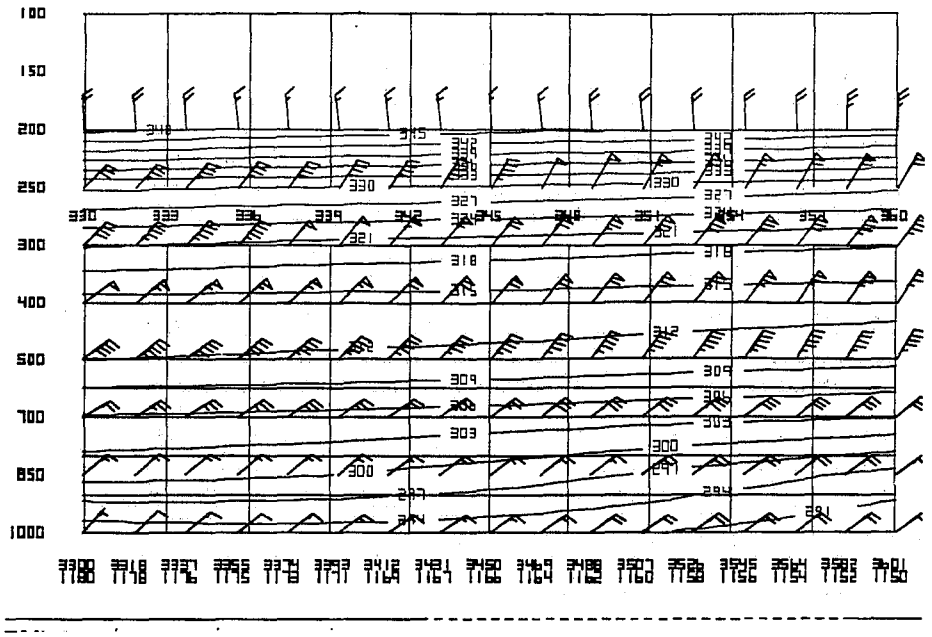

Figure 40. ETA crossection of winds (knots) and potential temperature (degrees kelvin) at 1200 UTC 2 November 1993. Potential temperature contours every 3 degrees kelvin.

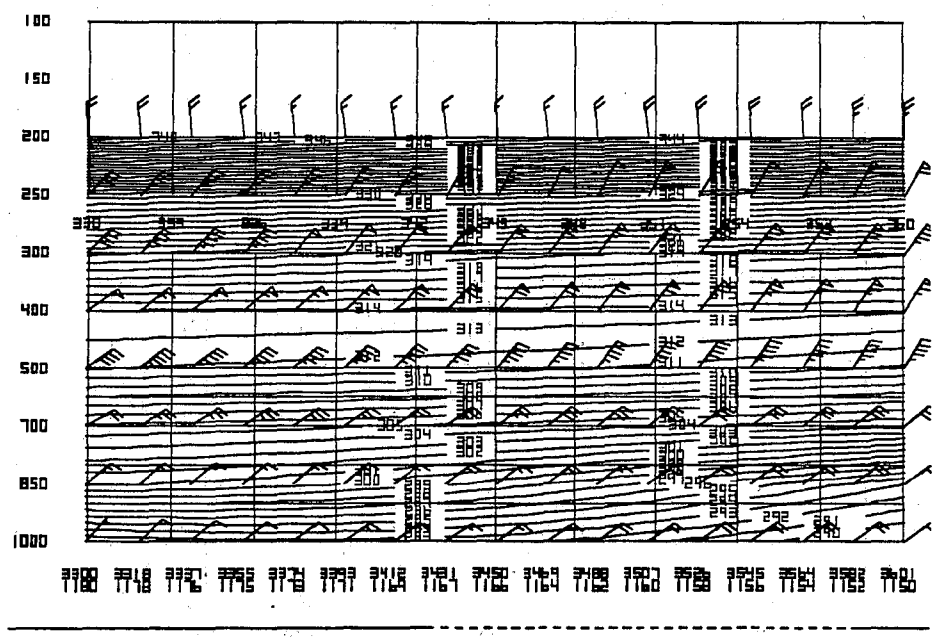

Figure 41. ETA crossection of winds (knots) and potential temperature (degrees kelvin) at 1200 UTC 2 November 1993. Potential temperature contours every 1 degree kelvin.

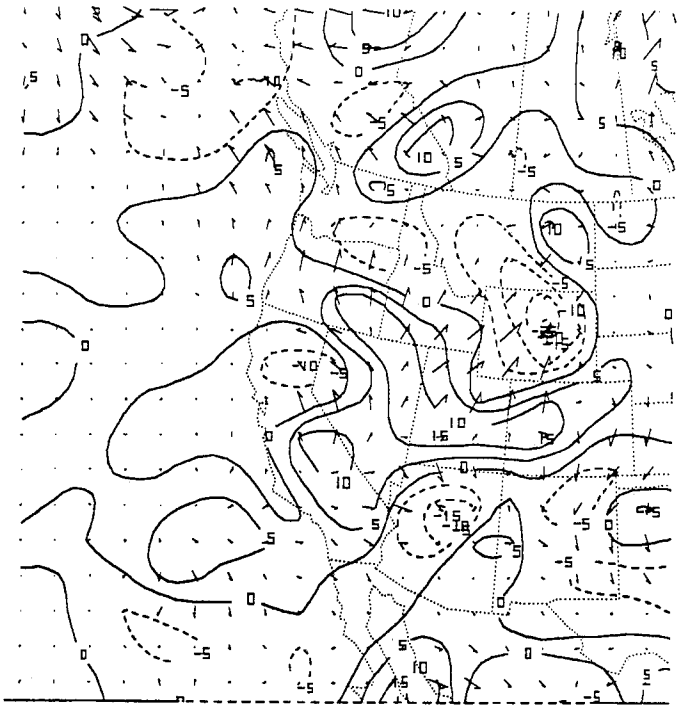

Figure 42. 1200 UTC 2 November 1993 700 millibar Q-vector divergence. Contours every 5×10^{-10} C m^{-2} s^{-1}.

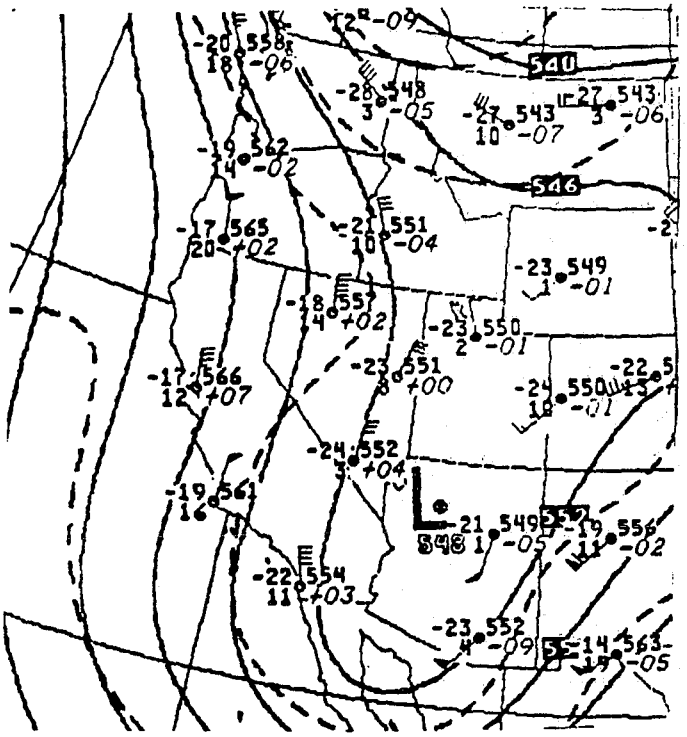

Figure 43a.
1200 UTC 13 November 1993
500mb analysis
heights/temperature

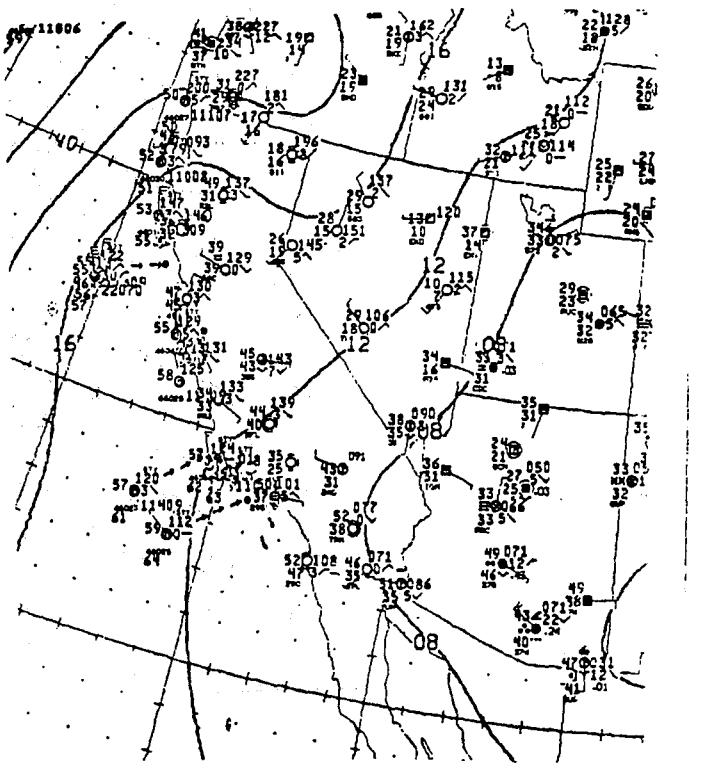

Figure 43b.
1200 UTC 13 November 1993
NMC surface analysis

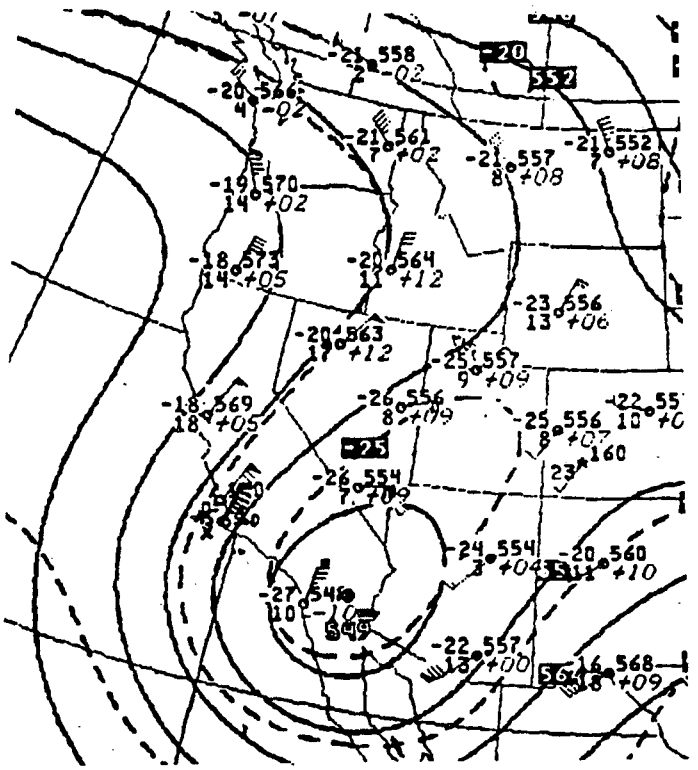

FIGURE 44a.
0000 UTC 15 November 1993
500mb analysis
heights/temperature

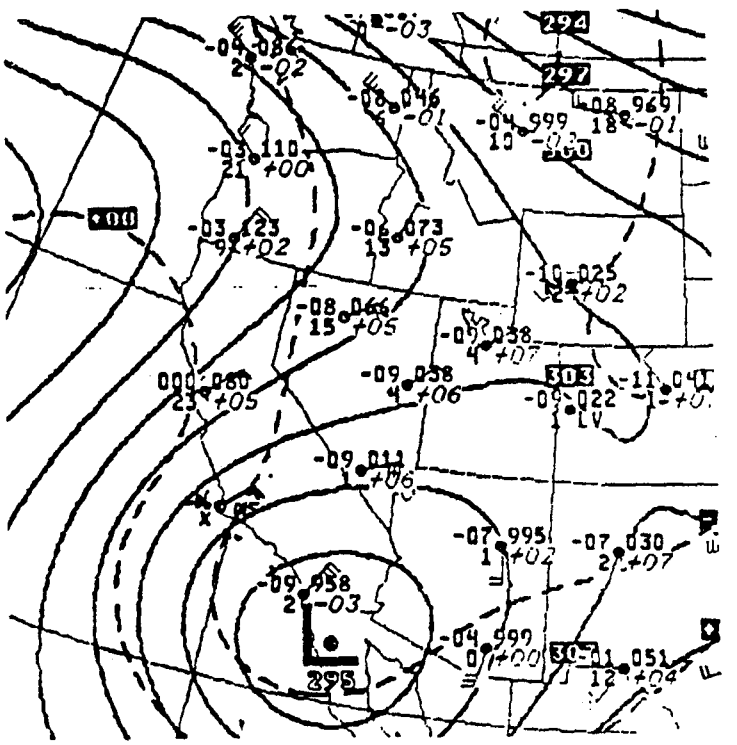

Figure 44b.
0000 UTC 15 November 1993
700mb analysis
heights/temperature

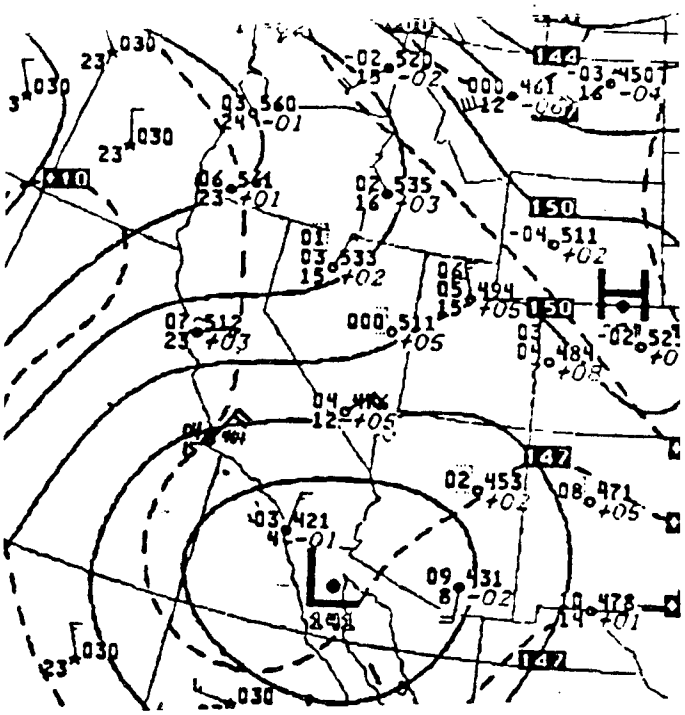

Figure 45a.
0000 UTC 15 November 1993
850mb analysis
heights/temperature

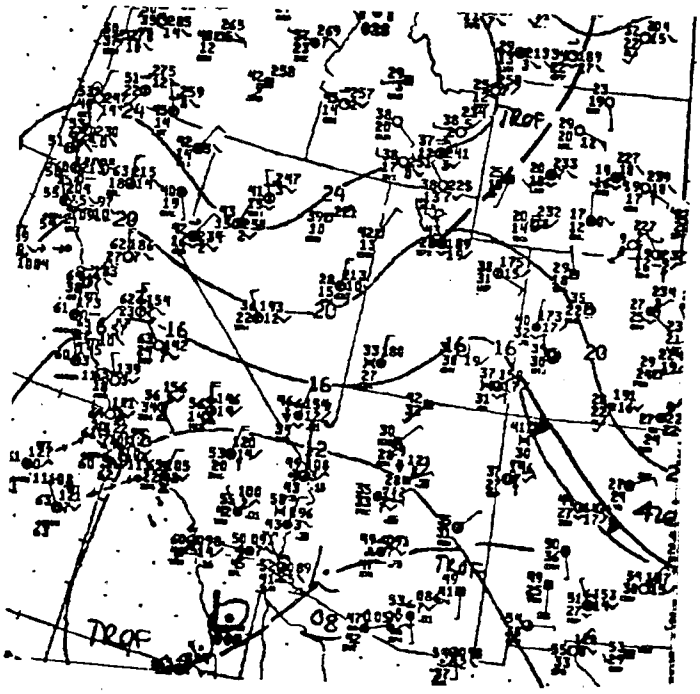

Figure 45b.
0000 UTC 15 November 1993
NMC surface analysis

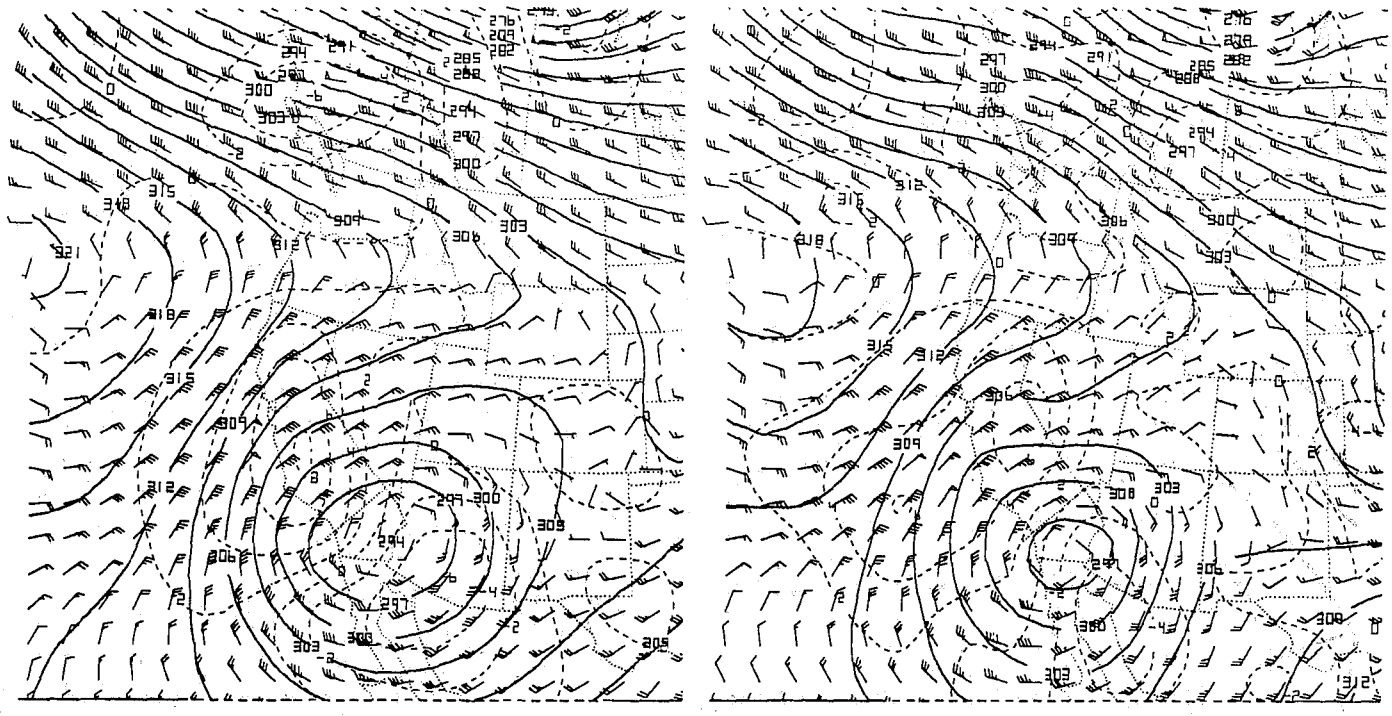

a. b.

Figure 46. (a) ETA 24 hour forecast 700 mb heights (dekameters), vertical velocities (microbars per second), and winds (knots) valid 0000 UTC 15 November 1993. Height contours (solid) every 30 meters and vertical velocity contours (dashed) every 2 microbars per second.
(b) ETA 700 mb heights, vertical velocities,and winds at 0000 UTC 15 November 1993. Same units and contour intervals.

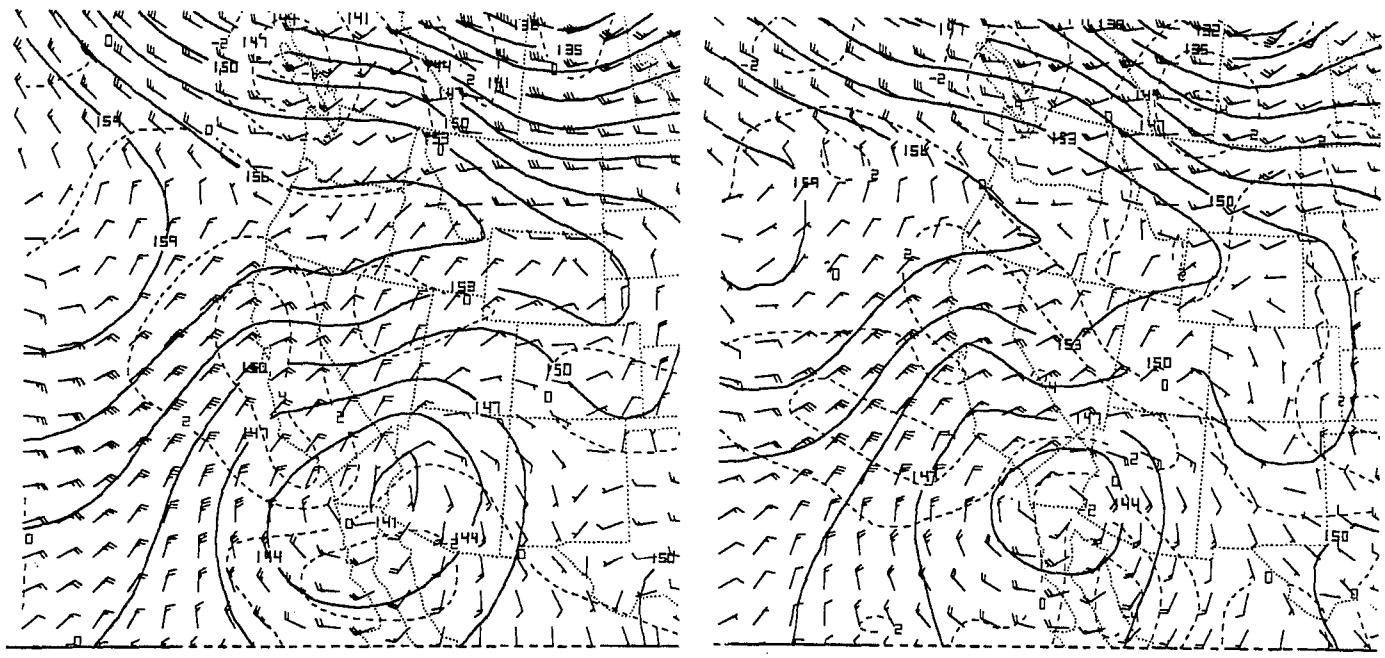

a. b.

Figure 47. (a) ETA 24 hour forecast 850 mb heights (dekameters), vertical velocities (microbars per second), and winds (knots) valid 0000 UTC 15 November 1993. Height contours are every 30 meters and vertical velocity contours are every 2 microbars per second.
(b) ETA 850 mb heights (dekameters), vertical velocities (microbars per second), and winds (knots) at 0000 UTC 15 November 1993. Same units and contour intervals.

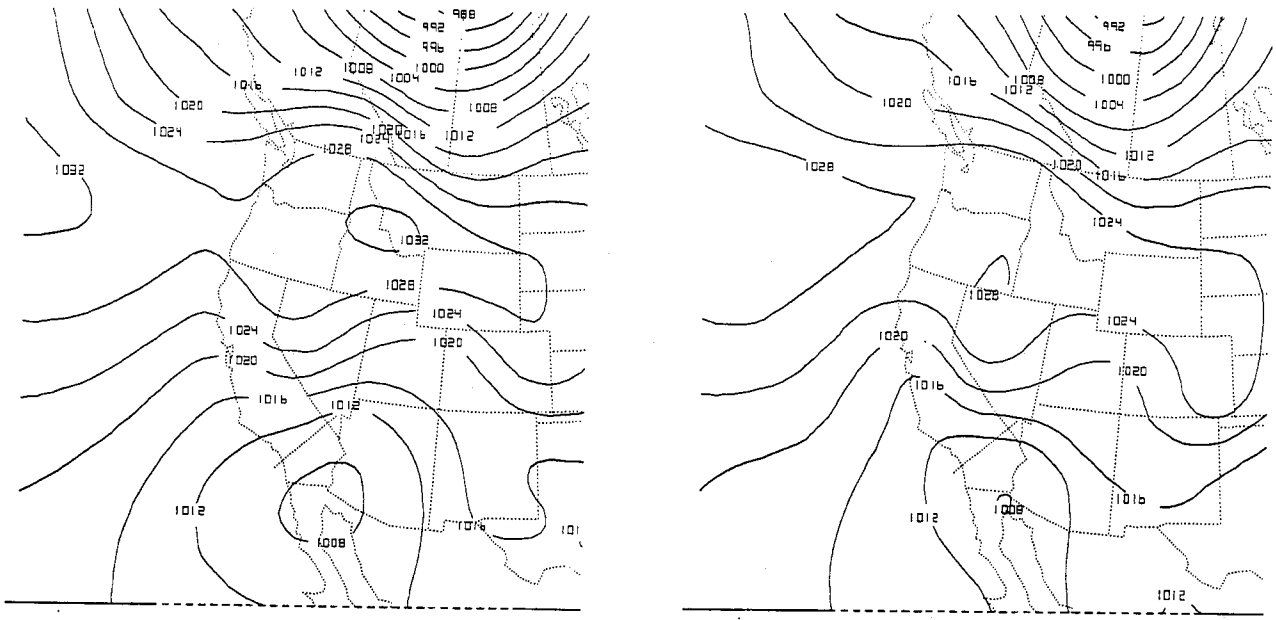

a. b.

Figure 48. (a) ETA 24 hour forecast Mean Sea Level Pressure (millibars) valid 0000 UTC 15 November 1993. Pressure contours every 4 millibars.
(b) ETA Mean Sea Level Pressure (millibars) at 0000 UTC 15 November 1993. Pressure contours every 4 millibars.

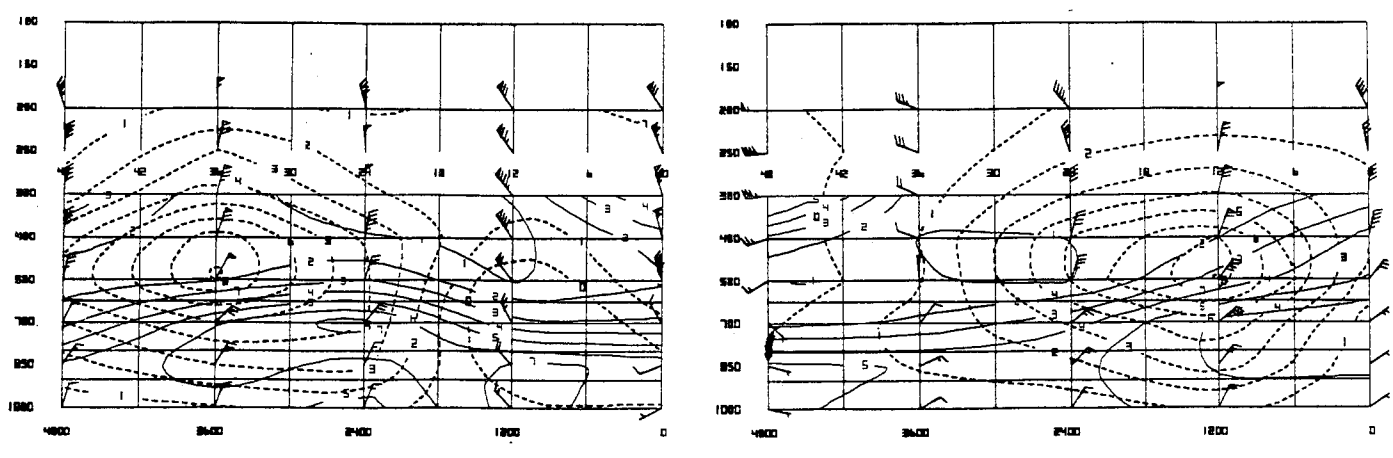

a. b.

Figure 49. (a) ETA Time/Height Crossection of winds (knots), vertical velocity (microbars per second) and relative humidity (percent) at 0000 UTC 14 November 1993. Vertical velocity (dashed) every 1 microbar per second, and relative humidity (solid) every 10 percent.
(b) Same, except at 0000 UTC 15 November 1993.

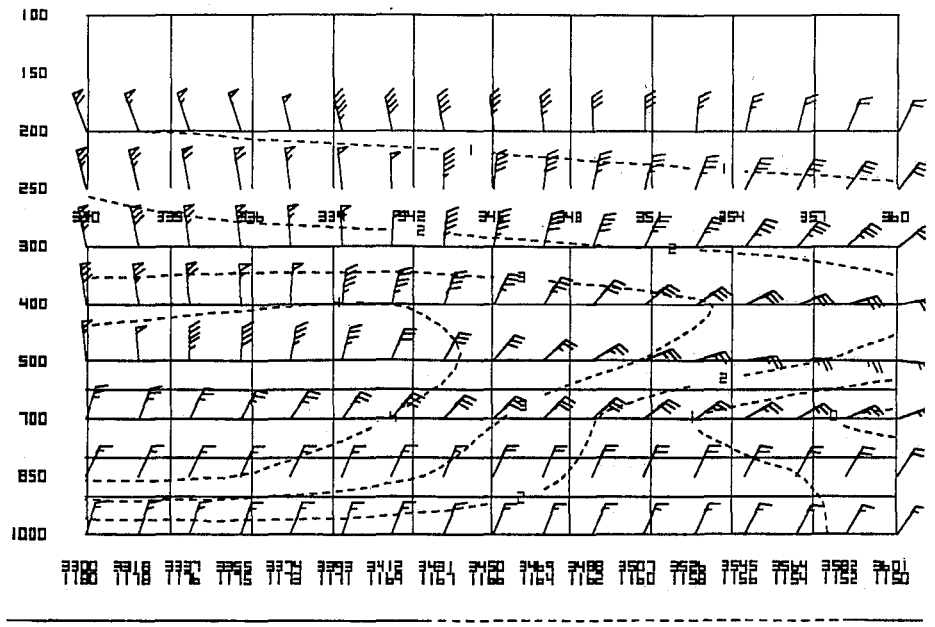

Figure 50. ETA 24 hour forecast crossection of winds (knots) and vertical velocity (microbars per second) valid 0000 UTC 15 November 1993. Vertical velocity (dashed) every 1 microbar per second.

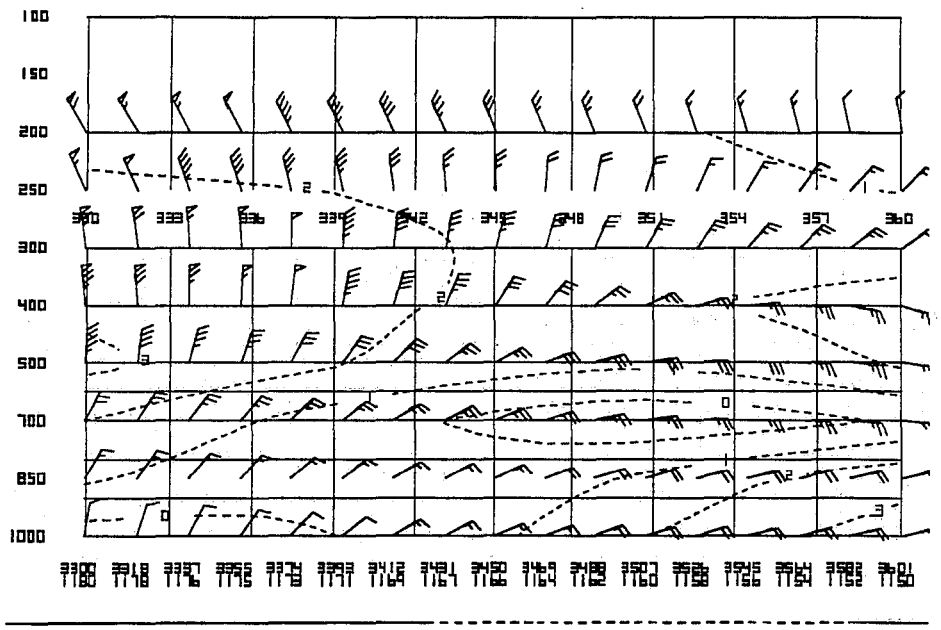

Figure 51. ETA crossection of winds (knots) and vertical velocity (microbars per second) at 0000 UTC 15 November 1993. Vertical velocity (dashed) every 1 microbar per second.

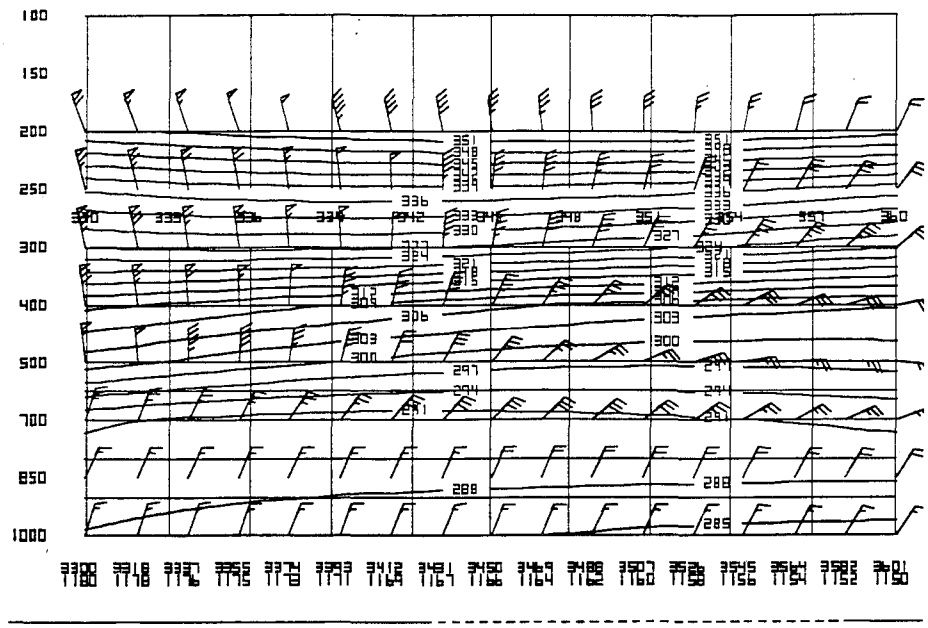

Figure 52. ETA 24 hour forecast crossection of winds (knots) and potential temperature (degrees kelvin) valid 0000 UTC 15 November 1993. Potential temperature contours every 3 degrees kelvin.

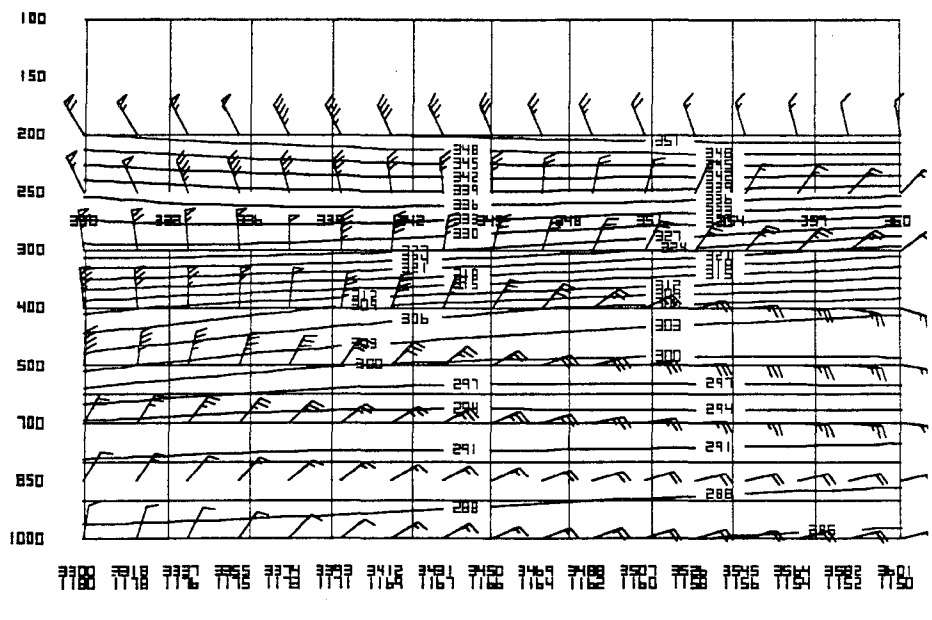

Figure 53. ETA crossection of winds (knots) and potential temperature (degrees kelvin) at 0000 UTC 15 November 1993. Potential temperature contours every 3 degrees kelvin.

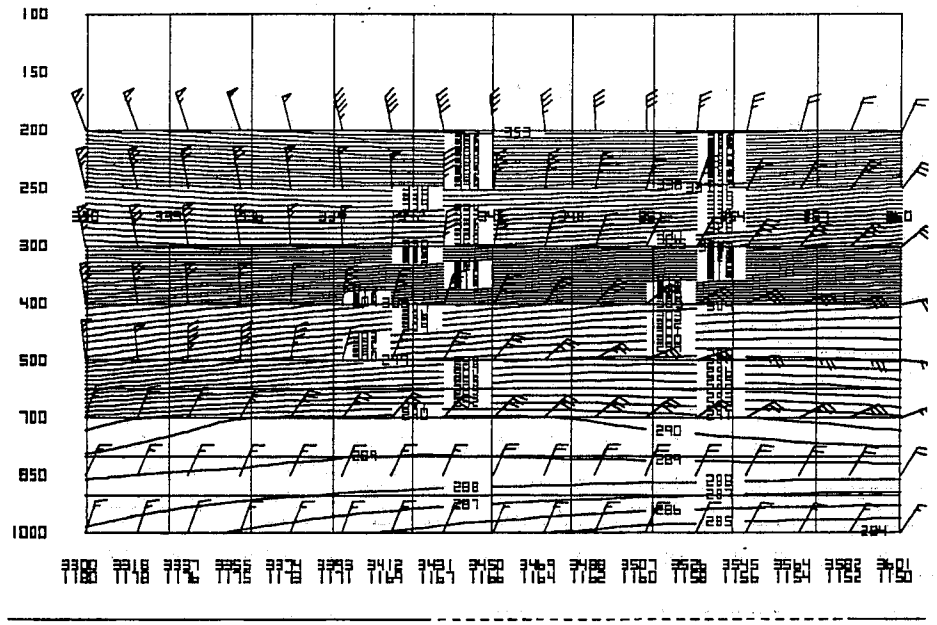

Figure 54. ETA 24 hour forecast crossection of winds (knots) and potential temperature (degrees kelvin) valid 0000 UTC 15 November 1993. Potential temperature contours every 1 degree kelvin.

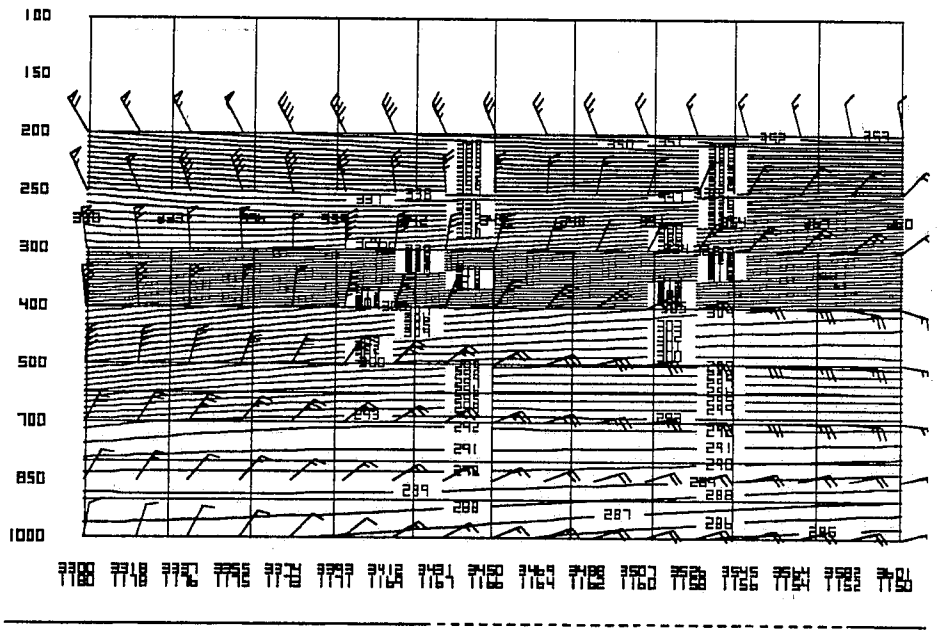

Figure 55. ETA crossection of winds (knots) and potential temperature (degrees kelvin) at 0000 UTC 15 November 1993. Potential temperature contours every 1 degree kelvin.

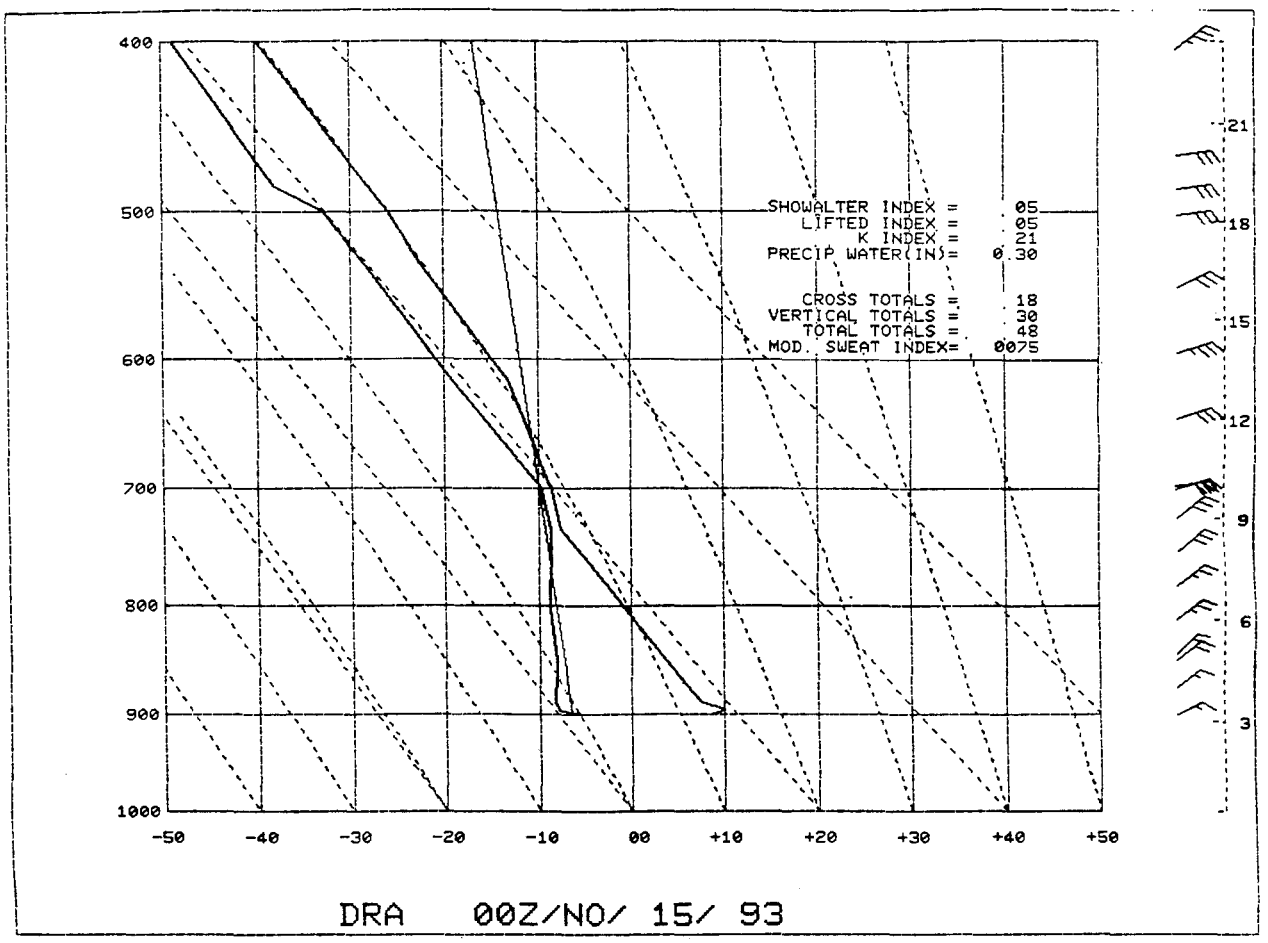

Figure 56. 0000 UTC 15 November 1993 Raob from Desert Rock (DRA) Nevada.

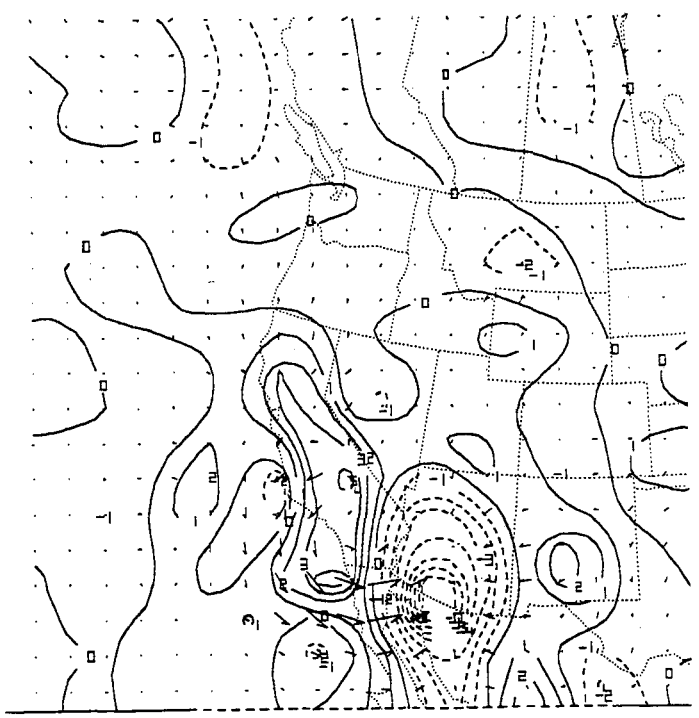

Figure 57. 0000 UTC 15 November 1993 700 millibar Q-vector divergence. Contours every 1×10^{-10} C m^{-2} s^{-1}.

142 The Usefulness of Data from Mountaintop Fire Lookout Stations in Determining Atmospheric Stability. Jonathan W. Corey, April 1979. (PB298899/AS)
143 The Depth of the Marine Layer at San Diego as Related to Subsequent Cool Season Precipitation Episodes in Arizona. Ira S. Brenner, May 1979. (PB298817/AS)
144 Arizona Cool Season Climatological Surface Wind and Pressure Gradient Study. Ira S. Brenner, May 1979. (PB298900/AS)
146 The BART Experiment. Morris S. Webb, October 1979. (PB80 155112)
147 Occurrence and Distribution of Flash Floods in the Western Region. Thomas L. Dietrich, December 1979. (PB80 160344)
149 Misinterpretations of Precipitation Probability Forecasts. Allan H. Murphy, Sarah Lichtenstein, Baruch Fischhoff, and Robert L. Winkler. February 1980. (PB80 174576)
150 Annual Data and Verification Tabulation - Eastern and Central North Pacific Tropical Storms and Hurricanes 1979. Emil B. Gunther and Staff, EPHC, April 1980. (PB80 220486)
151 NMC Model Performance in the Northeast Pacific. James E. Overland, PMEL-ERL, April 1980. (PB80 196033)
152 Climate of Salt Lake City, Utah. Wilbur E. Figgins (Retired) and Alexander R. Smith. Fifth Revision, July 1992. (PB92 220177)
153 An Automatic Lightning Detection System in Northern California. James E. Rea and Chris E. Fontana, June 1980. (PB80 225592)
154 Regression Equation for the Peak Wind Gust 6 to 12 Hours in Advance at Great Falls During Strong Downslope Wind Storms. Michael J. Oard, July 1980. (PB91 108367)
155 A Raininess Index for the Arizona Monsoon. John H. Ten Harkel, July 1980. (PB81 106494)
156 The Effects of Terrain Distribution on Summer Thunderstorm Activity at Reno, Nevada. Christopher Dean Hill, July 1980. (PB81 102501)
157 An Operational Evaluation of the Scofield/Oliver Technique for Estimating Precipitation Rates from Satellite Imagery. Richard Ochoa, August 1980. (PB81 108227)
158 Hydrology Practicum. Thomas Dietrich, September 1980. (PB81 134033)
159 Tropical Cyclone Effects on California. Arnold Court, October 1980. (PB81 133779)
160 Eastern North Pacific Tropical Cyclone Occurrences During Intraseasonal Periods. Preston W. Leftwich and Gail M. Brown, February 1981. (PB81 205494)
161 Solar Radiation as a Sole Source of Energy for Photovoltaics in Las Vegas, Nevada, for July and December. Darryl Randerson, April 1981. (PB81 224503)
162 A Systems Approach to Real-Time Runoff Analysis with a Deterministic Rainfall-Runoff Model. Robert J.C. Burnash and R. Larry Ferral, April 1981. (PB81 224495)
163 A Comparison of Two Methods for Forecasting Thunderstorms at Luke Air Force Base, Arizona. LTC Keith R. Cooley, April 1981. (PB81 225393)
164 An Objective Aid for Forecasting Afternoon Relative Humidity Along the Washington Cascade East Slopes. Robert S. Robinson, April 1981. (PB81 23078)
165 Annual Data and Verification Tabulation, Eastern North Pacific Tropical Storms and Hurricanes 1980. Emil B. Gunther and Staff, May 1981. (PB82 230336)
166 Preliminary Estimates of Wind Power Potential at the Nevada Test Site. Howard G. Booth, June 1981. (PB82 127036)
167 ARAP User's Guide. Mark Mathewson, July 1981, Revised September 1981. (PB82 196783)
168 Forecasting the Onset of Coastal Gales Off Washington-Oregon. John R. Zimmerman and William D. Burton, August 1981. (PB82 127051)
169 A Statistical-Dynamical Model for Prediction of Tropical Cyclone Motion in the Eastern North Pacific Ocean. Preston W. Leftwich, Jr., October 1981. (PB82195298)
170 An Enhanced Plotter for Surface Airways Observations. Andrew J. Spry and Jeffrey L. Anderson, October 1981. (PB82 153883)
171 Verification of 72-Hour 500-MB Map-Type Predictions. R.F. Quiring, November 1981. (PB82 158098)
172 Forecasting Heavy Snow at Wenatchee, Washington. James W. Holcomb, December 1981. (PB82 177783)
173 Central San Joaquin Valley Type Maps. Thomas R. Crossan, December 1981. (PB82 196064)
174 ARAP Test Results. Mark A. Mathewson, December 1981. (PB82 198103)
176 Approximations to the Peak Surface Wind Gusts from Desert Thunderstorms. Darryl Randerson, June 1982. (PB82 253089)
177 Climate of Phoenix, Arizona. Robert J. Schmidli, April 1969 (Revised December 1986). (PB87 142063/AS)
178 Annual Data and Verification Tabulation, Eastern North Pacific Tropical Storms and Hurricanes 1982. E.B. Gunther, June 1983. (PB85 106078)
179 Stratified Maximum Temperature Relationships Between Sixteen Zone Stations in Arizona and Respective Key Stations. Ira S. Brenner, June 1983. (PB83 249904)
180 Standard Hydrologic Exchange Format (SHEF) Version I. Phillip A. Pasteris, Vernon C. Bissel, David G. Bennett, August 1983. (PB85 106052)
181 Quantitative and Spacial Distribution of Winter Precipitation along Utah's Wasatch Front. Lawrence B. Dunn, August 1983. (PB85 106912)
182 500 Millibar Sign Frequency Teleconnection Charts - Winter. Lawrence B. Dunn, December 1983. (PB85 106276)
183 500 Millibar Sign Frequency Teleconnection Charts - Spring. Lawrence B. Dunn, January 1984. (PB85 111367)
184 Collection and Use of Lightning Strike Data in the Western U.S. During Summer 1983. Glenn Rasch and Mark Mathewson, February 1984. (PB85 110534)
185 500 Millibar Sign Frequency Teleconnection Charts - Summer. Lawrence B. Dunn, March 1984. (PB85 111359)
186 Annual Data and Verification Tabulation eastern North Pacific Tropical Storms and Hurricanes 1983. E.B. Gunther, March 1984. (PB85 109635)
187 500 Millibar Sign Frequency Teleconnection Charts - Fall. Lawrence B. Dunn, May 1984. (PB85 110930)
188 The Use and Interpretation of Isentropic Analyses. Jeffrey L. Anderson, October 1984. (PB85 132694)
189 Annual Data & Verification Tabulation Eastern North Pacific Tropical Storms and Hurricanes 1984. E.B. Gunther and R.L. Cross, April 1985. (PB85 1878887AS)
190 Great Salt Lake Effect Snowfall: Some Notes and An Example. David M. Carpenter, October 1985. (PB86 119153/AS)
191 Large Scale Patterns Associated with Major Freeze Episodes in the Agricultural Southwest. Ronald S. Hamilton and Glenn R. Lussky, December 1985. (PB86 144474AS)
192 NWR Voice Synthesis Project: Phase I. Glen W. Sampson, January 1986. (PB86 145604/AS)
193 The MCC - An Overview and Case Study on Its Impact in the Western United States. Glenn R. Lussky, March 1986. (PB86 170651/AS)
194 Annual Data and Verification Tabulation Eastern North Pacific Tropical Storms and Hurricanes 1985. E.B. Gunther and R.L. Cross, March 1986. (PB86 170941/AS)
195 Radid Interpretation Guidelines. Roger G. Pappas, March 1986. (PB86 177680/AS)
196 A Mesoscale Convective Complex Type Storm over the Desert Southwest. Darryl Randerson, April 1986. (PB86 190998/AS)
197 The Effects of Eastern North Pacific Tropical Cyclones on the Southwestern United States. Walter Smith, August 1986. (PB87 106258AS)
198 Preliminary Lightning Climatology Studies for Idaho. Christopher D. Hill, Carl J. Gorski, and Michael C. Conger, April 1987. (PB87 180196/AS)
199 Heavy Rains and Flooding in Montana: A Case for Slantwise Convection. Glenn R. Lussky, April 1987. (PB87 185229/AS)
200 Annual Data and Verification Tabulation Eastern North Pacific Tropical Storms and Hurricanes 1986. Roger L. Cross and Kenneth B. Mielke, September 1987. (PB88 110895/AS)
201 An Inexpensive Solution for the Mass Distribution of Satellite Images. Glen W. Sampson and George Clark, September 1987. (PB88 114038/AS)
202 Annual Data and Verification Tabulation Eastern North Pacific Tropical Storms and Hurricanes 1987. Roger L. Cross and Kenneth B. Mielke, September 1988. (PB88 101935/AS)
203 An Investigation of the 24 September 1986 "Cold Sector" Tornado Outbreak in Northern California. John P. Monteverdi and Scott A. Braun, October 1988. (PB89 121297/AS)
204 Preliminary Analysis of Cloud-To-Ground Lightning in the Vicinity of the Nevada Test Site. Carven Scott, November 1988. (PB89 128649/AS)
205 Forecast Guidelines For Fire Weather and Forecasters -- How Nighttime Humidity Affects Wildland Fuels. David W. Goens, February 1989. (PB89 162549/AS)
206 A Collection of Papers Related to Heavy Precipitation Forecasting. Western Region Headquarters, Scientific Services Division, August 1989. (PB89 230833/AS)
207 The Las Vegas McCarran International Airport Microburst of August 8, 1989. Carven A. Scott, June 1990. (PB90-240268)
208 Meteorological Factors Contributing to the Canyon Creek Fire Blowup, September 6 and 7, 1988. David W. Goens, June 1990. (PB90-245085)
209 Stratus Surge Prediction Along the Central California Coast. Peter Felsch and Woodrow Whitlatch, December 1990. (PB91-129239)
210 Hydrotools. Tom Egger. January 1991. (PB91-151787/AS)
211 A Northern Utah Soaker. Mark E. Struthwolf, February 1991. (PB91-168716)
212 Preliminary Analysis of the San Francisco Rainfall Record: 1849-1990. Jan Null, May 1991. (PB91-208439)
213 Idaho Zone Preformat, Temperature Guidance, and Verification. Mark A. Mollner, July 1991. (PB91-227405/AS)
214 Emergency Operational Meteorological Considerations During an Accidental Release of Hazardous Chemicals. Peter Mueller and Jerry Galt, August 1991. (PB91-235424)
215 WeatherTools. Tom Egger, October 1991. (PB93-184950)
216 Creating MOS Equations for RAWS Stations Using Digital Model Data. Dennis D. Gettman, December 1991. (PB92-131473/AS)
217 Forecasting Heavy Snow Events in Missoula, Montana. Mike Richmond, May 1992. (PB92-196104)
218 NWS Winter Weather Workshop in Portland, Oregon. Various Authors, December 1992. (PB93-146785)
219 A Case Study of the Operational Usefulness of the Sharp Workstation in Forecasting a Mesocyclone-Induced Cold Sector Tornado Event in California. John P. Monteverdi, March 1993. (PB93-178697)
220 Climate of Pendleton, Oregon. Claudia Bell, August 1993. (PB93-227536)
221 Utilization of the Bulk Richardson Number, Helicity and Sounding Modification in the Assessment of the Severe Convective Storms of 3 August 1992. Eric C. Evenson, September 1993. (PB94-131943)
222 Convective and Rotational Parameters Associated with Three Tornado Episodes in Northern and Central California. John P. Monteverdi and John Quadros, September 1993. (PB94-131943)
223 Climate of San Luis Obispo, California. Gary Ryan, February 1994. (PB94-162062)
224 Climate of Wenatchee, Washington. Michael W. McFarland, Roger G. Buckman, and Gregory E. Matzen, March 1994. (PB94-164308)
225 Climate of Santa Barbara, California. Gary Ryan, December 1994. (PB95-173720)
226 Climate of Yakima, Washington. Greg DeVoir, David Hogan, and Jay Neher, December 1994. (PB95-173688)
227 Climate of Kalispell, Montana. Chris Maier, December 1994. (PB95-169488)
228 Forecasting Minimum Temperatures in the Santa Maria Agricultural District. Wilfred Pi and Peter Felsch, December 1994. (PB95-171088)
229 The 10 February 1994 Oroville Tornado--A Case Study. Mike Staudenmaier, Jr., April 1995.

NOAA SCIENTIFIC AND TECHNICAL PUBLICATIONS

The National Oceanic and Atmospheric Administration was established as part of the Department of Commerce on October 3, 1970. The mission responsibilities of NOAA are to assess the socioeconomic impact of natural and technological changes in the environment and to monitor and predict the state of the solid Earth, the oceans and their living resources, the atmosphere, and the space environment of the Earth.

The major components of NOAA regularly produce various types of scientific and technical information in the following kinds of publications.

PROFESSIONAL PAPERS--Important definitive research results, major techniques, and special investigations.

CONTRACT AND GRANT REPORTS--Reports prepared by contractors or grantees under NOAA sponsorship.

ATLAS--Presentation of analyzed data generally in the form of maps showing distribution of rainfall, chemical and physical conditions of oceans and atmosphere, distribution of fishes and marine mammals, ionospheric conditions, etc.

TECHNICAL SERVICE PUBLICATIONS--Reports containing data, observations, instructions, etc. A partial listing includes data serials; prediction and outlook periodicals; technical manuals, training papers, planning reports, and information serials; and miscellaneous technical publications.

TECHNICAL REPORTS--Journal quality with extensive details, mathematical developments, or data listings.

TECHNICAL MEMORANDUMS--Reports of preliminary, partial, or negative research or technology results, interim instructions, and the like.

Information on availability of NOAA publications can be obtained from:

NATIONAL TECHNICAL INFORMATION SERVICE

U. S. DEPARTMENT OF COMMERCE

5285 PORT ROYAL ROAD

SPRINGFIELD, VA 22161